

## Invited Review

### Review of asteroid, meteor, and meteorite-type links

Peter JENNISKENS <sup>1,2\*</sup> and Hadrien A. R. DEVILLEPOIX<sup>3</sup>

<sup>1</sup>SETI Institute, Mountain View, California, USA

<sup>2</sup>NASA Ames Research Center, Moffett Field, California, USA

<sup>3</sup>Space Science and Technology Centre and International Centre for Radio Astronomy Research, Curtin University, Perth, Western Australia, Australia

#### \*Correspondence

Peter Jenniskens, SETI Institute, 339 Bernardo Ave, Mountain View, CA 94043, USA.

Email: [petrus.m.jenniskens@nasa.gov](mailto:petrus.m.jenniskens@nasa.gov)

(Received 13 October 2024; revision accepted 27 January 2025)

**Abstract**—With the goal to determine the origin of our meteorites in the asteroid belt, video and photographic observations of meteors have now tracked 75 meteorite falls. Six years ago, there were just hints that different meteorite types arrived on different orbits, but now, the number of orbits ( $N$ ) is high enough for distinct patterns to emerge. In general, 0.1–1-m sized meteoroids do not arrive on similar orbits as the larger ~1-km sized near-Earth asteroids (NEA) of corresponding taxonomic class. Unlike larger NEA, a group of H chondrite meteoroids arrived on low-inclined orbits from a source just beyond the 5:2 mean-motion resonance with Jupiter ( $N = 12$ ), three of which have the 7 Ma cosmic ray exposure (CRE) age from a significant collision event among H chondrites. There is also a source of H chondrites low in the inner main belt with a ~35 Ma CRE age ( $N = 8$ ). In contrast, larger H-like taxonomic S-class NEA arrive from high-inclined orbits out of the 3:1 resonance. Some H chondrites do so also, four of which have a 6 Ma CRE age and two have an 18 Ma CRE age. L chondrites arrive from a single source low in the inner main belt, mostly via the  $\nu_6$  secular resonance ( $N = 21$ ), not the 3:1 resonance as most L-like NEA do. LL chondrites arrive too from the inner main belt ( $N = 5$ ), as do larger LL-like NEA. CM chondrites are delivered from a low  $i < 3^\circ$  inclined source beyond the 3:1 resonance ( $N = 4$ ). Source asteroid families for these meteorite types are proposed, many of which have the same CRE age as the asteroid family's dynamical age. Also, two HED achondrites are now traced to specific impact craters on asteroid Vesta.

## INTRODUCTION

The quest to find the source of our meteorites in the asteroid belt so far has yielded 75 laboratory-classified meteorite falls with an instrumentally recorded approach orbit. Meteorites typically fall from 0.1 to 1 m sized meteoroids and somewhat larger asteroids. Meteorites are thought to sample up to 95–148 distinct parent bodies (Burbine et al., 2002; Greenwood et al., 2020; Meibom & Clark, 1999), but the meteorites with known approach orbits sample only about 15. Earlier reviews of this work

were given by Ceplecha (1977), Ceplecha et al. (1998), Borovička, Spurný, and Brown (2015), Borovička, Spurný, Šegon, et al. (2015), Granvik and Brown (2018), and Jenniskens (2014, 2018).

The goal is shared by the quest to find the source of our larger 20-m to 35-km sized near-Earth asteroids (NEA) in the asteroid belt, which has yielded several hundred spectroscopically classified NEA with orbits derived from asteroid astrometry (e.g., Brož, Vernazza, Marsset, Binzel, et al., 2024; Marsset et al., 2024; Sanchez et al., 2024). Results are put in context by comparative

studies of the reflection spectra of asteroids and meteorites and dynamical studies of the asteroid family collisional histories (e.g., Nesvorný et al., 2023; reviews by Brož, Vernazza, Marsset, DeMeo, et al., 2024; Burbine et al., 2024; Masiero et al., 2015).

The sources considered here (Figure 1) are large asteroids and families of asteroids that are the product of catastrophic and cratering collisions (Nesvorný et al., 2015, 2024; Novaković et al., 2022). Asteroids in a family tend to have the same taxonomic type because most originate from the target asteroid not the smaller projectile (e.g., Masiero et al., 2015; Parker et al., 2008). Conditions of the impact and properties of the target asteroid determine the size frequency distribution (SFD) of fragments. The original number of small fragments created and the total surface area of all remaining fragments factor into the likelihood of meteoroid delivery to Earth. If all fragments are small, then, the debris field may not be apparent in the current asteroid surveys, which mostly detect objects with diameter  $D > 0.5$  km at the inner edge of the main belt and  $D > 1.2$  km near the outer edge.

The influx at Earth of a given meteorite type is dominated by debris from a relatively small number of large collisions that occurred in the last 100 Myr, as shown by peaks in the distribution of meteorite cosmic ray exposure (CRE) ages (David & Leya, 2019; Eugster, 2003, 2006). The CRE age is the period of time a meteoroid was small enough to be exposed to cosmic rays (<2-m sized) and thus build up both stable and radioactive nuclides. In the past decade, a number of asteroid families have now been identified that are younger than 100 Myr, so they are in the same age range as CRE ages of meteorites reaching Earth.

There is also a background of non-family asteroids, but they too tend to originate from the limited number of parent asteroids that are mostly represented in the known asteroid families (Dermott et al., 2018; Morbidelli et al., 2009). The background asteroids are about as abundant as the family asteroids, with a similar or slightly shallower size distribution (Parker et al., 2008).

For some large asteroids, such as (4) Vesta, the surface area dominates that of associated largest asteroid

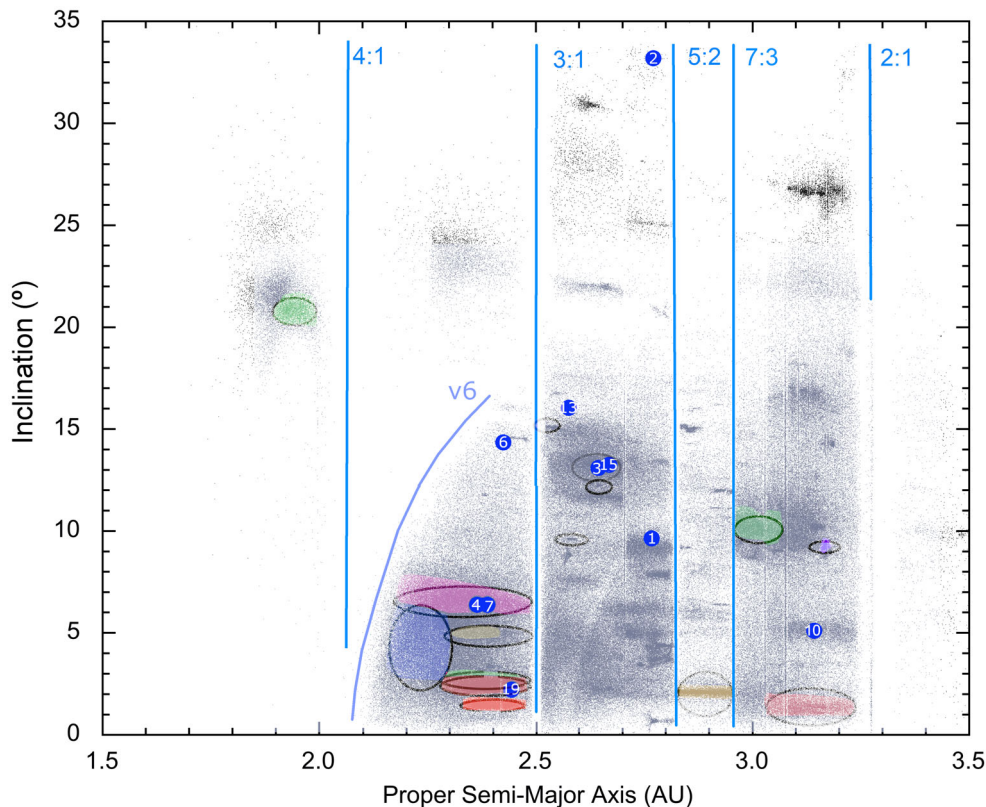


FIGURE 1. Meteorite source regions and delivery resonances. Proper elements of asteroids, with blue symbols marking the large asteroids (4) Vesta, (7) Iris, (6) Hebe, (19) Fortuna, (13) Egeria, (15) Eunomia, (3) Juno, (1) Ceres, (2) Pallas, and (10) Hygiea. Some of the asteroid families discussed in the text are: Hungaria (green); inner main belt: Flora (blue), Vesta (magenta), Erigone (brown), Polana/Eulelia (green), Hertha (red), and Massalia (orange); central main belt: Maria/Crescentia (yellow), Nele (green), and Brangäne (magenta); outer main belt: Koronis (brown), Eos (green), Themis (red), and Veritas (purple).

family members, large enough to produce enough fragments to be detected at Earth as a peak in the CRE age distribution. As an order-of-magnitude estimate, to create enough m-sized fragments to cause the 22 Ma peak in the CRE age distribution of Howard-Eucrite-Diogenites (HED), a crater on Vesta should be at least 10-km in size or a 1-km or larger asteroid needs to be catastrophically destroyed. Many of the known young asteroid families were created from asteroids 1–10 km in size, but the Vesta family has few such large members. Vesta's surface area is larger than that of all Vesta family asteroids >300-m in size. Because of that, most HED meteorites likely originated from Vesta itself (Jenniskens et al., 2020; Unsalan et al., 2019).

Following a collision event, these orbits of asteroid family members evolve by non-gravitational forces, notably Yarkovsky forces, to gain or lose energy and thus evolve into longer or shorter orbits, until the orbital period is matched by a resonance (Bottke et al., 2002). Meter-sized objects have high Yarkovsky mobility, typically 0.001 to 0.01 AU Myr<sup>-1</sup> (Bottke, Vokrouhlický, et al., 2006). This enables them to reach resonances on timescales on the order of a couple of million years, and sometimes shorter if they start close to a resonance. For iron meteoroids, the Yarkovsky effect is inefficient due to high thermal conductivity and thus, the drift is slow (Bottke, Vokrouhlický, et al., 2006), largely explaining the long, up to 1500 Ma, CRE ages of iron meteorites (Eugster, 2003).

Mean motion resonances with Jupiter divide the low-inclined ( $i < 19.2^\circ$ ) main belt asteroid population into the inner main belt ( $v_6$ -3:1), the central main belt (3.1–5:2), the pristine main belt (5:2–7:3), and the outer main belt (7:3–2:1). Resonances are responsible for delivering the meteoroids to Earth (Wetherhill, 1985; Morbidelli & Gladman, 1998). Quickly, they change the eccentricity, lower the perihelion distance, and increase the aphelion distance, while keeping the orbital period (energy of the orbit) constant. Some resonances will also increase the inclination.

Because of the disturbing gravity of Jupiter near aphelion, the fraction of small asteroids to hit Earth exponentially decreases for source regions further out into the asteroid belt. Bottke, Nesvorný, et al. (2006) calculated that delivery by the  $v_6$  resonance ( $a \sim 2.05$  AU) near the inner edge of the asteroid belt (Figure 1) has an efficiency of about 1%. The 3:1 mean-motion resonance with Jupiter at 2.50 AU has an efficiency of about 0.03%, and the 5:2 resonance near 2.82 AU has an efficiency of only about 0.003%. The collision probability with Earth is higher if the inclination of the orbit is near zero and the semi-major axis is short, so that the collision cross section is high due to a low relative velocity.

If all things are equal, a majority of our meteorites are expected to arrive from the  $v_6$  resonance in no-inclined orbits. In reality, that is not the case, confirming that the impact population is dominated by discrete collision events, and the approach orbits are dominated by the dynamical evolution of the meteoroids generated in these collisions.

Once in the resonance, Figure 2 shows the principal ways in which the semi-major axis ( $a$ ) and inclination ( $i$ ) of 20-cm sized meteoroid orbits evolve after 50 Ma of dynamical evolution (Jenniskens et al., 2020). The figure shows all orbits that evolved to perihelion distance  $q < 1.1$  AU from sources in the inner main belt (left) or central main belt (right), either ejected from a high  $10^\circ$  inclination orbit (top) or low  $0^\circ$  initial inclination (bottom). For each case, the orbital element distributions of  $a$  and  $i$  on impact at Earth are distinctly different. The calculation shows that many orbits still have the semi-major axis of the delivery resonance. Qualitatively, meteorites are delivered to Earth principally via the  $v_6$  secular resonance and the 3:1 mean-motion resonance (Figure 1), with the 3:1 mean motion resonance pumping up the inclination. After they reach Earth orbit, close encounters with Earth tend to be most efficient at evolving the orbit when the source is low inclined, by lowering or raising the semi-major axis out of the resonance and dispersing the inclination.

During their orbital evolution from the asteroid belt to Earth, small asteroids can be disrupted by thermal stresses, from collisions with smaller asteroids and meteoroids, or by mass-shedding events from spin-up, among others. This is thought to be the main reason for the short (<1 Ma) CRE ages of some meteorites (e.g., Granvik et al., 2016; Jenniskens et al., 2012; McMullan et al., 2024; Shober et al., 2024). Carbonaceous chondrite asteroids only survive briefly at perihelion distances  $q < 0.2$  AU, while even ordinary chondrites survive only of order 0.01–0.5 Ma at those heliocentric distances (Toliou et al., 2021). Based on similarities in orbits, it has been proposed that up to 25% of meteorites may originate from NEA that had already evolved into Earth-orbit crossing orbits (e.g., Carbognani & Fenucci, 2023) but that likely depends on the meteorite type. Mass shedding events do not typically lead to recognizable asteroid families because the Lyapunov lifetimes are only 60–200 years for orbits in near-Earth space so that orbits rapidly diverge (Pauls & Gladman, 2005; Shober et al., 2025).

The role of collisions is less clear. Most of its lifetime as a small asteroid or meteoroid, the object moves in eccentric orbits with an aphelion in the outer main belt or beyond. The collisional lifetime of asteroids in the main belt is about  $1.4\sqrt{r}$ , with  $r$  the radius of the meteoroid in cm (Wetherhill, 1967, 1985). For those that produced meteorite falls, these are typically in the range of 6–12 Ma

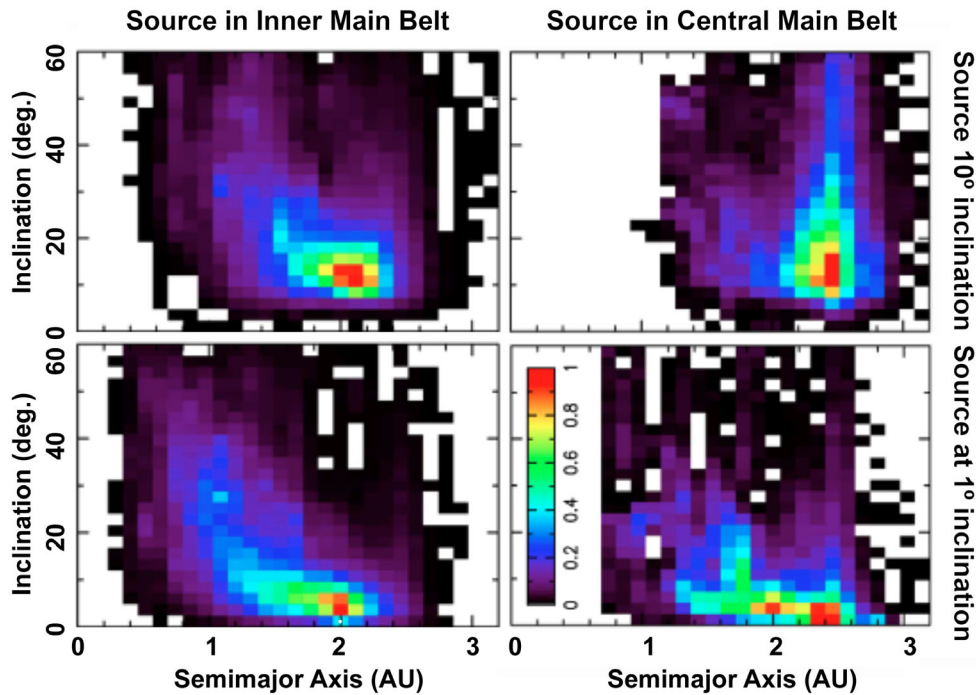


FIGURE 2. Statistical distribution of impact orbits (those with  $q < 1.1$  AU) from dynamical modeling of 20-cm meteoroids ejected from the inner main belt ( $a = 2.1$ – $2.4$  AU) or the central main belt ( $a = 2.55$ – $2.85$  AU), at initial inclinations of  $1^\circ$  and  $10^\circ$ , respectively, after 50 Ma of dynamical evolution. From calculations provided by D. Nesvorný (Jenniskens et al., 2020).

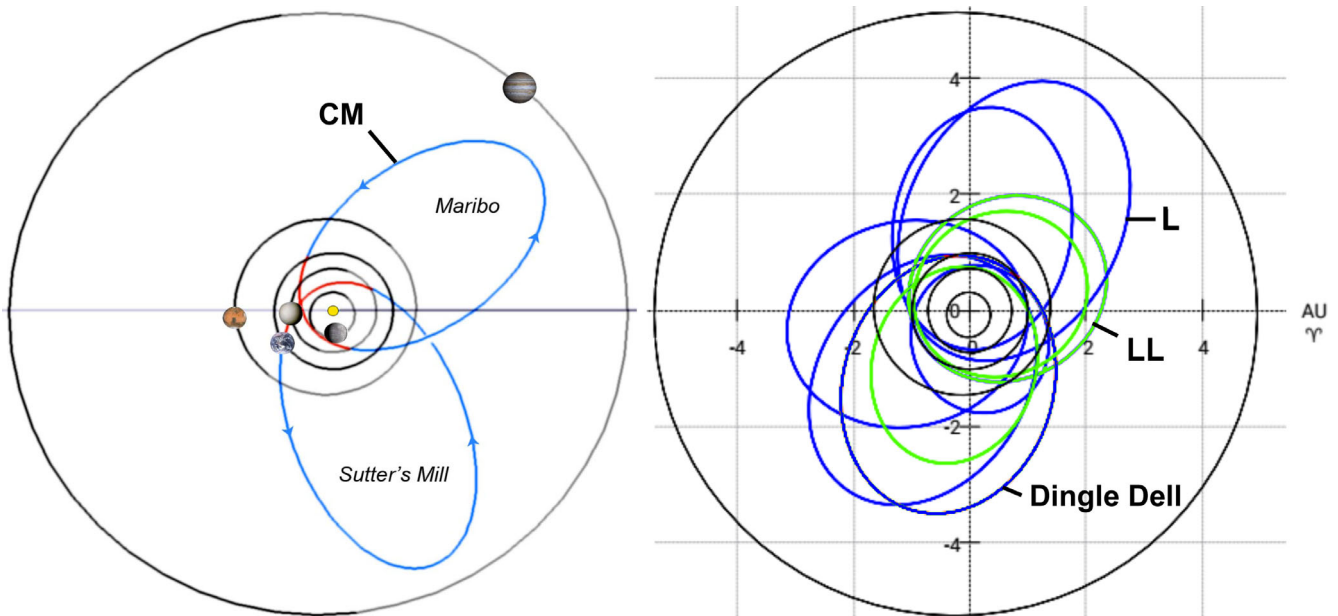


FIGURE 3. In 2018, similarities between the impact orbits of CM-type carbonaceous chondrites (left) and LL- compared to L-type ordinary chondrites (right) provided hints that different meteorite types approached Earth on different orbits. Dingle Dell (L/LL) was an exception on the short LL type orbits. From: Jenniskens et al. (2018).

(e.g., Jenniskens et al., 2019, 2020). However, we have many meteorites with higher CRE ages that imply they survived longer than this. The collisional lifetime of

meteoroids in eccentric orbits with  $q > 0.2$  AU appears to be longer by a factor of at least 3–5 (Jenniskens, 2018), which is possible considering the lower collisional

TABLE 1. Camera networks that tracked and documented meteors from recovered meteorite falls.

Abb.	Network	Coordinators	<i>N</i>	Ref.
V	Video and dashcam footage, digital still photos	—	36	—
EN	European Fireball Network	Z. Ceplecha, P. Spurný	18	[1]
USG	US Government Satellite Network	E. Tagliaferri	17	[2]
DFN/ GFO	Desert Fireball Network/ Global Fireball Observatory	P. Bland, E. Samson	17	[3]
Allsky7	AllSkyCams	H. Devillepoix	—	[4]
FRIPON/ PRISMA	Fireball Recovery and InterPlanetary Observations Network First Network for the Systematic Surveillance of Meteors and Atmosphere	M. Hankey F. Colas D. Barghini	10 6 —	[5] [6] [7]
GMN	Global Meteor Network	D. Vida	5	[8]
CAMS	Cameras for Allsky Meteor Surveillance	P. Jenniskens	4	[9]
A <sup>3</sup> N	Alpe-Adria All-sky Network	J. Kac	2	[10]
ASGARD	NASA Allsky Fireball Network	W. J. Cooke	2	[11]
FFN	Finnish Fireball Network	URSA, E. Lyytinen, M. I. Gritsevich	2	[12]
SACN	Spalding Allsky Camera Network	R. Spalding, D. Free, C. Palotai	2	[13]
SPMN	Spanish Meteor Network	J. Trigo-Rodríguez	1	[14]
AMOS	Automatic Meteor Orbit System	J. Tóth	1	[15]
BRAMON	Brazil Meteor Observation Network	L. S. Amaral	1	[16]
CMN	Croatian Meteor Network	D. Šegon	1	[17]
DMS	Dutch Meteor Society	H. Betlem	1	[18]
MORP	Meteorite Orbit and Recovery Project	I. Halliday	1	[19]
NORSK	Norwegian Meteor Network	S. Midtskogen	1	[20]
PN	Prairie Fireball Network	R. E. McCrosky	1	[21]
SOMN	Southern Ontario Meteor Network	P. Brown	1	[22]
SonotaCo	SonotaCo Network	T. Kanamori	1	[23]
USC	Escola Politécnica Superior de Enxerñaría	J. A. Docobo	1	[24]
SWEMN	Spanish Southwestern Europe Meteor Network	J. M. Madiedo	1	[25]
SKiYMET	SKiYMET meteor radar	W. Singer	1	[26]

*Note:* References: [1] Borovička et al. (2022); [2] Tagliaferri et al. (1994); [3] Bland et al. (2011); [4] Devillepoix et al. (2020); [5] Hankey et al. (2023); [6] Colas et al. (2020); [7] Barghini et al. (2023); [8] Vida, Segon, Gural, et al. (2021); [9] Jenniskens et al. (2011); [10] Kac (2005); [11] Ehlert and Blaauw Erskine (2020); [12] Visuri and Gritsevich (2021); [13] Palotai et al. (2019); [14] Eloy and Trigo-Rodríguez (2021); [15] Tóth et al. (2018); [16] Amaral et al. (2017); [17] Segon et al. (2018); [18] Betlem et al. (1998); [19] Halliday et al. (1978); [20] At website <http://norskmeteornettverk.no> (last accessed November 14, 2024); [21] McCrosky et al. (1971); [22] Brown et al. (2011); [23] Kanamori (2009); [24] Andrade et al. (2022); [25] Madiedo (2022); [26] Schult et al. (2015).

frequency in the region beyond the outer main belt and in the inner solar system.

At the time of our last review of asteroid-meteor-meteorite type links in 2018 (Jenniskens, 2018), there were only hints that meteorites of different type impacted Earth on different orbits. Figure 3, for example, shows the available orbits of CM carbonaceous chondrites (left) and the L and LL ordinary chondrites (right) at the time. Since that time, the number of recovered meteorites with known impact orbits from the triangulation of video and photographic recorded fireballs has doubled. As of July 2024, our records show that 75 falls have been documented in this manner, up from 36 discussed in Jenniskens et al. (2018). In four cases, the asteroid was detected in space prior to its recovery as meteorites (asteroids 2008 TC3, 2018 LA, 2023 CX1 and 2024 BX1), the most recent of which

caused the January 2024 fall of the aubrite Ribbeck in Germany.

This paper is a brief appraisal of the ongoing meteorite-type dependent orbital element survey of small asteroids and large meteoroids and what the results so far say about the possible source regions of our meteorites. An early version of this review was presented at the 86th Annual Meeting of the Meteoritical Society held in Brussels, Belgium, on August 1, 2024.

## EXPERIMENTAL METHODS

### Trajectory and Orbit

Data for this work are gathered by large and small camera networks spread over the globe, some of which are dedicated to the documentation of meteorite falls.

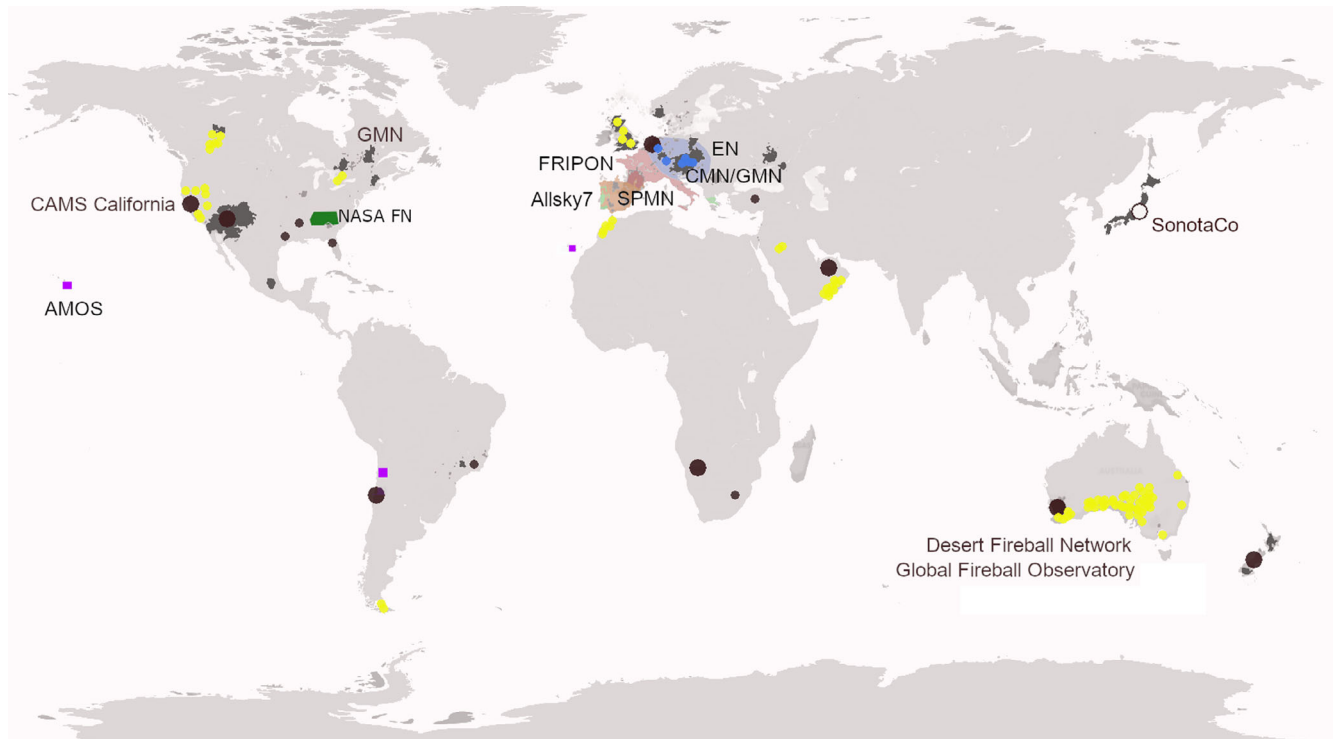


FIGURE 4. The approximate global area coverage and distribution of camera networks aimed at measuring the approach orbit of meteorite falls.

The main photographic and video camera networks are listed in Table 1. The total land coverage of these dedicated networks is shown in Figure 4. Only about 1% of land mass is covered.

The oldest and most prolific effort is that of Ondřejov Observatory in the Czech Republic, which first captured photographic records of the Příbram meteorite fall in 1959, using rotating shutters to create stop-motion records of the meteor in long exposures (Ceplecha, 1961). This event led to the establishment of the European Fireball Network, which recorded numerous meteorite falls, but no meteorites were recovered until the 2002 fall of Neuschwannstein (Spurný et al., 2003). It proved difficult to find meteorites from recorded falls in dedicated searches. The recovery of Neuschwannstein was made after more people learned about the trajectory calculations via social media. Only recently was it recognized that a meteorite fall near Ischgl, Austria, may have been recorded by this network in 1970 (Gritsevich et al., 2024). Also, the Benešov meteorite fell in 1991 but was recovered only in 2011 after the strewnfield was recalculated and the search was concentrated on small fragments (Spurný, Haloda, et al., 2013). In the USA, the Prairie Network recovered one meteorite, Lost City, in 1970 (McCrosky et al., 1971), while the Canadian Meteorite Orbit and Recovery Project (MORP) recovered one meteorite, Innisfree, in 1977 (Halliday et al., 1978).

In 1992, Peekskill was the first meteorite fall to be documented by video cameras (Brown et al., 1994). Video cameras became prolific with the advent of cell phones, door cameras, and dash cams, and videos are now ubiquitously spread by social media, which has resulted in a larger fraction of falls being documented. More falls were recovered after visual observations were systematically collected via social media (Hankey et al., 2013) and it was found that Doppler weather radar data can confirm the survival of meteorites to the ground from those fireballs and narrow down their fall locations (Fries & Fries, 2010).

At the same time, the European Fireball Network cameras were improved (still based on photographic detection) and expanded to include four remote stations in the Nullarbor Desert of southern Australia. This Desert Fireball Network (Bland et al., 2011) was later updated using digital still cameras, operated by Curtin University, and has recently expanded into a Global Fireball Observatory (Devillepoix et al., 2020). The airburst over Chelyabinsk resulted in a new push in 2013, after which the FRIPON network was created (Colas et al., 2020), later expanded into Italy as PRISMA (Barghini et al., 2023). In recent years, Allsky7 (Hankey et al., 2023) and the Global Meteor Network (Vida, Segon, Gural, et al., 2021) greatly added to existing networks of dedicated video cameras such as CAMS (Jenniskens et al., 2011). On average, there

are now about 13 meteorite falls reported globally each year (e.g., lists maintained at websites <https://galactic-stone.com/pages/falls>, <https://karmaka.de/>, and other online reports), up from about 6 a year in the early 2000s.

### CRE Age and Meteorite Type

Once a meteorite is recovered and the fall documented by recording the fireball trajectory and lightcurve and by tracing the fall location of the meteorites, it is necessary to determine from which collision event it originated. For that reason, the meteorite is analyzed for the isotopic signature of noble gases and cosmogenic radionuclides to determine the time since the object became  $<2$  m in size, the CRE age. It is also necessary to determine the mineralogic group and petrologic type, oxygen isotopes, and organic signatures, in order to determine the meteorite type, as well as the original target's terrain collisional and thermal history (e.g., the Ar-Ar, K-Ar and U,Th-He ages), the level of brecciation and the presence of xenoliths, magnetic signatures, and the level of aqueous alteration. Information on bulk chemistry, the formation age, and circumstances that created the original parent body can also help identify the source. Methods are described in the citations to Table 2.

## RESULTS

The 75 documented meteorite falls published to date are listed in Table 2. A partial list of 55 published orbits is maintained at <https://www.meteoriteorbits.info/> (Meier, 2017). Details from 26 falls still remain to be published in scientific journals (marked by an asterisk in Table 2) and at least 26 are still awaiting some or all meteorite analyses. Preliminary results presented here were often derived from data provided to facilitate the meteorite searches, published online and in reports such as the Meteoritical Bulletin, unless otherwise indicated. Five meteorites reported in Table 2 still need their name (and classification) approved by the Nomenclature Committee. Some applications are pending, others have their analysis delayed by meteorite ownership disputes. The provisional names are given between brackets.

Table 2 tabulates the date of fall, name of the meteorite, type of meteorite, the camera network that collected the data, the peak visible magnitude of the fireball, the estimated initial mass, the apparent entry speed, the entry angle, the altitude of the peak brightness, and the orbital elements: the perihelion distance, the semi-major axis, and the inclination. Also given are the CRE age and a reference to publications from which this data was derived. Regarding the remaining orbital elements node ( $\Omega$ ) and argument of perihelion ( $\omega$ ),  $\Omega$  is a

function of the date and time of impact, while  $\omega$  is a strong function of  $q$  (for  $a > 1$  AU) due to the encounter geometry.

Table 3 provides a tally of the different meteorite types so far documented. The tally is compared to all meteorites listed as “falls” in the Meteoritical Bulletin. About 5% of ordinary chondrite falls have documented impact orbits. The fraction is significantly higher at 18% for CM chondrites because an effort was made to document rare meteorite types and because CM chondrites are probably less likely to survive terrestrial alteration if they are not recovered quickly after the fall, so very few CM chondrite falls were recovered before 2000. The fraction of iron meteorites is only 2% and perhaps underrepresented due to a lack of recent iron falls.

The number of orbits has doubled since the review of Jenniskens (2018). Some patterns are now emerging from the distribution of semi-major axis and inclination for each meteorite type. Those will be examined now, starting with the group that has the lowest mean CRE age.

Figure 5 (left panel) shows the orbital elements of impacting CM2 carbonaceous chondrites on a backdrop of the proper elements of small asteroids detected to date (gray). All have a short CRE age (Table 2). As a group, CM2 chondrites have young CRE ages  $\leq 8$  Ma (Figure 5, right panel; Meier et al., 2016). It is expected that they impact on orbits that still have the semi-major axis of their delivery resonance, even if they originated from larger asteroids in near-Earth orbit that are now decaying. All four CM2-type meteorites arrived on low  $i < 3^\circ$  orbits with a semi-major axis around  $a = 2.5$  AU. The two best studied cases are Maribo, with  $a = 2.43 \pm 0.12$  AU,  $i = 0.25 \pm 0.16^\circ$  (Borovička et al., 2019) and Winchcombe with  $a = 2.586 \pm 0.008$  AU,  $i = 0.460 \pm 0.014^\circ$  (King et al., 2022). Both have an inclination  $< 1^\circ$ . Note that Winchcombe arrived from slightly outside of the 3:1 resonance with Jupiter at 2.50 AU. It is possible that Winchcombe broke from a larger NEA that had evolved to near-Earth space via the 5:2 resonance, instead. The entry velocity of Winchcombe and Aguas Zarcas was about  $14 \text{ km s}^{-1}$ , in the range of other meteorite falls, while those of Sutter's Mill and Maribo were on the high side at  $28 \text{ km s}^{-1}$  (Table 2), so that the prevalence of low-inclination orbits is not due to a higher collision cross-section with Earth.

The carbonaceous chondrite with CM-affinity, but classified as C1-ungrouped, Flensburg arrived from a slightly higher inclined orbit with a semi-major axis in the 5:2 mean-motion resonance ( $a = 2.82 \pm 0.03$  AU,  $i = 6.82 \pm 0.06^\circ$ ). Flensburg has one of the shortest CRE ages measured to date: around 5000 years (Bischoff et al., 2021). The 5:2 resonance is capable of rapid delivery of meteorites to Earth (Nesvorný et al., 2009), but it is likely that Flensburg broke from a larger asteroid

TABLE 2. List of meteorite falls with instrumentally recorded trajectories and orbits.

#	Fall date (UT)	Name ( $\theta$ ) = provisional	Type	Mv (mag)	M (kg)	$V_{\infty}$ (km s <sup>-1</sup> )	$h$ (°)	$H$ (km)	$q$ (AU)	$a$ (AU)	$i$ (°)	CRE (Ma)	Network	Ref.
75	2024-03-13	Takapō <sup>a</sup>	L5	-10	1	18.8	40	33	0.674	0.870	28.9	—	GM/CA/A7	[75]
74	2024-01-21	Ribbeck	Aubrite	-14	140	15.2	76	35	0.835	1.336	7.29	70	A/EN/A7/F	[74]
73	2023-12-29	La Posa Plain <sup>a</sup>	LL3-6	-10.4	—	13.5	51	30	0.859	1.173	3.6	—	GF/GM/A7/NA/V	[73]
72	2023-12-23	Raja <sup>a</sup>	EH3	-9	—	12.7	59	46	0.982	1.61	6.3	—	GF	[72]
71	2023-09-09	(Ménétréol-sur-Sauldre) <sup>a</sup>	H5	-10.5	—	17.2	40	32	0.86	2.58	0.0	—	F	[71]
70	2023-04-25	Elmshorn <sup>a</sup>	H3-6	-14	180	20.0	80	—	0.89	2.5	19.4	18.5	A7	[70]
69	2023-02-14	Matera <sup>a</sup>	H5	-11.1	10	16.3	57	33	0.966	2.10	14.5	—	PR	[69]
68	2023-02-13	Saint-Pierre-Le-Viger	L5-6	-17	780	14.0	49	27	0.918	1.685	3.56	30	A/V/GM/F/A7/EN/ GF	[68]
67	2023-01-20	Mvskoke Merkv <sup>a</sup>	L6	-14	—	13.2	32	26	0.977	1.61	7.7	—	V	[67]
66	2022-12-15	Tanxi <sup>a</sup>	H6	-13	—	13.5	70	28	0.984	2.39	2.0	—	V	[66]
65	2022-09-26	Junction City <sup>a</sup>	L5	-12	25	16.7	71	—	0.841	1.80	6.4	—	A7/NA	[65]
64	2022-08-13	Great Salt Lake <sup>a</sup>	H5	-16	—	21.2	27	26	0.753	2.5	1.0	—	V	[64]
63	2022-06-25	Pusté Ulany <sup>a</sup>	H5	-13.5	50	19.8	57	28	1.009	1.70	27.2	4	EN/A7	[63]
62	2022-03-08	Al-Khadhaf <sup>a</sup>	H5-6	-9	0.6	14.0	69	—	0.946	1.72	4.4	—	GF	[62]
61	2021-10-04	Golden	L/LL5	-12.3	70	17.9	54	31	1.000	1.58	23.5	25	GF/V/SN/GM	[61]
60	2021-08-06	Taghzout <sup>a</sup>	H5	-10	—	17.1	29	—	0.878	2.216	3.8	—	GF/SM	[60]
59	2021-07-15	Antonin	L4-5	-15	75	17.7	53	25	0.869	1.127	24.2	7.3 <sup>b</sup>	EN	[59]
58	2021-04-01	(Kybo-Lintos) <sup>a</sup>	H4/5	-12	—	25.4	64	—	0.595	2.597	0.36	—	DF	[58]
57	2021-02-28	Winchcombe	CM2	-10.5	12.5	13.6	42	34	0.987	2.586	0.46	0.3	GF/GM/A7	[57]
56	2021-01-18	Traspena	L5	-17	2600	16.4	77	29	0.691	1.125	4.6	—	USC/V/SP	[56]
55	2020-11-19	Kindberg <sup>a</sup>	L6	-12	270	14.1	17	42	0.951	2.02	5.9	—	EN/A7/F	[55]
54	2020-11-07	(Adalen)	Iron	-17.5	8500	17.4	70	—	0.893	1.90	15.2	—	FF/NO/USG	[54]
53	2020-08-19	Santa Filomena	H5-6	-16	—	16.3	43	—	0.945	2.10	0.15	—	V/BR	[53]
52	2020-07-01	Narashino <sup>a</sup>	H5	-18	6900	14.1	36	23	0.865	1.44	7.8	40	SC	[52]
51	2020-06-19	Madura Cave	L/LL5	-13	64	14.0	58	24	0.599	0.889	0.12	—	DF	[51]
50	2020-05-08	Tiros <sup>a</sup>	How.	-15	240	15.4	16	41	0.957	2.24	8.1	—	V	[50]
49	2020-02-28	Novo Mesto	L5	-16	470	22.1	48	35	0.568	1.451	8.76	—	V/USG	[49]
48	2020-01-01	Cavezzo	L5-an.	-9.5	3.5	12.8	68	33	0.983	1.82	4.0	—	PR	[48]
47	2019-11-18	Puli Ikariguru <sup>a</sup>	H5	-11	—	17.9	33	—	0.988	2.76	19.4	—	DF	[47]
46	2019-09-12	Fiensburg	C1 ung.	-20.7	15 k	19.4	65	41	0.843	2.82	6.82	0.005	A7/V/USG	[46]
45	2019-06-01	Arpu Kuilpu	H5	-9	2.2	17.6	50	—	0.905	2.75	2.0	7	DF	[45]
44	2019-04-24	Aguas Zarcas	CM2	-12.5	300	14.2	81	25	0.983	2.62	1.4	2.1	V	[44]
43	2019-02-01	Vinales	L6	-22	—	16.6	35	22	0.826	1.17	8.8	9.4 <sup>b</sup>	V/USG	[43]
42	2018-07-10	Renchen <sup>a</sup>	L5-6	-13.4	17	18.6	78	28	0.952	1.49	24.0	42	EN	[42]
41	2018-06-21	Ozerki	L6	-20.7	9.4 k <sup>c</sup>	14.9	78	27	0.673	0.84	18.4	1.2	V/USG	[41]
40	2018-06-02	Motopi Pan	How.	-23.2	5700	17.0	25	28	0.782	1.376	4.30	23	A/V/USG	[40]

TABLE 2. *Continued.* List of meteorite falls with instrumentally recorded trajectories and orbits.

#	Fall date (UT)	Name ( $\emptyset$ ) = provisional	Type	Mv (mag)	M (kg)	$V_{\infty}$ (km s <sup>-1</sup> )	$h$ (°)	$H$ (km)	$q$ (AU)	$a$ (AU)	$i$ (°)	CRE (Ma)	Network	Ref.
39	2018-01-17	Hamburg	H4	-16.3	140	15.8	66	—	0.926	2.73	0.60	12	V	[39]
38	2017-09-05	(Crawford Bay) <sup>a</sup>	H6	-15.2	—	16.2	28	36	0.922	2.68	1.4	—	V/USG	[38]
37	2016-10-31	Dingle Dell	L/LL6	-14	140	15.4	39	36	0.923	2.254	4.05	8.6	DF	[37]
36	2016-06-02	Dishchi' bikoh	LL7	-15.9	1050	16.3	46	27	0.897	1.129	21.2	11	CA/SN/V/USG	[36]
35	2016-05-17	Hradec Králové <sup>a</sup>	LL5	-11.5	90	13.3	47	31	1.011	1.75	8.5	—	EN/V	[35]
34	2016-03-06	Stubenberg <sup>a</sup>	LL6	-15.5	600	13.9	70	22	0.924	1.525	2.07	36	EN	[34]
33	2016-02-06	Ejby	H5/6	-14.0	120	14.5	62	31	0.968	2.81	0.96	83	V/EN	[33]
32	2016-01-24	Oseola <sup>a</sup>	L6	-16	>1.8 k	13.8	43	—	0.980	1.49	13.2	18 <sup>b</sup>	V	[32]
31	2015-11-27	Murrili	H5	-12	38	13.7	69	28	0.985	2.521	3.32	6.6	DF	[31]
30	2015-10-24	Creston	L6	-12	50	16.0	51	25	0.767	1.300	4.2	45 <sup>b</sup>	DF/SN/CA/V	[30]
29	2015-09-02	Sarıççek	How.	-16.8	1700	17.3	53	27	1.009	1.44	22.6	22	V/USG	[29]
28	2015-01-09	Porangaba	L4	-16	—	16.9	29	—	0.914	2.54	8.6	—	V/USG	[28]
27	2014-12-09	Žďár nad Sázavou	L3.9	-15.3	170	21.9	26	37	0.672	2.093	2.8	25	EN/AM	[27]
26	2014-04-19	Annama	H5	-18.3	470	24.2	30	35	0.634	1.99	14.7	30	FF/V	[26]
25	2013-07-31	(Benghazi Dam) <sup>a</sup>	H5	-19	7900	15.3 <sup>d</sup>	44	29	0.984	(2.8) <sup>a</sup>	2.3	—	DF/USG	[25]
24	2013-02-15	Chelyabinsk	L/LL5	-27.5	1.2e7	19.2	18	30	0.739	1.76	4.9	1.2	V/USG	[24]
23	2012-10-18	Novato	L6	-13.8	80	13.7	19	36	0.988	2.09	5.5	9 <sup>b</sup>	CA	[23]
22	2012-04-22	Sutter's Mill	CM2	-18.3	50 k	28.6	26	48	0.456	2.59	2.4	0.05	V	[22]
21	2011-02-04	Křiževci	H6	-13.7	63	18.2	65	31	0.740	1.544	0.64	—	CM/AN/EN	[21]
20	2010-04-15	Miffin <sup>a</sup>	L5	-17	1000	13.7	14	28	0.866	1.34	1.2	25	V	[20]
19	2010-04-13	Mason Gully	H5	-9.4	40	14.6	54	36	0.982	2.470	0.8	14	DF	[19]
18	2010-02-28	Košice	H5	-18	3.5 k	15.0	60	36	0.957	2.71	2.0	6	V/EN/USG	[18]
17	2009-09-26	Grimsby	H5	-14.8	33	20.9	55	39	0.982	2.04	28.1	35	SO	[17]
16	2009-04-09	Jesenice	L6	-15	170	13.8	59	26	0.997	1.75	9.6	1.6, 17	EN/AN	[16]
15	2009-01-17	Maribo	CM2	-19.7	2000	28.3	31	37	0.475	2.43	0.3	0.8	V/SK/DM/EN	[15]
14	2008-11-21	Buzzard Coulee <sup>a</sup>	H4	-20	15 k	18.6	67	34	0.961	1.25	25.0	6	V/USG	[14]
13	2008-10-07	Almahata Sitta	Ur	-19.7	83 k	12.4	19	38	0.900	1.308	2.54	19.5	A/USG	[13]
12	2007-07-20	Bunburra Rockhole	Eu,ann	-9.6	22	13.4	31	36	0.646	0.853	8.9	22	DF	[12]
11	2004-01-04	Villalbeto de la Peña	L6	-18	760	16.9	29	28	0.860	2.3	0.0	48 <sup>b</sup>	V	[11]
10	2003-03-27	Park Forest	L5	-21.7	11 k	19.5	61	29	0.811	2.53	3.2	17 <sup>b</sup>	V/USG	[10]
9	2002-04-06	Neuschwanstein	EL6	-17.2	300	21.0	50	21	0.793	2.40	11.4	48	EN	[9]
8	2000-05-06	Morávka	H5	-20.0	1500	22.5	20	33	0.982	1.85	32.2	6.7	V/USG	[8]
7	2000-01-18	Tagish Lake	C2 ung	-22	75 k	15.8	18	34	0.884	1.98	2.0	7.8	V/USG	[7]
6	1992-10-09	Peekskill	H6	-16	5000	14.7	3	42	0.886	1.49	4.9	32	V	[6]
5	1991-05-07	Benešov	LL3.5, H5	-19.5	4100	21.3	81	24	0.925	2.483	24.0	11	EN	[5]
4	1977-02-06	Innisfree	L/LL5	-12.1	42	14.7	68	36	0.986	1.872	12.3	26	MO	[4]

TABLE 2. *Continued.* List of meteorite falls with instrumentally recorded trajectories and orbits.

Fall date (UT)	Name $\theta =$ provisional	Mv (mag)	M (kg)	$V_\infty$ (km s <sup>-1</sup> )	$h$ (°)	$H$ (km)	$q$ (AU)	$a$ (AU)	$i$ (°)	CRE (Ma)	Network	Ref.
3 1970-11-24	Ischgl	-15	130	21.3	19	—	0.907	1.223	31.6	1.7	EN	[3]
2 1970-01-04	Lost City	-11.6	165	14.1	38	32	0.967	1.66	12.0	7.0	PN	[2]
1 1959-04-07	Příbram	-19.2	1300	20.9	43	46	0.790	2.401	10.5	17	EN	[1]

*Note:* Mv is the peak absolute visual magnitude (from 100 km distance),  $V_\infty$  the apparent entry speed,  $h$  the entry angle measured from the horizontal,  $H$  the altitude of peak brightness,  $q$  the perihelion distance,  $a$  the semi-major axis,  $i$  the inclination of the impact orbit, and CRE the cosmic ray exposure age. Networks are listed that contributed imaging and photometry to the trajectory and light curve data, including data not used for analysis. Meteorite provisional names are given between brackets. Camera networks: V = video and still photographs from cameras not typically used for meteor observations, A = Asteroid, A7 = Allsky7, AM = AMOS, AN = Alpe-Adria All-sky Network, BR = BRAMON, CA = CAMS, CM = CMIN, DF = DFN, DM = DMS, F = FRIPON; FF = Finnish Fireball Network; GF = GFO, GM = GMN, MO = MORP, NA = NASA Allsky Fireball Network, NO = Norsk Meteor Network, PR = Prisma, SC = Sonotaco, SK = SKIYMET meteor radar, SM = Spanish Southwestern Europe Meteor Network, SN = Spalding Allsky Camera Network, SO = SOMN, SP = SPMN, USC = Universidade de Santiago de Compostela, USG = United State Government satellite network. References: [1] Ceplecha (1961), Bagolia et al. (1980), Spurný et al. (2003), Meier et al. (2022); [2] McCrosky et al. (1971), Ceplecha (1996), Ceplecha and ReVelle (2005), Bogard et al. (1971), Graf and Marri (1995); [3] Gritsevich et al. (2024); [4] Halliday et al. (1978), Halliday et al. (1996), Ceplecha and ReVelle (2005); [5] Spurný (1994), Spurný, Haloda, et al. (2013), Ceplecha and ReVelle (2005), Spurný et al. (2014), Meier et al. (2019); [6] Brown et al. (1994), Graf et al. (1997); [7] Brown et al. (2000), Hildebrand et al. (2006); [8] Borovička, Spurný, et al. (2003) and Borovička, Weber, et al. (2003); [9] Spurný et al. (2003), Oberst et al. (2004); [10] Brown et al. (2004), Meier et al. (2017); [11] Llorea et al. (2005), Trigo-Rodríguez et al. (2006); [12] Bland et al. (2009), Spurný, Bland, Shrubny, et al. (2012), Welten et al. (2012); [13] Jenniskens et al. (2012), Kozubal et al. (2011), Farnocchia et al. (2017), Riebe et al. (2017); [14] Milley (2010), Milley et al. (2010), Meier et al. (2019); [15] Haack et al. (2010, 2012), Jenniskens et al. (2012), Zolqdek et al. (2013), Spurný, Borovička, et al. (2015), Borovička et al. (2019); [16] Spurný et al. (2010), Welten et al. (2016); [17] Brown et al. (2011), Cartwright et al. (2011); [18] Borovička, Toth, et al. (2013), Ozdín et al. (2015); [19] Spurný et al. (2011); Spurný, Bland, Borovička, et al. (2012), Meier et al. (2019); [20] Kita et al. (2013), and this work; [21] Borovička, Spurný, Segon, et al. (2015); [22] Jenniskens et al. (2012), Nishiizumi et al. (2014); [23] Jenniskens et al. (2014); [24] Borovička, Spurný, et al. (2013); [25] Devillepoix (2022), and this work; [26] Trigo-Rodríguez et al. (2015); [27] Spurný et al. (2016, 2020); [28] Ferus et al. (2020); [29] Unsalan et al. (2019); [30] Jenniskens et al. (2019); [31] Bland et al. (2016), Sansom et al. (2020), Townner et al. (2022); [32] Meier et al. (2020); [33] Spurný et al. (2017); [34] Spurný et al. (2016), Welten and Caffee (2024); [35] Spurný et al. (2019), Borovička et al. (2020), and this work; [36] Jenniskens et al. (2020); [37] Devillepoix et al. (2018); [38] Hildebrand et al. (2018), Jenniskens et al. (2018), and this work; [39] Brown et al. (2019); [40] Jenniskens et al. (2021); [41] Shrubny et al. (2022), Kartashova et al. (2020), Smith et al. (2021), Spurný et al. (2019), Borovička et al. (2020), Shrubny et al. (2022); [43] Zuluaga et al. (2019), Ceballos et al. (2021), and this work; [44] Garvie (2021), Kerraouch et al. (2022), Jenniskens et al. (2024), Dionnet et al. (2022); [45] Shober et al. (2022), Anderson et al. (2021), Heinlein et al. (2020); [47] Devillepoix (2020), and this work; [48] Gardiol et al. (2021), Pratesi et al. (2021); [49] Vida, Segon, et al. (2021), Gardiol et al. (2021), Zurita et al. (2020), and this work; [50] Zurita (2020), Zurita et al. (2020), and this work; [51] Devillepoix et al. (2022); [52] Kanamori (2020), Yamaguchi et al. (2020), Takenouchi et al. (2021), Okazaki et al. (2023); [53] Moutinho et al. (2020), Tosi et al. (2023); [54] Kyrylenko et al. (2022), Shrubny et al. (2022); [55] Spurný (2020), Ferrière et al. (2022); [56] Andrade et al. (2022); [57] King et al. (2022), McMullan et al. (2024); [58] Anderson et al. (2022), and this work; [59] Bischoff et al. (2022), Shrubny et al. (2022), Kóvágó (2021), Krzesinska et al. (2024), and this work; [60] Chennaoui-Aoudjehane, Agee and Devillepoix (2024), Chennaoui-Aoudjehane and Ross (2024), Chennaoui-Aoudjehane, Agee and Ziegler (2024), Guennou et al. (2024); [61] Brown et al. (2023); [62] Zappatini et al. (2022), Zappatini, Hofmann, et al. (2024); [63] Spurný et al. (2022), Ozdín et al. (2024), and this work; [64] Karner et al. (2022), and this work; [65] Branch et al. (2022), Hankey and Branch (2025); [66] Li et al. (2025), and this work; [67] Distel et al. (2023), and this work; [68] Zande et al. (2023), Bischoff et al. (2023); [69] Barghini et al. (2023), Barghini et al. (2024); [70] Heinlein et al. (2024), Möller and Knöfel (2023), Bischoff, Patzek, Alostius, et al. (2024) and Bischoff, Patzek, Barrat, et al. (2024), Hankey Bischoff, Patzek, Barrat, et al. (2024); [71] Anier (2023), Colas (2023); [72] Zappatini et al. (2024b); [73] Devillepoix (2024), Matson et al. (2024), and this work; [74] Spurný et al. (2024a), Hamann et al. (2024), Bischoff, Patzek, Barrat, et al. (2024); [75] Scott et al. (2024), Palmer and Scott (2024).

<sup>a</sup>Preliminary results, unpublished in journals.

<sup>b</sup>Has 468 Ma Ar-Ar age resetting age.

<sup>c</sup>Nominal reported value (<https://eneos.jpl.nasa.gov/fireballs/>) for entry speed  $V_\infty = 17.8$  km s<sup>-1</sup>, here lowered to 15.3 km s<sup>-1</sup> to arrive at a semi-major axis in the 5:2 mean-motion resonance.

<sup>d</sup>For adjusted luminous efficiency of 2%.

TABLE 3. Tally of documented meteorite falls by type. The last columns give the most likely corresponding asteroid taxonomic classes for the reflection spectra of freshly fallen meteorites and those of space-weathered asteroids.

Type	2018	2024	All falls <sup>a</sup>	Asteroid taxonomy class (Tholen/Bus-DeMeo)	
				Fresh	Space- weathered
Ordinary chondrites					
H	14	28	410	Q	S/Sr
L	8	20	469	Q	S
LL	5	6	113	Q	S/Sq
L/LL	2	5	—	Q	S
LL, H Mix	0	1	1	Q	S
H/L	0	0	—	Q	S
K	0	0	1	K	S, A/Sa
R	0	0	1	K	S, A/Sa
Carbonaceous chondrites					
CI	0	0	5	C, B	F, B, C, P, D/ Cb
CM	2	4	22	C, X/ Xc	C, P, D/Ch, Cgh
C1 ung	0	1	1	C, X	X, P
C2 ung	1	1	6	P	T, D
C3 ung	0	0	1	C/X	C/K
CR	0	0	3	L, Xk	L
CB/CH	0	0	1	X/Xc	X, B/Xk
CO	0	0	7	K, L	S/K, L, Xk
CV	0	0	8	K, L	S/K, L, Xk
CK	0	0	2	K	S/K, L
CL	0	0	0	K	S/K, L
Basaltic achondrites					
Howardite (HED)	1	3	20	V	V/Sv
Eucrite (HED)	1	1	40	V	V/Sv
Diogenite (HED)	0	0	12	V	V/Sv
Enstatite chondrites and achondrites					
EH	0	1	9	E/Xc, Xe	E, M/L, Xc, Xe
EL	1	1	8	E/Xe	E, M/L, Xe
Aubrite	0	1	12	E/Xe	E/Xe
Ureilites					
Ureilite	1	1	6	F	L
Primitive achondrites					
Acapulcoite/ Lodranite	0	0	2	Q	S, R
Angrites	0	0	1	A, S	A, S/Sr
Brachinites	0	0	0	A	A/Sa
Winonaites	0	0	1	Q/L	S
Irons and stony-irons					
Iron	0	1	49	M/Xk	D/Xk
Mesosiderites	0	0	7	M, Q	M, S
Pallasites	0	0	4	A/L	A, S/L, Sa

Note: For lack of one-on-one asteroid and meteorite classifications, see e.g. DeMeo et al. (2015) and Burbine et al. (2024).

<sup>a</sup>Current tally of observed falls published in the Meteoritical Bulletin.

that already had evolved in the 5:2 resonance to cross the Earth's orbit (Jenniskens et al., 2012; Scott & Herzog, 2021; Shober et al., 2024).

C2-ungrouped meteorite Tagish Lake ( $a = 1.98 \pm 0.20$  AU,  $i = 2.0 \pm 0.9^\circ$ ) was delivered by the  $v_6$  resonance instead (Brown et al., 2000). It has a CRE age of  $\sim 7.8$  Ma years (Brandon et al., 2005), older than most CM2-type carbonaceous chondrites (Figure 5) and old enough for some interactions with the terrestrial planets to have modified its semi-major axis and inclination.

In recent years, there have been some CO and CV meteorite falls, but none were documented. Those include a nighttime fall at Boorama in Somalia on 3 December 2023 (CO3), a daytime fall at Moss in Norway on 14 July 2006 (CO3.6), and a nighttime fall at Bukhara in Uzbekistan on 9 July 2001 (CV3).

Figure 6 shows the distribution of orbital elements for H-type ordinary chondrites. The population of H chondrites has a dominant CRE age peak at  $7.1 \pm 0.1$  Ma ("A" in Figure 6, right panel). The meteorites for which such CRE age  $\sim 7$  Ma was measured are shown as open circles in the left panel of Figure 6. The 7 Ma peak has a full width at half-maximum (FWHM) of  $2.0 \pm 0.1$  Ma. Several other peaks are present too at  $12.0 \pm 0.5$  Ma ("C"),  $23.0 \pm 0.5$  Ma ("D"),  $33.5 \pm 0.5$  Ma ("E"), and about 42 Ma ("F"), with FWHM = 3, 5, 6, and  $\sim 7$  Ma, respectively, suggesting that the typical CRE age measurement has an uncertainty of about 18%. The 7 Ma peak is broader, suggesting that more than one collision event contributed to it. The relative integrated intensity of the peaks A, C–F is  $116 \pm 10$ ,  $9 \pm 2$ ,  $40 \pm 8$ ,  $24 \pm 5$ , and  $14 \pm 5$  meteorites, respectively. There is also an excess of H chondrites with short CRE ages  $< 5$  Ma ("B" in Figure 6).

Now more H chondrites have been tracked, a cluster of orbit solutions has emerged with low inclination and semi-major axis between the 3:1 and 5:2 mean-motion resonances. Three of the meteorites in that cluster also have the low CRE age of 7 Ma age (Košice, Murrili, and Arpu Kuilpu), pointing to one source of 7-Ma CRE age H chondrites being low in the Pristine Main Belt beyond the 5:2 resonance. Some others in this group have a CRE age that differs from  $\sim 7$  Ma.

Previously, the only two known cases with  $\sim 7$  Ma CRE age were Lost City ( $a = 1.66$  AU,  $i = 11.98^\circ$ , with unknown error bars) and Morávka ( $a = 1.85 \pm 0.07$  AU,  $i = 32.2 \pm 0.5^\circ$ ), both well observed, suggesting that a second source of 7-Ma H chondrites might be high in the asteroid belt (Jenniskens, 2018). This age is too young to explain both the short semi-major axis and high inclination by the normal dynamical evolution from a source at low- $i$  and high- $a$  in the pristine main belt (Figure 2). Now, we can add two more high-inclined H

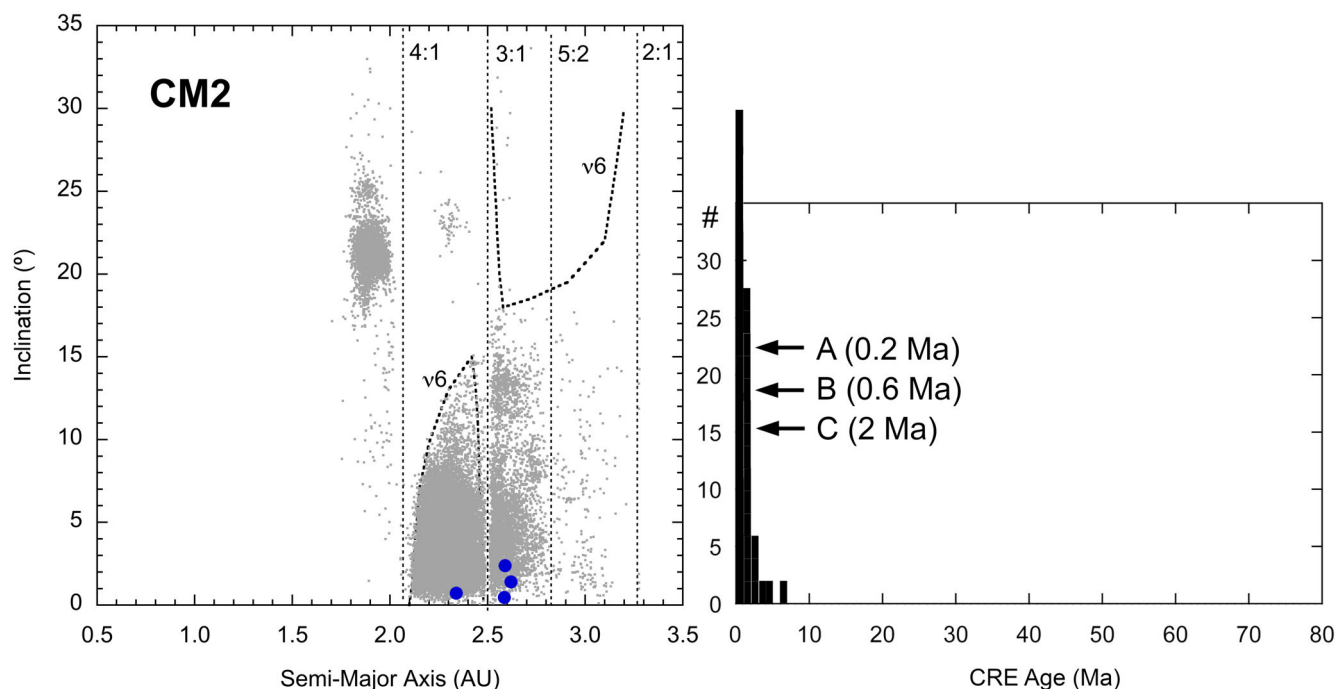


FIGURE 5. CM affinity carbonaceous chondrites. Left: Orbital elements of the impacting orbits on a gray background of proper elements of small asteroids. Right: CRE age distribution of CM2 carbonaceous chondrites with possible discrete collision events marked by letters, after Jenniskens (2018), updated with data from Zolensky et al. (2021).

chondrites with such short CRE ages: Mason Gully and Pusté Úlány.

There may be even more sources of H chondrites. H chondrites as a group have CRE ages up to 80 Ma (Figure 6). There is a peak around CRE age = 32 Ma (Graf & Marti, 1995), examples being the H5 Grimsby with a CRE age  $\sim 35$  Ma (Cartwright et al., 2011), the H5 Annama with a  $30 \pm 4$  Ma CRE age (Kohout et al., 2016), and the H6 Peekskill with a 32 Ma CRE age (Graf et al., 1997). The higher CRE age implies more time for interactions with the terrestrial planets, resulting in more evolved orbits. Grimsby has  $a = 2.04 \pm 0.05$  AU,  $i = 28.1 \pm 0.3^\circ$  (Brown et al., 2011). Annama has  $a = 1.99 \pm 0.12$  AU,  $i = 14.7 \pm 0.5^\circ$  (Trigo-Rodríguez et al., 2015). Peekskill has  $a = 1.49 \pm 0.03$  AU and  $i = 4.9 \pm 0.2^\circ$  (Brown et al., 1994). H5 Narashino has  $a = 1.44 \pm 0.13$ ,  $i = 7.8 \pm 2.1^\circ$  (Kanamori, 2020) and 40 Ma CRE age and may also belong to this group (Okazaki et al., 2023). It is possible that these were delivered via both the  $v_6$  and 3:1 resonances from a source in the Inner Main Belt. Other possible members with  $a \leq 2.05$  AU and  $i < 15^\circ$  are Kríževci ( $a = 1.54 \pm 0.01$  AU,  $i = 0.64 \pm 0.03^\circ$ ), Al-Khadaf ( $a = 1.72 \pm 0.02$ ,  $i = 4.36 \pm 0.06^\circ$ ), and Santa Filomena ( $a = 2.10 \pm 0.15$  AU,  $i = 0.15 \pm 0.05^\circ$ ). If so, these would be predicted to have a  $\sim 35$  Ma CRE age, but CRE ages are not available yet. The median inclination for this group (without outliers Annama and Grimsby) is

$4.4 \pm 3.2^\circ$ , but the source region is expected to be at lower inclination because the inclination dispersion is expected to increase over time. Two of these meteorites have inclinations near  $0^\circ$ . Because it is hard to lower the inclination below the source region, this suggests that the source of inner-main-belt H chondrites is near the ecliptic plane.

We examined if the different H chondrite source regions have different compositions or physical properties (e.g., Flynn et al., 2017) not caused by the meteoroids coming close to the Sun such as the  $^3\text{He}$  loss (Graf & Marti, 1995). Figure 7 shows the low-calcium pyroxene ferrosilite content (Fs, mole%) versus the olivine fayalite (Fa, mole%) content as listed in the meteoritical bulletin. In our sample, pristine main belt H chondrites have systematically lower Fs content for given Fa. If this is a common property of the two source regions, then the low-Fs meteorite Taghzout, with  $a = 2.22 \pm 0.01$  AU and low  $i = 3.80 \pm 0.01^\circ$  (Guennoun et al., 2024), may also belong to the pristine main belt H chondrite group.

Table 4 compiles the bulk elemental composition of the H chondrites for which such data has been published. For error bars, we refer to the original publications. The table does show subtle differences in the Fe content between the instrumentally observed Pristine Main Belt and Inner Main Belt H-chondrite elemental abundances in our sample, but more data is needed to be certain.

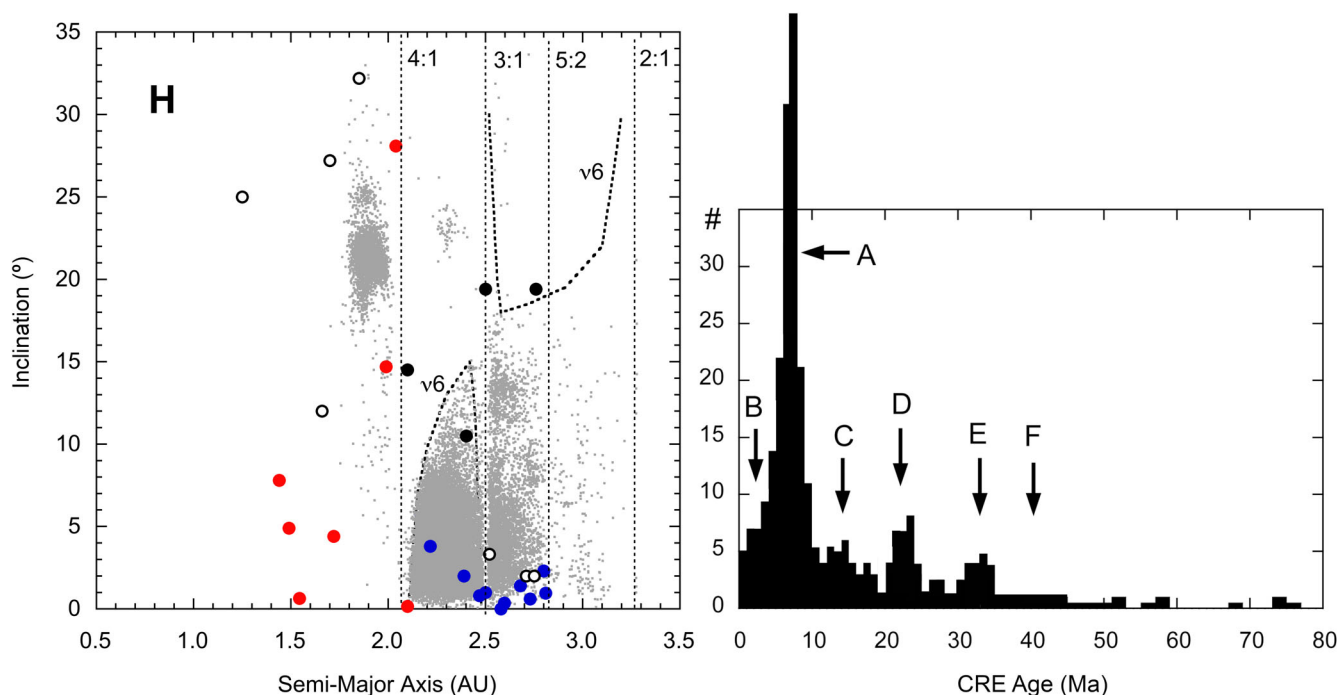


FIGURE 6. H affinity ordinary chondrites. Left: orbital elements of the impacting orbits on a gray background of proper elements of small asteroids. Open circles are meteorites with CRE ages of  $\sim 7$  Ma, including four that may have originated from a high-inclined source (black). H-chondrites that may have originated in the outer main belt are shown in blue, those from a low-inclination source in the inner main belt are in red, and others are in black. Right: CRE age distribution of H chondrites with possible discrete collision events marked by letters, after Jenniskens (2018) and updated with data from Herzog and Caffee (2014).

Figure 8 shows the same diagram as Figure 6 but for the LL-type ordinary chondrites. So far, LL chondrites arrived on mostly evolved short- $a$  ( $< 2$  AU) orbits, delivered via the  $\nu_6$  resonance from the inner main belt. The median value of the low inclination orbits is  $\langle i \rangle = 3.3 \pm 2.9^\circ$  ( $N = 4$ , including that of the recent LL chondrite fall at Haag, Austria; Spurný et al., 2024b). The population follows the expected behavior for a source low in the inner main belt (Figure 2). Orbits still close to the  $\nu_6$  resonance are missing due to a lack of LL chondrites with short CRE ages in our sample. The distribution shows peaks at 3, 8, 16, 29, and  $\sim 40$  Ma (Figure 8). The relative integrated intensity is  $N = \sim 5$ ,  $13 \pm 3$ ,  $19 \pm 4$ ,  $12 \pm 3$ , and  $< 5$  meteorites, respectively.

Figure 9 shows the same diagrams for L-type ordinary chondrites (excluding those typed as L/LL). The orbital elements are similarly widely distributed as H chondrites, but lack the cluster at high- $a$  and low- $i$  seen among H chondrites. The distribution shows the larger dispersion in inclination for a smaller semi-major axis expected for a source low in the inner main belt. Two L chondrites arrived while still in or near the 3:1 mean-motion resonance, but most appear to be delivered by the  $\nu_6$  resonance. The eccentricity decreases with a decreasing semi-major axis, intersecting the 2.1 AU semi-major axis

of the  $\nu_6$  resonance at the expected  $e = 0.52$  when orbits first reach Earth's orbit ( $q = 1.0$  AU). Even the two L chondrites in the 3:1 resonance fall along this trend and have higher eccentricity than expected for a new arrival from the 3:1 resonance. Orbits between the  $\nu_6$  and 3:1 resonance have median  $\langle i \rangle = 4.4 \pm 3.0^\circ$  ( $N = 6$ ). The source family of L chondrites is in a dense region, given the numerous peaks in the CRE distribution (Figure 9). The peaks are centered on about 2.5, 5.8, 10.5, 23.7, 28, and 39 Ma and have a relative integrated intensity of  $10 \pm 3$ ,  $17 \pm 4$ ,  $18 \pm 3$ ,  $25 \pm 4$ ,  $8 \pm 2$ , and  $24 \pm 5$  meteorites, respectively.

Unlike previous hints (Jenniskens et al., 2019), there is now no indication that shocked and un-shocked L chondrites have a different source family. Open symbols show the shocked meteorites with a 468-Ma Ar-Ar resetting age, corresponding to a high flux of L chondrites on Earth (Liao & Schmitz, 2023; Lindskog et al., 2017; Schmitz et al., 2019). They scatter among the other L chondrites with no clear distinction in  $a$  or  $i$ , also being delivered from both the 3:1 and  $\nu_6$  resonances from a source low in the inner main belt. However, the shocked L-chondrites may originate from different collision events within that family: three have a CRE age of 7.3–9.4 Ma (two in highly evolved orbits), two have a CRE age of

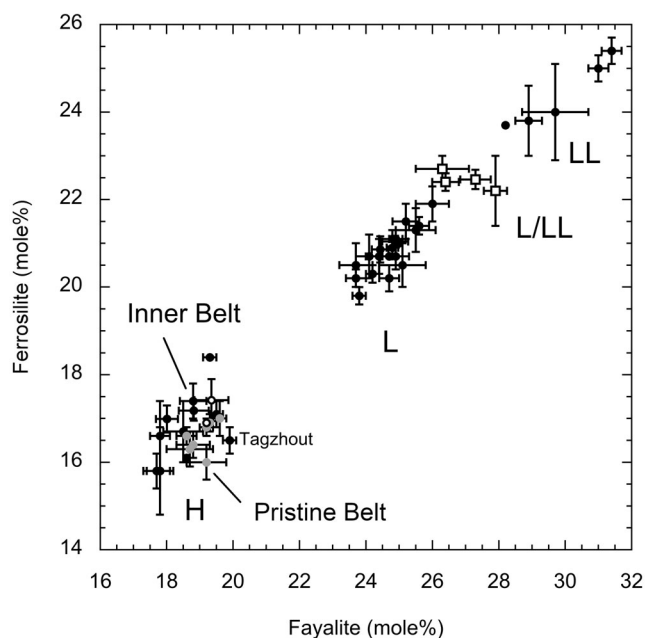


FIGURE 7. Ferrosilite versus Fayalite composition of ordinary chondrites from instrumented falls. Among H chondrites, meteorites that likely originate in the pristine main belt are gray solid circles, those in the inner main belt are black solid circles, while high- $i$  asteroids of  $\sim 7$  Ma CRE age are shown as open circles.

17–18 Ma, and two have a CRE age of 45–48 Ma. Note that these values do not necessarily coincide with the peaks in the overall L chondrite CRE age distribution.

Some ordinary chondrites fall in the LL domain but plot close to the L domain (open squares in Figure 7). These meteorites, classified as L/LL, scatter just above the high- $i$  upper edge of the LL-chondrite distribution in Figure 8, distributed more similar to that of L chondrites in Figure 9. However, the sample size is too small to be certain that this is a significant difference. The group follows the same trend as other inner main belt sources. The median value of the low inclination orbits is  $\langle i \rangle = 4.1 \pm 2.6^\circ$  ( $N = 3$ ). The Chelyabinsk impactor plots in this group, which at 20 m diameter (Popova et al., 2013) is about a factor of 20 larger than the typical meteoroids responsible for LL type meteorite falls. The Madura Cave meteorite with an unusual evolved low-inclined orbit also plots in this group but is classified as L. Given the wide dispersion of compositions, it is possible that the LL group has more than one component. Innisfree and Golden have CRE ages = 25–26 Ma and Dingle Dell has CRE age = 8.6 Ma, while the CRE age of Chelyabinsk is a young 1.2 Ma (Table 2).

The influence of Earth encounters on the orbit of meteorites is illustrated in Figure 10, which shows the distribution of perihelion distance ( $q$ ) versus semi-major axis ( $a$ ) for the three ordinary chondrite groups and

howardite–eucrite–diogenites (HED). Starting at  $0^\circ$  in steps of  $2^\circ$ , the inclination distribution of this sample is: 12, 12, 10, 3, 8, 1, 3, 2, 0, 3, 1, 2, 4m, 1, 2, 1, 1, and 0 meteorites. Those with high inclination  $i > 18^\circ$  are distributed along a thin arc that has  $q = 1$  AU at  $a = 1.5$ – $1.8$  AU and lower and higher values of  $q$  for higher and lower values of the semi-major axis, respectively (lower right diagram of Figure 10). In contrast, most known NEA follow the  $q = a(1-e)$  line for all  $a = 1.0$ – $2.8$  AU, as most are detected with  $q \sim 1.0$  AU (e.g., Granvik et al., 2018; figure 17 in Tosi et al., 2023).

As a group, LL and L chondrites show a very similar behavior as the L/LL chondrites (Figure 10, upper right and lower left diagrams). Again, L chondrites with the 468-Ma signature do the same, with no distinction in the distribution. The observed evolution to lower  $q$ , lower  $e$ , lower  $a$ , and on-average higher  $i$  is not linear in time; in particular, meteorites Antonin and Ozerki have evolved orbits but with a short CRE age. Three of the five meteorites with CRE age  $< 10$  Ma are in evolved (high  $i$  and low  $e$ ) orbits. The most “fresh out of the resonance” L-chondrite Novato ( $a \sim 2.0$  AU,  $e \sim 0.5$ ) has a 9 Ma CRE age and  $i = 5.5^\circ$ .

Again, the cluster of low- $i$  and high- $a$  H-chondrites stands out (marked in blue in the upper left diagram of Figure 10). The cluster shows a trend of more dispersed  $q$  with lower semi-major axis away from the 5:2 mean-motion resonance. We interpret this to mean that the delivery resonance to a near-Earth orbit is likely the 5:2 mean-motion resonance, but subsequent close encounters with Earth lowered the semi-major axis. For the dominant delivery resonance to be the 5:2 resonance, the source of these H chondrites is most likely at  $a \geq 2.82$  AU (at low inclination) in the pristine main belt or outer main belt. There are also some H chondrites with  $a \sim 2.5$  AU orbits and  $q \sim 1$  AU that perhaps suggest that there is an evolutionary pathway crossing the 5:2 resonance until capture in the 3:1 resonance without significant interactions with Earth. 3:1 is the more efficient pathway for meteoroid delivery to Earth.

Figure 11 shows the inclination as a function of eccentricity for the three ordinary chondrite groups. Dashed lines are the expected values of eccentricity that had the meteoroid come fresh out of the resonance and arrived at  $q = 1.0$  AU. Both pristine main belt ( $\bullet$ ) and inner main belt (gray solid dots) H-chondrites show mostly a steady increase of inclination for lower values of eccentricity. L and LL chondrites show the same, but more dispersed, perhaps due to a range of CRE ages. Annama has an unusually high eccentricity for an inner main belt H-chondrite, while Benešov has an unusually high inclination for LL chondrites.

TABLE 4. Bulk elemental compositions (wt%) of pristine main belt, central main belt, and inner main belt H-chondrites.

Element	Pristine Main Belt 7, 12 and 83 Ma				CMB 6 Ma	CMB 18 Ma	Inner Main Belt 35 Ma	
	Ejby [1]	Murrili [2]	Mason Gully [3]	Košice [4]	Morávka [5]	Elmshorn <sup>b</sup> [6]	Annama [7]	Peekskill <sup>c</sup> [8]
O	—	—	—	—	—	—	35.3	35.6
Na	0.67	—	0.66	0.60	0.58	0.60	0.74	—
Mg	15.0	14.2	14.3	13.8	16.2	12.6	13.5	14.2
Al	1.10	1.06	1.06	1.07	1.19	—	1.04	1.28
Si	—	—	—	16.5	18.1	—	18.5	18.5
K	0.095	0.10	0.09	0.09	—	0.100	0.080	—
Ca	1.28	1.20	1.16	1.14	1.45	1.08	1.32	1.16
Ti	0.062	0.058	0.047	0.060	0.077	0.058	0.055	0.058
Cr	0.31	—	—	0.35	0.38	0.36	—	—
Mn	0.26	0.20	0.24	0.23	0.26	0.24	0.223	—
Fe	28.7	28.7 <sup>a</sup>	28.6	28.9	24.0	31.7	27.8	27.3
Co	0.075	0.092 <sup>a</sup>	0.096	0.087	0.058	0.111	0.088	—
Ni	2.11	1.92 <sup>a</sup>	1.96	1.00	1.38	2.05	1.92	—

Note: References: [1] Haack et al. (2019), Bischoff, Patzek, Alosius, et al. (2024) and Bischoff, Patzek, Barrat, et al. (2024); [2] Anderson et al. (2022); [3] Dyl et al. (2016); [4] Ozdín et al. (2015); [5] Borovicka et al. (2003); [6] Bischoff, Patzek, Alosius, et al. (2024) and Bischoff, Patzek, Barrat, et al. (2024); [7] Kohout et al. (2016); [8] Graf et al. (1997).

<sup>a</sup>For assumed 15% FeNi fraction.

<sup>b</sup>Anomalous H3–6 breccia.

<sup>c</sup>Only stone fraction measured. Metal fraction assumed to contain 90 wt% Fe, 9.0 wt% Ni and 0.45 wt% Co, respectively (Wasson & Kallemeyn, 1988).

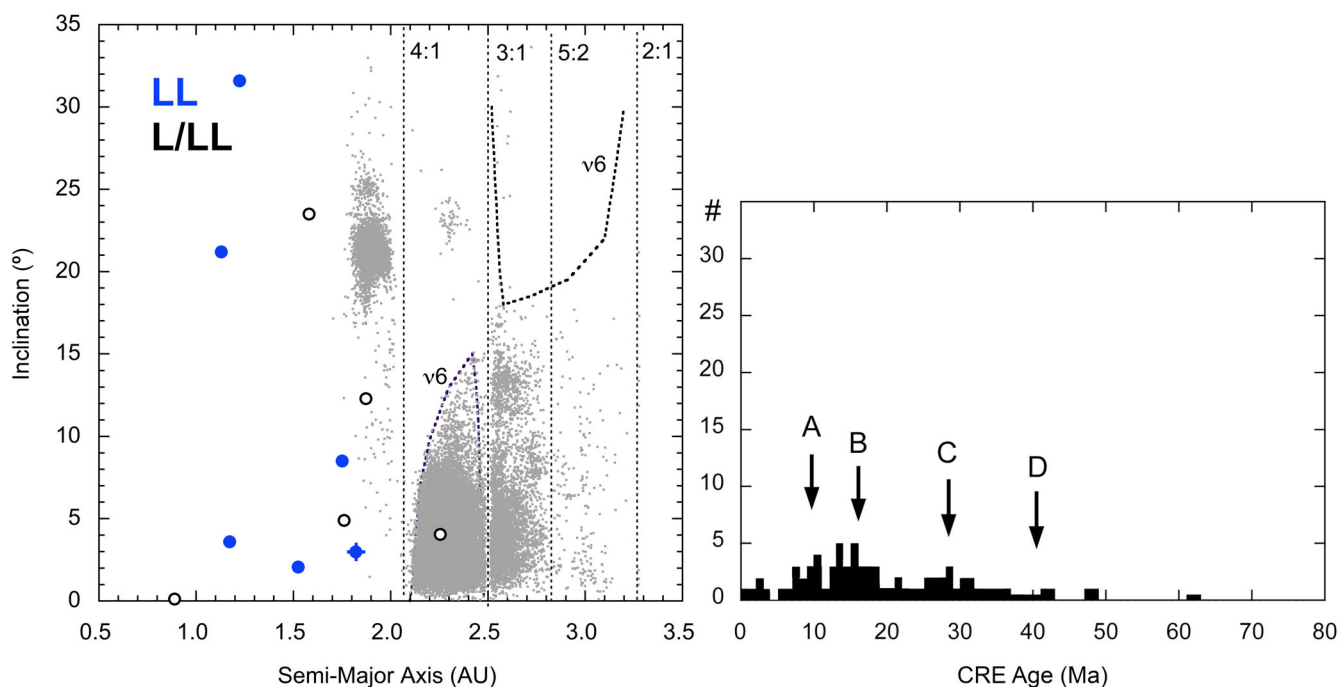


FIGURE 8. LL affinity ordinary chondrites. Left: orbital elements of the impacting orbits on a gray background of proper elements of small asteroids. The recent LL meteorite fall near Haag, Austria, is also plotted, marked by a cross. L/LL chondrites are shown as open circles. Right: CRE age distribution of LL chondrites with possible discrete collision events marked by letters, updated from Jenniskens (2018) with data from and David & Leya (2019).

Figure 12 shows the same diagrams as Figures 5, 6 and 9 for HED meteorites. HEDs are thought to have originated from Vesta or the Vesta family (McCord et al., 1970). In addition to two main-group howardites

with the common 22 Ma CRE-age (Sarıççek and Motopi Pan), also plotted are howardite Tiros and the preliminary results for the recent August 25, 2024 *Nqweba* (provisional name) fall in South Africa (Glass &

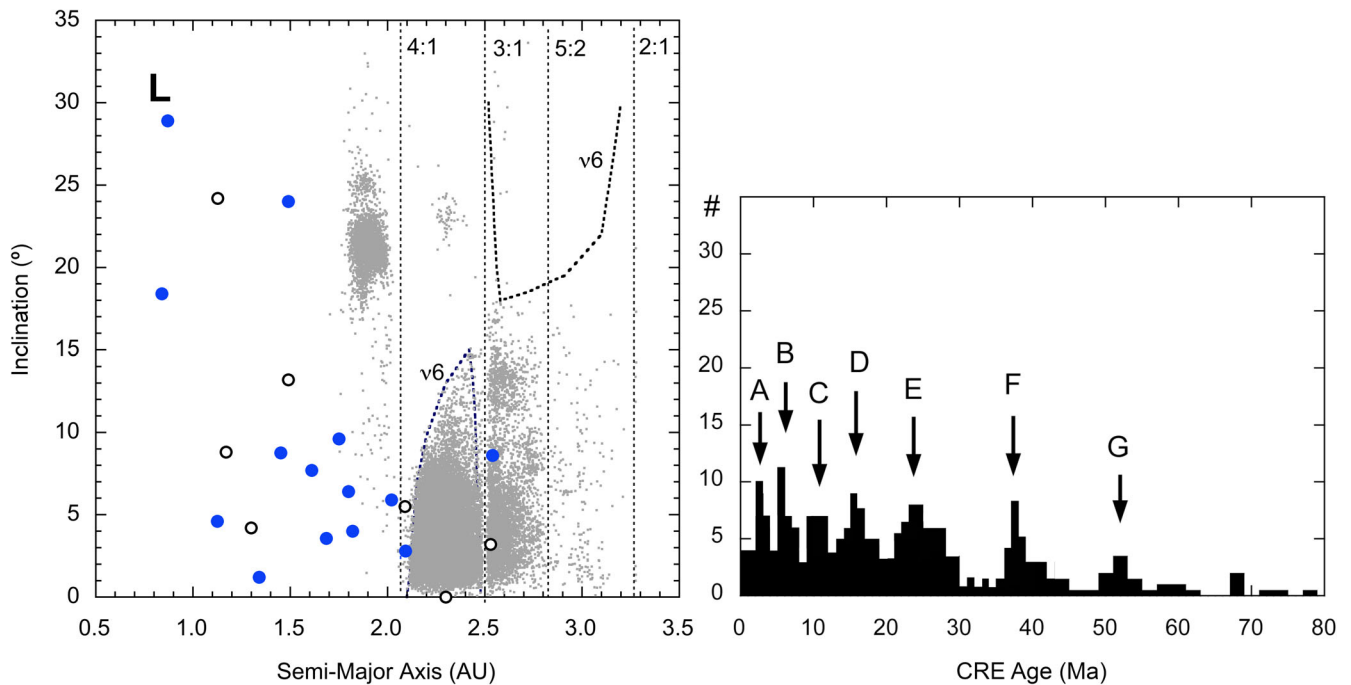


FIGURE 9. L type ordinary chondrites. Left: orbital elements of the impacting orbits on a gray background of proper elements of small asteroids. Right: CRE age distribution of L chondrites with possible discrete collision events marked by letters, after Jenniskens (2018) and updated with data from Herzog and Caffee (2014).

Cooper, 2024) based on the USG satellite data ( $a \sim 1.01$  AU,  $i \sim 9.0^\circ$ , and  $q \sim 0.45$  AU). In this case, the meteor entered at a shallow angle, so that the observed trajectory was long. Motopi Pan (asteroid 2018 LA:  $a = 1.3764 \pm 0.0001$  AU,  $i = 4.2974 \pm 0.0004^\circ$ ), Tiros ( $a \sim 2.24$  AU,  $i \sim 8.1^\circ$ ) and *Nqweba* arrived on a low-inclined orbit with an inclination similar to the  $7^\circ$  of Vesta. The orbits all have a short semi-major axis, and all but one have a low  $q < 0.79$  AU (shown by a symbol “+” in Figure 10). They follow the same evolutionary trend as L-chondrites, which have a similar median CRE age. This confirms that L-chondrites likely originate from the inner main belt. The small sample of orbits measured so far lacks high- $a$  orbits in part because most have the higher  $\sim 22$  Ma CRE age, but also because most likely originated from the  $v_6$  resonance rather than the 3:1 resonance.

The eucrite Bunburra Rockhole has unusual oxygen and chromium isotopic signatures (Benedix et al., 2017) that suggest it did not originate from Vesta. Surprisingly, the CRE age of 22 Ma is similar to that of other eucrites, and the bulk composition also suggests a large parent body, only slightly smaller than Vesta. The meteoroid arrived on an Aten type orbit ( $a = 0.8529 \pm 0.0004$  AU,  $i = 8.95 \pm 0.03^\circ$ ) and likely had its source in the inner main belt.

Several other meteorite types are represented now also (Table 3). An EL (Neuschwanstein) arrived from the 3:1 resonance ( $a = 2.40 \pm 0.02$  AU,  $i = 11.41 \pm 0.03^\circ$ ).

An EH (Raja) arrived from an evolved orbit ( $a = 1.61 \pm 0.09$  AU,  $i = 6.31 \pm 0.34^\circ$ ). In addition, one ureilite (meteorite Almahata Sitta, asteroid 2008 TC3) had  $a = 1.308205 \pm 0.000008$  AU and  $i = 2.54222 \pm 0.00004^\circ$ , and one aubrite (Ribbeck, asteroid 2024 BX1) arrived on an orbit with  $a = 1.33649 \pm 0.00002$  AU and  $i = 7.2931 \pm 0.0002^\circ$ . Finally, an iron meteorite *Ådalen* (provisional name) arrived on  $a = 1.90 \pm 0.03$  AU and  $i = 15.22 \pm 0.14^\circ$  (Table 2). All of these latter orbits have evolved away from their delivery resonance by close encounters with the terrestrial planets and suggest delivery from the inner main belt via the  $v_6$  resonance.

All impact orbits show a strong sinusoidal variation of perihelion distance  $q$  and argument of perihelion  $\omega$ , with  $q = 1.0$  AU orbits having  $\omega = 180^\circ$  (and  $0^\circ$ ). In that geometry, the other node is near aphelion and farthest from Earth’s orbit. H and CM chondrites suspected to have arrived from the pristine and outer main belt tend to cluster near  $\omega = 180^\circ$  and  $0^\circ$ . Orbits originating in the inner main belt favor  $\omega > 100^\circ$ , clustering near  $\omega = 220^\circ$ .

## DISCUSSION

### Meteoroid Sources

Some relevant information on the more likely asteroid family sources of our meteorites, and the large asteroids that are potential parent bodies, is summarized in Tables 5

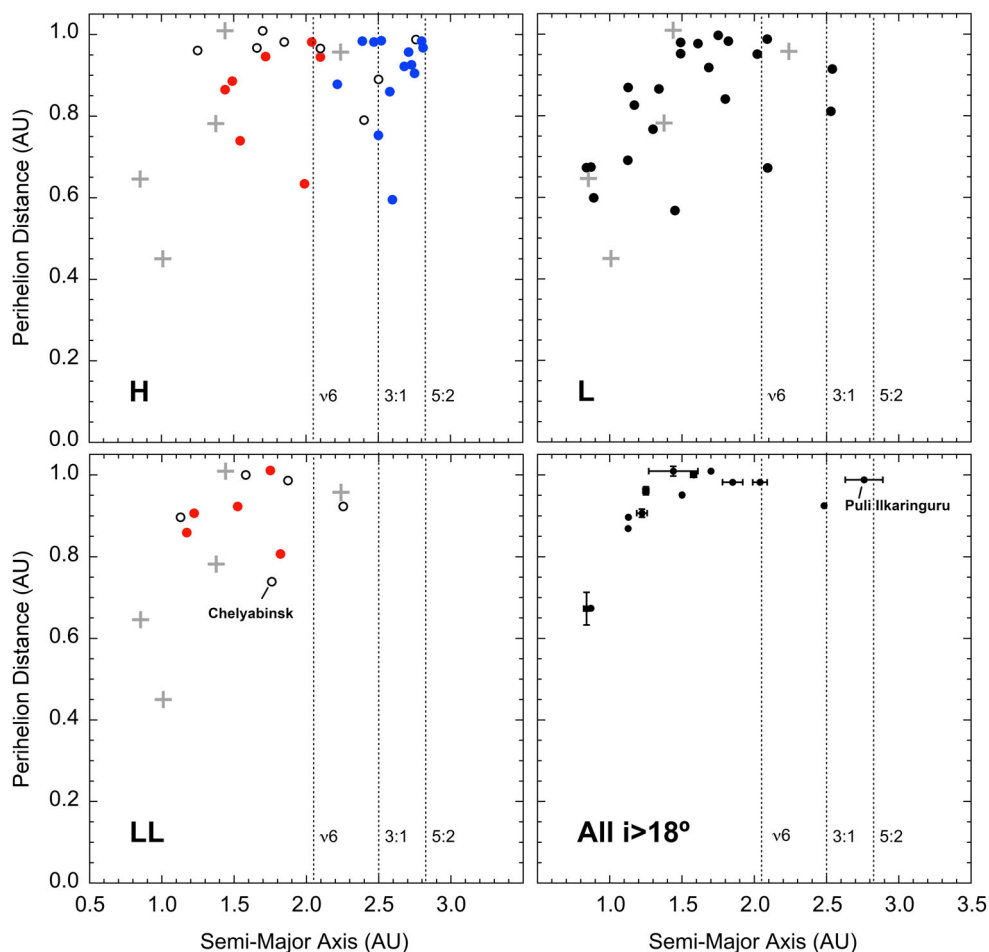


FIGURE 10. Perihelion distance as a function of semi-major axis of impact orbits for the three types of ordinary chondrites ( $\bullet$ ). In each diagram, also shown are the positions of HED meteorites (+, including *Nqweba*) that have a known source region in the inner main belt. Top left: H-chondrites that may have originated at Koronis are shown in blue, those from a low-inclination source in the inner main belt are in red. Others in open circles. Bottom left: LL chondrites in red, L/LL chondrites in open circles. Bottom right diagram includes all inner main belt chondrite classes and HED meteorites with inclination  $i > 18^\circ$ .

and 6. Table 5 includes most asteroid families in the inner main belt, some of the richer families in the central main belt, and the most abundant families in the pristine and outer main belt, as well as some young families with CRE ages of 1–100 Ma (Nesvorný et al., 2015, 2024). Table 5 gives the family's name, taxonomic class, and location in the asteroid belt. The geometric visible albedo ( $\langle p_v \rangle$ ) and size frequency distribution (SFD) slope are from Masiero et al. (2015), and ages are from Carruba and Nesvorný (2016) and Paolicchi et al. (2019), unless they were updated from more recent references cited. Table 6 lists all asteroids larger than about 200 km in diameter and some other large unusual asteroids, their location in the asteroid belt, their diameter, and their taxonomic class. In each table, the column “Meteorite Type” gives the inferred meteorite type based on asteroid taxonomic studies. In many cases, that information is still uncertain.

## H Ordinary Chondrites and the Koronis Family

Low-inclined H chondrites from the 7-Ma CRE age peak likely originate from a source low in the pristine or outer main belt beyond the 5:2 mean-motion resonance. As it happens, there is a known young debris field of S-class asteroids with H-type affinity (Lindsay et al., 2015) at low inclination just outside the 5:2 mean-motion resonance in the pristine main belt, called Koronis (brown in Figure 1), which was suggested as a source of H chondrites by Vernazza et al. (2014) from similarities in the shape of reflectance spectra and the young age of the family. Asteroid (243) Ida, visited by NASA's *Galileo* spacecraft in 1993, is part of the Koronis family. Koronis has a young cluster, called the Karin family, first identified by Nesvorný et al. (2002) with a dynamical age of  $5.8 \pm 0.2$  Ma, later refined to  $5.75 \pm 0.05$  Ma

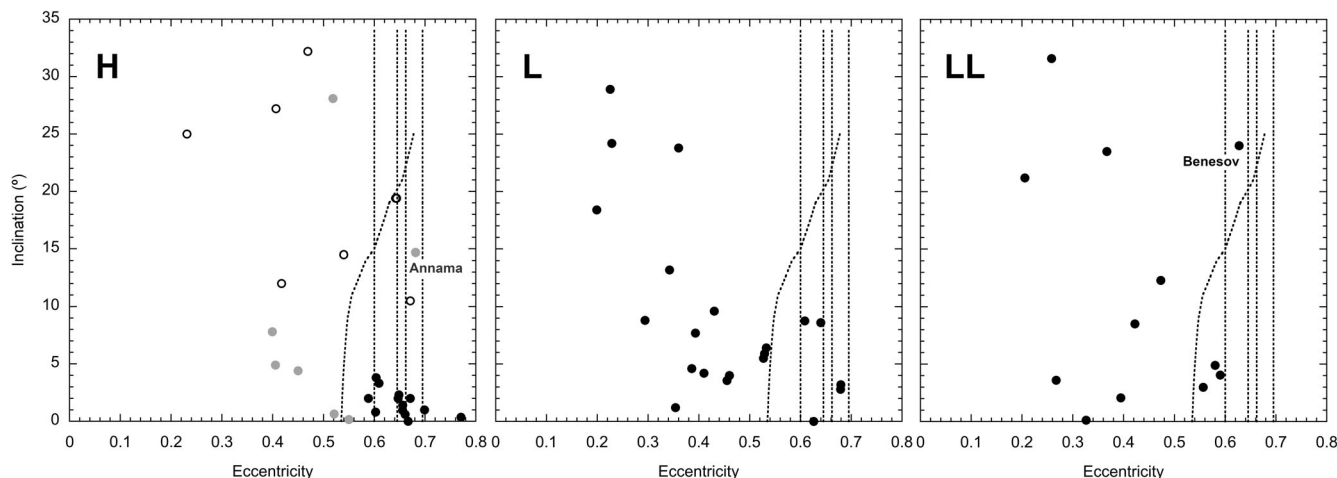


FIGURE 11. Inclination as a function of eccentricity of impact orbits for the three types of ordinary chondrites. H-chondrites are separated in groups as in Figure 10, with gray the likely inner main belt and solid black dots the pristine main belt H-chondrites. Dashed lines show the expected values had the meteorite been fresh from the resonance and arrived at  $q = 1.0$  AU.

(Carruba et al., 2020). There is also a Koronis<sub>2</sub> asteroid family from a cratering event on Koronis itself, which is older at 10–15 Ma (Nesvorný et al., 2015) or  $10 \pm 5$  Ma (Carruba et al., 2020). Koronis<sub>3</sub> is a more diffuse group with an age of <120 Ma (Brož, Vernazza, Marsset, Binzel, et al., 2024). Brož, Vernazza, Marsset, Binzel, et al. (2024) recently derived an age of  $7.6 \pm 0.2$  Ma for Koronis<sub>2</sub> and argued that this family had a steeper size distribution and therefore is the more likely source of  $\sim 7$  Myr old H chondrites.

Table 7 lists the H chondrites that may originate from the pristine main belt source. Those with known CRE ages are listed; others await such information. Three have known CRE ages that suggest they belong to the 7 Ma CRE age peak (average  $\sim 6.5$  Ma, not significantly different than the 5.8 Ma dynamical age of the Karin cluster). Two other H chondrites, Hamburg with CRE age of 12 Ma (Heck et al., 2020) and Mason Gully with CRE age of  $\sim 14$  Ma (Meier et al., 2019), have a CRE age the same as the dynamical age of the Koronis<sub>2</sub> family if it is 10–15 Ma. The Ejby meteorite also has a low- $a$  and low- $i$  orbit but has a CRE age of 83 Ma. If the third cluster in Koronis, named Koronis<sub>3</sub>, is the source of this meteorite, that would put the age of this cluster at  $83 \pm 11$  Ma.

### LL-Type Chondrites and the Flora Family

Based on returned samples in the *Hayabusa* mission, the asteroid Itokawa is a LL5–6 ordinary chondrite (Nakamura et al., 2011). Although it is much larger than typical meteoroids responsible for our meteorites, it has a similar evolved short- $a$  orbit with  $a = 1.32$  AU and

$i = 1.6^\circ$  as that of other recovered LL chondrite falls, including Chelyabinsk. All likely arrived to Earth via the  $v_6$  resonance. 1-km sized NEAs with LL-affinity also have orbits that point to delivery by the  $v_6$  resonance from a  $\sim 7^\circ$  inclined source (Dunn et al., 2013; Marsset et al., 2024; Sanchez et al., 2024).

As it happens, there is a large family called Flora with LL-type spectra (Lindsay et al., 2015; Vernazza et al., 2008) on the inner side of the Inner Main Belt, shown in blue in Figure 1. Satellite flyby missions visited Flora family asteroids (951) Gaspra, (5535) Anfrank, and (152830) Dinkinesh. The inclination of Chelyabinsk ( $a = 1.76 \pm 0.16$  AU,  $i = 4.93 \pm 0.48^\circ$ ) with CRE age = 1.2 Ma (Popova et al., 2013) is that of the Datura cluster within Flora ( $a = 2.24$  AU,  $i = 5.2^\circ$ ), but the 0.5 Ma dynamical age of Datura (Vokrouhlický et al., 2017) is perhaps too young to contribute to our NEA and meteorites. No clusters have been identified in the Flora family with ages that correspond to the CRE age peaks in Figure 8. LL6 chondrite Ischgl (CRE age = 1.7 Ma) arrived on an evolved highly inclined orbit from a previous close encounter with Earth and likely did not originate from the high inclined Eunomia family in the central main belt (Table 5) given its short semi-major axis.

There is also a large asteroid in the inner main belt, (7) Iris (Table 6), that has an LL-type spectrum (Noonan et al., 2019). Cratering of this asteroid could contribute to the influx of LL chondrites. Indeed, there are eight 10-km sized craters on Iris (Hanuš et al., 2019), even though the asteroid has no known associated family. This was interpreted to mean that these craters are very old, but they could also be young but having produced only asteroids that are too small to be detected by current

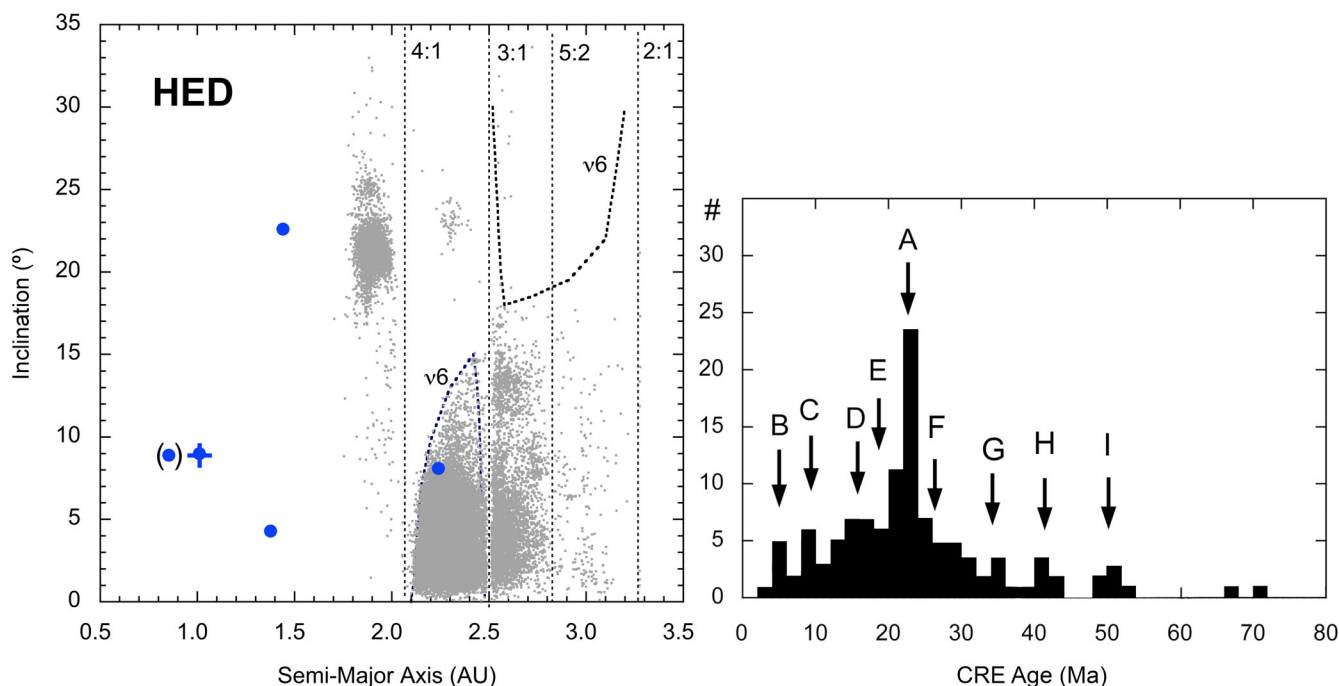


FIGURE 12. HED achondrites. Left: orbital elements of the impacting orbits on a gray background of proper elements of small asteroids. Between brackets is the anomalous eucrite Bunburra-Rockhole, while “+” is the preliminary result for the recent *Nqwaba* fall. Right: CRE age distribution of HED achondrites, each measurement with a reported average uncertainty of 4.7%, or  $\pm 1.0$  Ma at 22 Ma ( $1\sigma$ ), with possible discrete collision events marked by letters based on the individual CRE age distributions of H, E and D types; updated from Jenniskens (2018) with data summarized by Cartwright et al. (2013).

asteroid surveys. As it stands, Iris is not a likely source because of the large combined surface area of the larger Flora family members.

LL chondrites contain highly shocked members, such as the LL7 Dishchii’bikoh meteorite ( $a = 1.129 \pm 0.008$  AU,  $i = 21.2 \pm 0.3^\circ$ ). Shock-blackened meteorites are dark and have weak mineral bands. Some X-complex asteroids in the Flora family may represent shock-blackened LL chondrite material. The Flora family has about 9% X-complex asteroids (Oszkiewicz et al., 2015). The Baptistina family with X-class spectra has LL affinity and may also produce shock-blackened LL chondrites (Popova et al., 2013; Reddy et al., 2011, 2014). Dishchii’bikoh has a CRE age of 11 Ma, which is younger than the  $\sim 80$  Ma dynamical age of the Baptistina family (Table 5). It is possible that debris from the Baptistina formation event has now been lost due to collisions because the short semi-major axis orbit would keep their aphelion in the main belt even when the orbit evolves to intersect Earth’s orbit.

### L-Type Chondrites and the Hertha Family

It was recently argued that L-type ordinary chondrites originate from the Massalia family (Marsset et al., 2024) and that L-type ordinary chondrite like NEA

originate from the  $13^\circ$  inclined Juno family Brož, Vernazza, Marsset, Binzel, et al. (2024). Here, we argue that both may originate in the Hertha family instead.

We observe a strong increase in the dispersion of inclination from an initial  $i \sim 4.4 \pm 3.0^\circ$  for L-chondrite orbits with a low semi-major axis (Figure 2). This points to a source low in the inner main belt. Larger NEA with L-chondrite affinity also appear to originate in the inner asteroid belt at  $i \sim 5^\circ$  (Marsset et al., 2024). They are delivered mostly by the 3:1 resonance, not by both 3:1 and  $v_6$  like the smaller meteoroids. This means that the source is closer to the 3:1 resonance and young enough so that fewer 1-km asteroids have reached the  $v_6$  resonance.

First suggested by Gaffey and Fieber-Beyer (2019), the S-class Massalia family is at the right position ( $i = 1.4^\circ$ ) low in the inner main belt to be the source of L chondrites (Figure 1). Identified by Nesvorný, Bottke, et al. (2006), the family seems to have formed from a cratering event on the asteroid (20) Massalia  $\sim 150$  Myr ago (Milani et al., 2014; Vokrouhlický et al., 2006a). The family is rich in small asteroids (SFD slope =  $-3.5$ , Table 5), representing a large surface area for collisions. However, Hyden et al. (2020) concluded from asteroid spectral band analysis that the family was composed of H chondrites. In addition, the Massalia family may be too young to account for the 468 Ma Ar-Ar resetting age

TABLE 5. Selected asteroid families that are potential sources of our meteorites.

Asteroid family	Tax.	$\langle p_v \rangle$	$a$ (AU)	$e$	$i$ (°)	$N$	SFD	Age (Ma)	Notes	Type	Ref.
Hungaria	E/Xe	0.46	1.944	0.078	20.87	1870	—	150		Aub	[1]
Roxane (= Hawke?)	E/Xe	0.49	~2.26	~0.030	~1.7	6	—	—		Aub	[2]
Vesta	V	0.36	2.362	0.099	6.36	10,612	-3.4	3590 <sup>a</sup>	Rich in small	HED	[3]
2012 PM61	V?	—	2.364	0.112	6.71	35	—	—	Only small, too young?	HED	[4]
Athor	M/Xc	0.23	~2.38	~0.095	~8.2	77	—	3000	Diffuse	EL	[5]
Zita	X/Xk	0.10	~2.28	~0.18	~2.8	79	—	4500	Diffuse	EH	[6]
Baptistina	X	0.18	2.264	0.149	6.00	2500	-3.3	80	Rich in small	LL-sb	[7]
Flora	S	0.29	2.201	0.144	4.59	13,786	-2.7	950	Diffuse	LL	[8]
Datura	Sk,Sq,Q	0.29	2.235	0.156	5.21	6	—	0.5	Too young?	LL	[9]
Euterpe	S	0.27	2.347	0.187	0.72	474	—	>100		LL	[10]
Massalia	S	0.25	2.409	0.162	1.41	7820	-2.8	150		H or L	[11]
Massalia <sub>2</sub>	S	0.25	2.409	0.162	1.41	—	-3.5	40	Rich in small	H or L	[12]
<i>Nysa/Polana</i>											
Hertha	S	0.29	2.412	0.179	2.44	4785	-4.3	300	Rich in small	L or LL	[13]
Hertha <sub>2</sub>	X	0.14	2.426	0.174	2.58	75	—	<145		L-sb?	[14]
2000 FO47	S	—	2.360	0.205	2.35	84	—	—	Too young?	L or LL	[15]
Urania	S	0.22	~2.365	~0.11	~7.5	190	—	4400	Diffuse	L?	[16]
Lucienne	S	0.23	2.462	0.111	14.51	142	—	<100		L	[17]
Phocaea	S	0.29	2.400	0.228	23.41	1989	-2.7	1187		H	[18]
Tamara	C	0.04	2.318	0.203	23.22	140	—	264	Hydrated	CM	[19]
Nemausa	C	0.10	~2.37	~0.11	~5.0	125	—	4000	Diffuse, hydrated	CM?	[20]
Erigone	C,G/Ch	0.06	2.367	0.210	4.74	1776	-3.6	200	Rich in small; Hydrated	CM	[21]
Klio	Ch	0.06	2.362	0.193	9.38	330	-2.5	960	Hydrated	CM	[22]
Chaldaea	Ch	0.06	2.376	0.236	11.60	132	-3.1	—	Small, hydrated	CM	[23]
Chimaera	C/X	0.05	2.460	0.155	14.65	108	-2.6	—	Hydrated	CM?	[24]
Sulamitis	Ch	0.06	2.463	0.091	5.04	303	-2.4	320	Hydrated	CM	[27]
<i>Nysa/Polana</i>											
Polana	F/C	0.06	2.38	0.154	3.23	4020	-3.2	2200	Ryugu samples	CI	[25]
Eulalia	F/C	0.06	2.485	0.145	2.28	7143	-2.7	1200	Bennu samples	CI	[26]
Clarissa	F/C	0.05	2.406	0.107	3.35	236	-3.8	56	Small, Bennu/Ryugu	CI	[28]
Svea	C/X	0.05	2.476	0.088	16.09	48	—	<100	Bennu/Ryugu	CI	[29]
Eunomia	S	0.27	2.644	0.148	13.08	9856	-3.1	1500		LL	[30]
Juno	Sq	0.26	2.669	0.232	13.34	1693	-2.4	463		L	[31]
Gefion	S	0.27	2.784	0.129	9.01	2428	-3.3	1030		H	[32]
Maria	S	0.26	2.554	0.101	15.02	2858	-2.6	1750		H	[33]
Crescentia	S	0.33	2.534	0.103	15.19	805	—	<100	Near 3:1	H?	[34]
Agnia	S	0.24	2.783	0.066	3.58	753	-3.1	100	Rich in small	H	[35]
Mexia	S	0.25	2.745	0.133	4.85	329	-2.7	329	Rich in small	H	[36]
Nele (= Iannini)	S	0.32	2.644	0.267	12.19	150	-3.2	6	Rich in small	H	[37]

TABLE 5. *Continued.* Selected asteroid families that are potential sources of our meteorites.

Asteroid family	Tax.	$\langle p_v \rangle$	$a$ (AU)	$e$	$i$ (°)	$N$	SFD	Age (Ma)	Notes	Type	Ref.
Witt	S	0.26	2.760	0.030	5.79	1816	-3.1	$\leq 100$		?	[38]
Hansa	S	0.29	2.589	0.004	17.34	1162	-3.4	800		?	[39]
Barcelona	Sq	0.29	2.637	0.251	30.83	346	—	$\sim 200$		?	[40]
Aeternitas	A	0.32	2.787	0.097	10.14	447	—	$< 100$		Brach.	[41]
Henan	L	0.23	2.699	0.063	2.80	1872	-3.7	—	3 micron band	?	[42]
Brangäne	L	0.12	2.587	0.179	9.64	325	-3.9	45	Rich in small	Ur?	[43]
Pallas	B	0.16	2.771	0.281	33.20	128	-2.8	1700	Hydrated	CR	[44]
Jones	B	0.05	2.626	0.110	12.35	22	—	2	Too young?	?	[45]
Nipponia	DT	0.24	2.567	0.089	14.50	510	—	$< 100$		?	[46]
Dora	FB/Ch	0.06	2.797	0.198	7.83	506	-3.8	250	Rich in small, hydrated	CM	[47]
Adeona	FB/Ch	0.06	2.673	0.169	11.71	2236	-2.9	350	Hydrated, active asteroid	CM	[48]
Hoffmeister	F/C	0.05	2.787	0.047	4.36	332	-2.9	220		CI?	[49]
Aeolia	C/Xe	0.17	2.742	0.168	3.49	529	-3.3	25	Rich in small; active ast.	?	[50]
Karma	P/X	0.05	2.577	0.106	10.75	51	-2.7	140		?	[51]
Nemesis	G/C	0.07	2.750	0.088	5.18	1302	-4.3	150	Rich in small	CM?	[52]
Padua	G/X	0.07	2.747	0.035	5.09	320	-2.6	190		CM?	[53]
Misa	G/X	0.03	2.658	0.178	2.26	70	—	319		CM?	[54]
2000 EZ39	G/X	0.08	2.658	0.178	2.26	577	-4.1	112	Rich in small	CM?	[55]
König	C	0.05	2.571	0.139	8.85	578	-3.4	22	Rich in small	CM?	[56]
Lorre	C	0.05	2.745	0.263	26.55	19	-3.2	1.9		?	[57]
Astrid	C	0.06	2.788	0.048	0.66	548	-2.6	140	Only hint of 0.7 $\mu$ band	CM?	[58]
Hanna	C	0.05	2.807	0.180	4.17	150	-3.6	—	Rich in small	?	[59]
Koronis	S	0.24	2.869	0.045	2.15	7390	-2.5	1350		H	[60]
Karin	S	0.18	2.864	0.044	2.10	541	-2.9	5.8		H	[61]
Koronis <sub>2</sub>	S	0.18	2.864	0.045	2.16	246	-4.0	15	Rich in small	H	[62]
Koronis <sub>3</sub>	S	0.18	2.84	0.045	2.09	208	-3	$< 120$		H	[63]
Lau	A	0.27	2.929	0.195	6.30	56	—	—		Brach, CK	[64]
1999 XT <sub>17</sub>	A	0.19	2.939	0.119	10.71	58	—	—		Brach, CK	[65]
Seinajoki (=Brasilina)	X	0.18	2.862	0.127	14.98	845	-3.5	120	Rich in small	?	[66]
Naema	C	0.08	2.940	0.036	11.99	50	-4.3	150	Rich in small, hydrated	CM?	[67]
Tirela	S/Ld	0.24	3.116	0.195	17.06	1815	-3.5	300	Rich in small	Ur?	[68]
Watsonia	L	0.13	2.760	0.122	17.33	99	—	660		Ur?	[69]
Eos	K	0.16	3.012	0.077	9.94	16,038	-3.3	1466		CO/CV/CK	[70]
Zelima	K	0.20	3.015	0.069	10.33	33	—	2.9		CO/CV	[71]
Theobalda	F	0.06	3.178	0.263	14.05	376	-3.9	7	Rich in small; active ast.	CM?	[72]
Veritas	G/Ch	0.07	3.174	0.066	9.06	2139	-2.8	8.3	Hydrated	CM/CI-ung.	[73]
Themis	B/Cb	0.07	3.134	0.152	1.08	5612	-2.5	3024	Active asteroids	CM	[74]
Beagle	B/Cb	0.08	3.155	0.154	1.34	148	-3.0	$< 10$		CM	[75]
Hygiea	F/Cb	0.07	3.142	0.136	5.07	4854	-3.7	1347	Rich in small, active ast.	CM	[76]

TABLE 5. *Continued.* Selected asteroid families that are potential sources of our meteorites.

Asteroid family	Tax.	$\langle p_{\text{v}} \rangle$	$a$ (AU)	$e$	$i$ ( $^{\circ}$ )	$N$	SFD	Age (Ma)	Notes	Type	Ref.
Euphrosyne	Cb	0.06	3.155	0.208	26.54	2035	-4.4	280	Rich in small	CM heated	[77]
Alauda	C/B,X	0.07	3.194	0.021	21.66	1294	-2.8	2500	Hydrated, active asteroid	CM	[78]
Marconia	C/X	0.05	3.063	0.097	2.58	34	—	<20		CI?	[79]
Lixiaohua	P/X	0.04	3.153	0.201	10.06	1241	-3.6	155	No OH; active asteroids	CI?	[80]
Ursula	C/X	0.06	3.128	0.098	16.21	1466	-2.7	1800	No hydration	CI?	[81]

*Note:* Member names, proper element coordinates, and number tallies from Nesvorný et al. (2015, 2024), the geometric visible albedo ( $\langle p_{\text{v}} \rangle$ ) and size frequency distribution slope (SFD) are from Masiero et al. (2015) and Brož, Vernazza, Marsset, Binzel, et al. (2024), ages are formation ages of the family from Carruba and Nesvorný (2016) and Paolicchi et al. (2019), unless more recently updated in the references cited. The column “Type” gives the inferred meteorite types based on asteroid taxonomic studies, with sb = shock-blackened. References: [1] Gaffey et al. (1992), Brož, Vernazza, Marsset, Binzel, et al. (2024); [2] Fornasier et al. (2008), Hamann et al. (2024); [3] McCord et al. (1970), Kelley et al. (2003), Dermott et al. (2021); [4] Nesvorný et al. (2024); [5] Delbo et al. (2019), Avdelidou et al. (2022); [6] Delbo et al. (2011, 2014), Popova et al. (2013); [8] Vernazza et al. (2008), Erasmus et al. (2019), Oskiewicz et al. (2015); [9] Nesvorný, Vokrouhlický, and Bottke (2006), Vokrouhlický et al. (2017); [10] Bourdelle de Micas et al. (2022, 2024); [11] Nesvorný, Bottke, et al. (2006), Erasmus et al. (2019), Hyden et al. (2020), Marsset et al. (2024), Brož, Vernazza, Marsset, DeMeo, et al. (2024); [13] Celino et al. (2001), Brož, Vernazza, Marsset, DeMeo, et al. (2024); [14] Dykhuus and Greenberg (2015); [15] Nesvorný et al. (2024); [16] Ferrone et al. (2023), Bourdelle de Micas et al. (2024); [17] Huaman et al. (2018); [18] Noonan et al. (2019), Marsset et al. (2024); [19] Novaković et al., 2017, DeMeo et al. (2022); [20] Delbo et al. (2017, 2023); [21] Carruba et al. (2015), Vernazza et al. (2016), Bolin et al. (2018); Delbo et al. (2023), Harvison et al. (2024), Brož, Vernazza, Marsset, Binzel, et al. (2024); [22] Morate et al. (2019), Arredondo et al. (2020), Delbo et al. (2023); [23] Morate et al. (2019), Delbo et al. (2023); [24] Morate et al. (2019), Celino et al. (2001), Walsh et al. (2013), Erasmus et al. (2019), Delbo et al. (2023), Brož, Vernazza, Marsset, Binzel, et al. (2024); [26] Walsh et al. (2013), Tatsumi et al. (2021), Delbo et al. (2023); [27] Arredondo et al. (2021a), Delbo et al. (2023); [28] Morate et al. (2019), Lowry et al. (2020); Delbo et al. (2023); [29] Huaman et al. (2018), Morate et al. (2019), Delbo et al. (2023); [30] Foglia & Masi (2004), Lindsay et al. (2015), Marsset et al. (2024); [31] Noonan et al. (2019), Marsset et al. (2024); [32] Carruba et al. (2003), Nesvorný et al. (2009), Aljbaae et al. (2019), McGraw et al. (2022), Marsset et al. (2024); [33] Fieber-Beyer et al. (2011), Aljbaae et al. (2017), Marsset et al. (2024); [34] Nesvorný et al. (2024); [35] Vokrouhlický, Brož et al. (2006), Bottke, Vokrouhlický, et al. (2006), Marsset et al. (2024); [36] Bottke, Vokrouhlický, et al. (2006) and Bottke, Nesvorný, et al. (2006), Marsset et al. (2008), Chapman et al. (2009), Carruba et al. (2018), Brož, Vernazza, Marsset, Binzel, et al. (2024); [38] Hergenrother et al. (1996), Spoto et al. (2015), Brož, Vernazza, Marsset, Binzel, et al. (2024); [39] Nesvorný et al. (2015), Milani et al. (2019); [40] Foglia & Masi (2004), Carruba et al. (2011), Paolicchi et al. (2019); [41] Nesvorný et al. (2024); [42] Bus et al. (2002), Gomez Barrientos et al. (2024); [43] Cellino et al. (2019), Brož, Vernazza, Marsset, Binzel, et al. (2024); [44] Sato et al. (1997), De León et al. (2010), Marsset et al. (2020), MacLennan and Granvik (2024), Tatsumi et al. (2024); [45] Bolin et al. (2018), Brož, Vernazza, Marsset, Binzel, et al. (2024); [46] Paolicchi et al. (2019); [47] Nesvorný et al. (2024); [48] Carruba et al. (2003), Hsieh et al. (2024); [49] Carruba et al. (2017), Brož, Vernazza, Marsset, Binzel, et al. (2024); [50] Hsieh et al. (2020), Brož, Vernazza, Marsset, DeMeo, et al. (2024); [51] Pavela et al. (2021), Tatsumi et al. (2024); [52] Carruba and Barletta (2019), Brož, Vernazza, Marsset, Binzel, et al. (2024); [53] Carruba (2009), Bolin et al. (2018), Milani et al. (2018), Milani et al. (2019), Tatsumi et al. (2024); [55] Milani et al. (2019); [56] Pavela and Novaković (2019), Brož, Vernazza, Marsset, Binzel, et al. (2024); [57] Novaković et al. (2012), Hsieh et al. (2020); [58] Carruba (2016), Tatsumi et al. (2024); [59] Masiero et al. (2013); [60] Hirayama (1918), Milani et al. (2014), Lindsay et al. (2015), Erasmus et al. (2024); [61] Nesvorný et al. (2002), Brož, Vernazza, Marsset, DeMeo, et al. (2024); [62] Brož, Vernazza, Marsset, Binzel, et al. (2024); [63] Brož, Vernazza, Marsset, Binzel, et al. (2024); [64] Milani et al. (2014), Nesvorný et al. (2015); [65] DeMeo et al. (2022), Galinier et al. (2013), Milani et al. (2014), Nesvorný et al. (2015); [66] Carruba et al. (2013), Milani et al. (2014), Nesvorný et al. (2015), Bolin et al. (2018), Tatsumi et al. (2024); [68] Mothé-Diniz and Nesvorný (2008), Huaman et al. (2017), Balossi et al. (2024); [69] Celino et al. (2014), Brož, Vernazza, Marsset, Binzel, et al. (2024); [70] Hirayama (1918), Bell (1988), Gattacceca et al. (2020), Brož, Vernazza, Marsset, Binzel, et al. (2024); [71] Tsvirvoulis (2019), Carruba and Ribeiro (2020), Carruba et al. (2024); [72] Novaković et al. (2010), Hsieh et al. (2020); [73] Nesvorný et al. (2003), Brož, Vernazza, Marsset, Binzel, et al. (2024); [74] Hirayama (1918), Florczak et al. (1999), Tatsumi et al. (2021); [75] Fornasier et al. (2016), Carruba (2019); [76] Carruba et al. (2014), Hsieh et al. (2020); [77] Foglia & Masi (2004), Masiero et al., 2015, Yang et al. (2020); [78] Gill-Hutton (2006), Hsieh et al. (2020), and Brož, Vernazza, Marsset, Binzel, et al. (2024); [79] Carruba et al. (2018); [80] Novaković (2010), Hsieh et al. (2020); [81] De Prá, Píñilla-Alonso, et al. (2020).

<sup>a</sup>Based on Ar-Ar age of HED. Some estimates put age at only ~1000 Ma (e.g., Milani et al., 2014; Schenk et al., 2022).

TABLE 6. The largest asteroids, with diameter  $D \geq 200$  km, and some large unusual asteroids that are potential meteorite source parent bodies.

Asteroid	Tax. <sup>a</sup>	$p_v$	$a$ (AU)	$e$	$i$ (°)	$D$ (km)	Meteorite type	Ref.	$v_6$
4 Vesta <sup>b</sup>	V	0.42	2.362	0.099	6.39	<b>525</b>	HED	[1]	
7 Iris	S	0.28	2.386	0.211	6.39	200	LL	[2]	
336 Lacadiera	D/Xk	0.05	2.252	0.088	6.11	63	C2-ung.	[3]	
6 Hebe <sup>b</sup>	S	0.27	2.425	0.159	14.35	185	H	[4]	
44 Nysa	E	0.48	2.423	0.173	3.04	79	Aubrites	[5]	
19 Fortuna	G/Ch	0.04	2.442	0.135	2.22	210	—		3:1
15 Eunomia <sup>b</sup>	S	0.25	2.644	0.149	13.10	270	LL, partial differentiated	[6]	
3 Juno	S/Sk	0.24	2.669	0.234	13.25	254	H, but family L or LL	[7]	
64 Angelina	E	0.48	2.682	0.152	2.26	58	Aubrites	[8]	
324 Bamberga	CP/—	0.05	2.684	0.270	12.10	221	—		
88 Thisbe	CF/Cb	0.07	2.768	0.145	6.27	212	—		
13 Egeria	G/Ch	0.05	2.576	0.126	16.06	205	—		
1 Ceres	G/C	0.09	2.767	0.115	9.65	<b>939</b>	—		
2 Pallas <sup>b</sup>	B	0.16	2.771	0.280	33.20	<b>513</b>	CR?	[9]	5:2
16 Psyche	M/X	0.12	2.922	0.103	2.52	225	Mesosiderites?	[10]	7:3
704 Interamnia	F/B	0.08	3.061	0.105	18.79	306	Ureilites?	[11]	
451 Patientia	CU/—	0.09	3.062	0.071	13.99	254	—		
52 Europa	CF/C	0.06	3.097	0.119	6.37	314	—		
48 Doris	CG/Ch	0.07	3.112	0.064	6.61	216	—		
24 Themis <sup>b</sup>	C	0.07	3.135	0.153	1.085	198	CM		
10 Hygiea <sup>b</sup>	C	0.07	3.142	0.135	5.104	<b>407</b>	CM		
31 Euphrosyne	C/Cb	0.05	3.155	0.208	26.54	267	Heated CM		
94 Aurora	CP/C	0.04	3.158	0.074	8.24	199	—		
511 Davida	C	0.08	3.174	0.183	14.25	270	—		2:1

Note: Orbital elements are proper  $a$ ,  $e$  and  $i$ ,  $D$  is diameter, and meteorite type is that proposed from asteroid taxonomy. References that discuss context with meteorites: [1] McCord et al. (1970), Consolmagno and Drake (1977), Kelley et al. (2003), Unsalan et al. (2019), Jenniskens et al. (2021); [2] Migliorini et al. (1997), Hanuš et al. (2019), Noonan et al. (2019); [3] Rhoden et al. (2020); [4] Farinella et al. (1994), Gaffey and Gilbert (1998), Bottke et al. (2010), Marsset et al. (2017), Fieber-Beyer and Gaffey (2020); [5] Cloutis and Gaffey (1993); [6] Nathues et al. (2005), Brož, Vernazza, Marsset, DeMeo, et al. (2024); [7] Noonan et al. (2019, 2024), Marsset et al. (2024); [8] Clark et al., 2004; [9] Sato et al. (1997), De León et al. (2010), MacLennan and Granvik (2024); [10] Viikinkoski et al. (2018); [11] Jenniskens et al. (2010). Bold marks the largest asteroids.

<sup>a</sup>If two classifications are given separated by “/”, the first is in the Tholen classification, the second in (Bus-DeMeo) SMASS II classification scheme.

<sup>b</sup>Has collisional family.

among L ordinary chondrites. Marsset et al. (2024), however, argued that while (20) Massalia seems to be a H-type, other asteroid family members have band positions similar to L ordinary chondrites. They derived an age of  $450 \pm 50$  Ma for the family, as required for this family to be the source of L chondrites. The initial debris from this cratering event would since have been lost (CRE ages of our L-chondrite meteorites are typically  $<100$  Ma), but there appears to be at least one younger  $\sim 40$  Ma cluster in the family, and there may be more such clusters (Marsset et al., 2024). Note, however, that the 40 Ma peak in the L-chondrite CRE age distribution is not particularly prominent (Figure 9).

In our opinion, a more likely source region of L-type chondrites is the Hertha family, also known in the past as the Nysa or Mildred family of S-class asteroids (Dykhuis & Greenberg, 2015). This family is also located at a good location ( $i = 2.4^\circ$ ), just above the Massalia family in fact, but in a region with an overlapping and much older

C-class Polana family, together called the Nysa/Polana family (Celino et al., 2001). Because albedo or spectra are needed to distinguish the families, there is less information on the Hertha family. The Hertha family is rich in small  $<10$  km size asteroids, has a relatively steep size distribution, and appears to have originated from a cratering event on asteroid (135) Hertha (Dykhuis & Greenberg, 2015).

Marsset et al. (2024) classified the Hertha family (their “Nysa”) as LL-type based on near-IR spectra of 6 family members, but that classification may be in error. L spectra too provide a reasonable fit to the average spectrum of the 6 family members. Erasmus et al. (2019) did show that Hertha and Flora (LL class) family asteroids have similar V-I versus V-R band slopes, distinct from those of the Massalia and Koronis families, but Massalia and Koronis (H class) plots were similar. Looking at the olivine and pyroxene band strengths in Marsset et al. (2024), again Massalia members plot similar to those of Koronis (H

TABLE 7. H-type ordinary chondrites with a likely origin in the Koronis family.

Meteorite	Type	$a$ (AU)	$i$ (°)	CRE age (Ma)	Ref.
Karin cluster ( $5.75 \pm 0.05$ Ma)					
Košice, Slovakia	H5	2.71	2.0	$6.0 \pm 1.0$	[1]
Murrili, Australia	H5	2.52	3.3	$6.6 \pm 0.5$	[2]
Arpu Kuilpu, Australia	H5	2.75	2.0	$7.0 \pm 1.0$	[3]
Koronis <sub>2</sub> cluster ( $10 \pm 5$ Ma)					
Hamburg, USA	H4	2.73	0.6	$11.8 \pm 0.7$	[4]
Mason Gully, Australia	H5	2.47	0.8	~14	[5]
Koronis <sub>3</sub> cluster (<120 Ma)					
Ejby, Denmark	H5/6	2.81	1.0	$83 \pm 11$	[6]
Unknown					
Great Salt Lake, USA	H5	2.5	1	—	This work
(Crawford Bay), Canada	H6	2.68	1.4	—	[7]
(Ménétréol-sur-Sauldre), France	H5	2.58	0.0	—	[8]
(Kybo-Lintos), Australia	H4/5	2.60	0.4	—	[9]
Tanxi, China	H6	2.40	1.9	—	[10]
(Benghazi Dam), Australia	H5	(2.8) <sup>a</sup>	2.3	—	This work

Note: References: [1] Nesvorný et al. (2002), Carruba et al. (2020); [2] Povinec & Toth (2015); [3] Anderson et al. (2022); [4] Anderson et al. (2024); [5] Molnar and Haegert (2009), Nesvorný et al. (2015), Carruba et al. (2020); [6] Heck et al. (2020); [7] Haack et al. (2019); [8] Dyl et al. (2016), Meier et al. (2019); [9] Jenniskens et al. (2018); [10] Colas (2023); [11] Anderson et al. (2022); [12] Li et al. (2025).

<sup>a</sup>For this assumed semi-major axis.

class), while most Flora family members (LL class) plot significantly offset from those of the Hertha family members, and Hertha family members plot in between Massalia and Flora. The relatively low flux of LL chondrites and the lack of LL chondrites arriving to us from the 3:1 mean-motion resonance also argue against Hertha being a source of LL chondrites.

The formation of the Hertha family can explain better the high flux of L chondrites 468 Ma ago. This was an exceptional event in Earth's history, with only 1 out of 70 major family-forming break-ups in the past ~500 Ma having resulted in such a high flux of meteorites on Earth (Terfelt & Schmitz, 2021). The Hertha family resulted from a collision event that involved asteroid (135) Hertha, an asteroid that is now of M/ $X_k$  class, but that spread S-class fragments with an ejection speed of  $\sim 285$  m s<sup>-1</sup> over a large part of the inner main belt, the current distribution of the family limited by the 3:1 resonance and the Mars crossing line (Dykhuis & Greenberg, 2015). This compares to an ejection speed of  $\sim 44$  m s<sup>-1</sup> for the cratering event that created the Massalia family (Vokrouhlický et al., 2006a). Also, less of the original asteroid survived. The dynamical age of the Hertha family is  $300 \pm 60$  Ma (Dykhuis & Greenberg, 2015), which is closer than the age of Massalia to the 468 Ma required for shocked L chondrites. More recently, Paolicchi et al. (2019) estimated the age of the Hertha family at ~242 or ~761 Ma, while Brož, Vernazza, Marsset, DeMeo, et al. (2024) estimated the age at ~600 Ma.

Asteroid (135) Hertha experienced another collision event <145 Ma ago that created a cluster of X-class

asteroids called Hertha<sub>2</sub>, with weak 1- and 2- $\mu$ m bands that possibly indicate shock-blackened L chondrites (Dykhuis & Greenberg, 2015). It is possible that the 468 Ma collision that created the Hertha family left the asteroid covered in a shock-blackened material, which then experienced a second collision to create the Hertha<sub>2</sub> family (Scenario 4 of Dykhuis & Greenberg, 2015). In contrast, Massalia was not covered in shock-blackened fragments after the collision that created the Massalia family.

The oldest 42–48 Ma CRE age of some shocked L chondrites may well measure the dynamical age of the Hertha<sub>2</sub> family. If all L chondrites with the 468-Ma signature originated from the Hertha<sub>2</sub> family, then this compact family is expected to include even younger families of about 9 and 18 Ma. Alternatively, the extended Hertha family likely includes shock-blackened fragments and may include X-class families hard to differentiate from the Polana and Eulalia families. In the same way, the extended Hertha family is expected to include young S-class families of about the 3, 5, 24, and 52 Ma CRE age peaks (Figure 9). One of those peaks may be related to the undated compact 2000 FO47 family, part of the Hertha family (Nesvorný et al., 2024), but it is possible that this family is too young for delivering meteorites to Earth.

### H-Type Chondrites that Are not from Koronis

If we assign the cluster of meteoroids with low inclination and  $a > 2.5$  AU in Figure 6 to Koronis, then

the remaining population consists of two groups: one is a high 10–30° inclined population similar to that of the corresponding NEA in Marsset et al. (2024); the other is a population of low-inclined and short-semi major axis orbits that appear to have originated in the inner main belt (Jenniskens, 2018; Trigo-Rodríguez et al., 2015).

The need of a source of H chondrites in the inner main belt is another argument against the idea that Massalia could produce L chondrites. There is no ready alternative. If the Hertha family is the source of L chondrites and the Massalia family is H type instead (Hyden et al., 2020), then Massalia<sub>2</sub> may be the source of the 35-Ma CRE peak of H chondrites, which in our sample is represented by the meteorites Grimsby, Peekskill, Narashino, and Annama. Other possible members of this group are Santa Filomena, Križevci, and Al-Khadhaf (red in Figure 10). This number of meteorites ( $N = 7$ ) implies a significant source. Massalia does have a prominent ~40 Ma cluster (Marsset et al., 2024).

Marsset et al. (2024) pointed out that nearly all km-sized NEA of H type appear to arrive at Earth in highly 10–30° inclined orbits, out of the 3:1 resonance. Although the 3:1 resonance can pump up the inclination, there are no NEA observed with low  $i$  that suggests they originated from the Koronis family. A source high in the central main belt was suspected, most likely from Phocaea or the Maria families (Brož, Vernazza, Marsset, Binzel, et al., 2024). Asteroid (6) Hebe (“3” in Figure 1) has also long been proposed as a possible parent body of H chondrites based on its reflectance spectrum, relatively large size, and because the asteroid is located close to dynamical chaotic zones of the 3:1 mean motion resonance and the  $\nu_6$  secular resonance (Farinella et al., 1994; Gaffey & Gilbert, 1998; Migliorini et al., 1997; Morbidelli et al., 1994), but that asteroid has only a small and old cratering family associated with it (Fieber-Beyer & Gaffey, 2020).

The high inclination H chondrites may not originate from Phocaea as thought before (e.g., Jenniskens, 2018) but from a small S-class asteroid family in the central main belt that stands out in number density among nearby small asteroids (Brož, Vernazza, Marsset, DeMeo, et al., 2024): Nele (called “Iannini” in Nesvorný et al., 2024), at  $i \sim 12^\circ$  with an estimated dynamical age of  $6 \pm 2$  Ma (Brož, Vernazza, Marsset, Binzel, et al., 2024; Carruba et al., 2018). The relative band strength in near-IR spectra by Chapman et al. (2009) suggests to us that this is a H-chondrite family. Among all six possible H chondrites from this source, four have the low CRE ages of  $6.7 \pm 1.0$  Ma (Borovička et al., 2003) for Morávka ( $a = 1.85 \pm 0.07$  AU,  $i = 32.2 \pm 0.5^\circ$ ),  $7.0 \pm 0.4$  Ma (Bogard et al., 1971; Graf & Marti, 1995) for Lost City ( $a = 1.66$  AU,  $i = 12^\circ$ ),  $\sim 6$  Ma (Meier et al., 2019) for Buzzard Coulee ( $a = 1.25$  AU,  $i = 25^\circ$ ), and  $4 \pm 1$  Ma (Ozdín et al., 2024) for Pusté Úlany

( $a = 1.70$  AU,  $i = 27.2^\circ$ ), in good agreement with the dynamical age of this family. A source in the central main belt can account for high inclination orbits from pumping up inclination in the 3:1 mean-motion resonance. Other members of this group possibly include Matera ( $a = 2.10 \pm 0.07$  AU,  $i = 14.5 \pm 0.2^\circ$ ). This would make the Nele family composed of H-chondrite types and not Acapulcoites/Lodranites as proposed in Brož, Vernazza, Marsset, Binzel, et al. (2024). If so, both Nele and Karin/Koronis<sub>2</sub> contribute to the 7 Ma CRE peak of H chondrites.

Two other relatively high inclined H chondrites, Příbram ( $a = 2.401 \pm 0.005$  AU,  $i = 10.4820 \pm 0.0004^\circ$ ) and Elmshorn ( $a \sim 2.50 \pm 0.07$  AU,  $i = 19.4^\circ$ ), have CRE ages ~18 Ma. While Příbram might have originated from Koronis<sub>2</sub> based on an earlier CRE age measurement of  $11.5 \pm 1.5$  Ma (Bagolia et al., 1980), the re-evaluation of the CRE age based on old measurements ( $14.7 \pm 1.1$  Ma from Graf & Marti, 1995) yielding an age of  $17 \pm 2$  Ma by Meier et al. (2022) implies otherwise. That age overlaps with the age of  $18.5 \pm 1.5$  Ma measured for Elmshorn by Bischoff, Patzek, Alosius, et al. (2024) and Bischoff, Patzek, Barrat, et al. (2024). Perhaps, these H chondrites originated from the Maria family, in particular the cluster of asteroids centered on (660) Crescentia (Aljbaae et al., 2017; Nesvorný et al., 2024) between asteroid (170) Maria and the 3:1 mean-motion resonance (Figure 1). Until now, this structure has not been dated separate from the older rest of the Maria family.

### An LL/H Mix and the Eunomia Family

Benešov ( $a = 2.483 \pm 0.002$  AU,  $i = 23.981 \pm 0.007^\circ$ ) is a rare mixed bag of meteorites, dominated by LL chondrites. The recovered meteorites (20 years after the fall) were a 7.72 g LL3.5 chondrite with an achondrite-like inclusion, a 1.99 g LL3.5 chondrite, but also a 1.56 g H5 chondrite now listed as Benešov(b) (Spurný, Haloda, et al., 2013; Spurný et al. 2014). Because of its uncertain identity, the meteorite is not included in Figure 8. It arrived on Earth from a highly inclined orbit out of the 3:1 resonance, an odd case among LL chondrites (Figure 11), suggesting that it did not originate in the Flora family but from a source high in the central main belt. Eunomia is the largest asteroid family in the central main belt (at  $a = 2.64$  AU,  $i = 13.1^\circ$ ) and perhaps the only source of LL chondrites (Vernazza et al., 2014; Marsset et al., 2024). There are several sources of H chondrite clasts nearby. Eunomia also has several known clusters: 1998 GC3, 1990 SB1, 2008 OV23, 1998 TA6, and 1996 WU2 (Nesvorný et al., 2024). To date, no dynamical ages have been determined for these. The 11 Ma CRE age for Benešov is uncertain because of terrestrial weathering (Meier et al., 2019; 2022).

TABLE 8. The largest-for-its-age-bracket rayed (young) impact craters on asteroids (4) Vesta that can be a source of HED meteorites.

Crater	$D$ (km)	Age <sub>Lunar</sub> (Ma)	Age <sub>Asteroid</sub> (Ma)	Ejecta blanket	CRE age peak (Ma) <sup>a</sup>	Main type	Meteorite example	Ref.
Arruntia	10.5	2.5 ± 0.4	14.6 ± 2.3	Fa rich exposures from impact melt	(too young)			[1]
—	—	—	—		5.2 ± 0.5	D, E	Nobleborough (E, polym.)	
Vibidia	7.1	9.6 ± 1.3	98 ± 7	On slope Veneneia, many type ejecta	8.9 ± 0.5	E	Juvinas (E)	[2]
Cornelia	14.9	11.2 ± 2.1	~58	Diverse, crater floor pitted terrain, impact melt	15.2 ± 1.9	E	Ibitira (E)	[3]
Rubria	10.3	17.9 ± 3.4	~84	On topographic high, no solar wind Ne	18.2 ± 1.3	H	Motopi Pan (H)	[4]
Antonia	16.7	21.1 ± 3.7	89 ± 3	On slope Rheasilvia, solar wind Ne	22.2 ± 1.2	D, E, H	Sarıçiçek (H)	[5]
—	—	—	—		25.8 ± 1.2	E	Millbillillie (E)	
—	—	—	—		32.6 ± 1.6	E, H	Lakangaon (E)	
—	—	—	—		41.3 ± 1.2	H, D	Roda (D)	
Licinia	24.1	49.5 ± 4.6	~172	Highland crater, many type ejecta	50.5 ± 1.5	H, D, E	Macibini (E, polymict)	[6]
Marcia	67.6	120 ± 40	294 ± 130	Eucritic ejecta, floor pitted terrain, impact melt	(too old)			[7]

Note: Ages in lunar chronology scheme by Schmedemann et al. (2014), ages in the asteroid-based chronology scheme by Marchi et al. (2012) and O'Brien et al. (2014). References: [1] Ruesch et al. (2014); [2] Kneissl et al. (2014); [3] Krohn et al. (2014); [4] Krohn et al. (2014); [5] Kneissl et al. (2014), Unsalan et al. (2019); [6] Ruesch et al. (2014); [7] Ruesch et al. (2014), Williams et al. (2014).

<sup>a</sup>CRE age groups as in Figure 12, modified from Eugster and Michel (1995) and Welten et al. (1997).

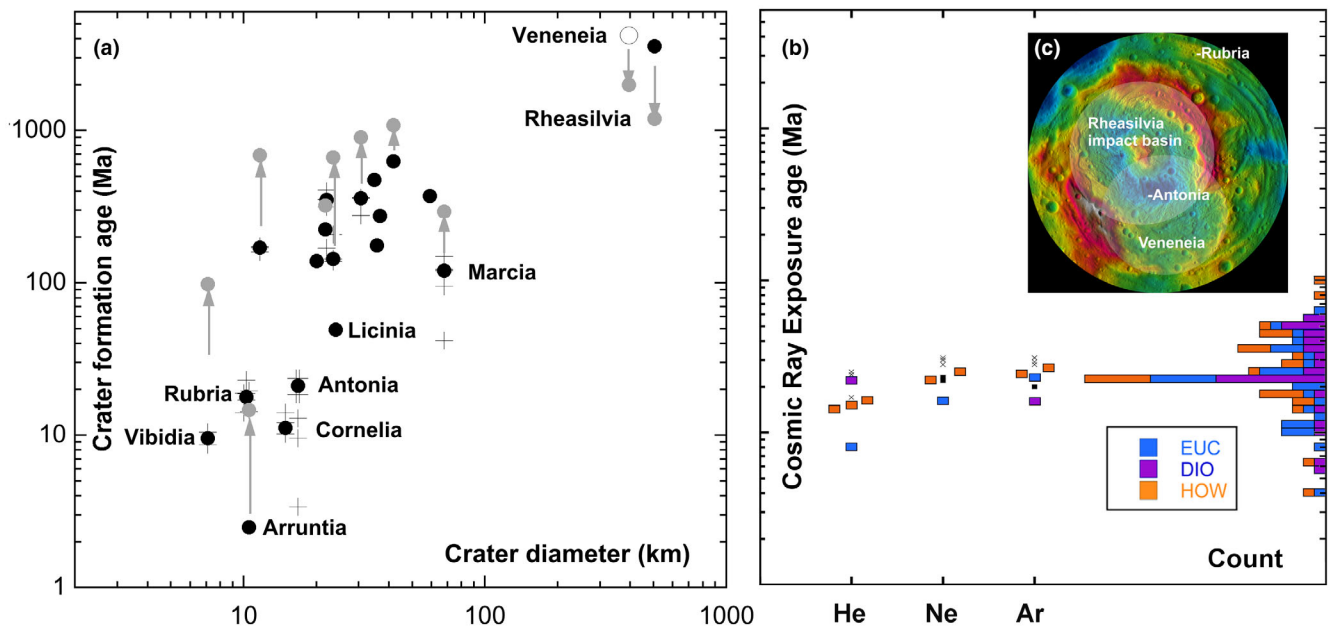


FIGURE 13. Relation of crater ages on (4) Vesta to CRE ages of recovered HED meteorites. Left: Age of young impact craters in Moon-based (dark) and Asteroid-based (gray) chronology schemes; Right: The cosmic ray exposure age of HED meteorites, with example of Motopi Pan. From: Jenniskens et al. (2021).

## HED-Type Achondrites and Asteroid Vesta

The lack of large asteroids in the Vesta asteroid family makes asteroid (4) Vesta itself the likely source of our meteorites (Unsalan et al., 2019). Only a handful of the largest craters on Vesta are likely source craters for HED meteorites as the debris from those will dominate that of smaller impacts in their age bracket. Those are listed in Table 8. Their ages are derived from crater counts on the ejecta blankets. Calibrations of those counts have resulted in different age estimates. In the asteroid-derived chronology, all these rayed craters are too old to be the source of our meteorites and the one crater that could be the source would have ejected impact melt, contrary to the nature of HEDs. Instead, there is good agreement between peaks in the CRE age distribution and the age of source craters in the lunar-based chronology (Figure 13).

That does not exclude the possibility that some HED are from collisions with Vesta family members. Recently, a compact 35-member family was identified in the Vesta family associated with asteroid 2012PM61, consisting only of small objects (Nesvorný et al., 2024). It is unclear if enough fragments were generated in this collision to cause one of the unassigned peaks in Table 8. Moreover, this family may be too young to produce meteorites at Earth now.

Assigning meteorites to specific impact craters can only be achieved from space missions like Dawn that map the crater terrain. Dawn also visited asteroid Ceres, the largest asteroid in the main belt and found that 26-km sized crater Kupalo is ~4 Myr old (e.g., Hernandez et al., 2022). That is a possible source crater for meteorites, but no meteorites are known associated with Ceres.

The isotopic signatures and orbit of Bunburra-Rockhole imply that there is also a population of eucrites in the inner main belt unrelated to Vesta (Benedix et al., 2017). That source remains unidentified.

## CM Carbonaceous Chondrites and the Themis Family

At least half of the CM chondrites have such short CRE ages (~0.05–2 Ma) that they likely originate from larger NEA that already evolved into the near-Earth orbit. Maribo and Sutter's Mill arrived on low-*q* orbits (Table 2), suggesting that larger NEA did survive to evolve to such lower *q* orbits but then fragmented by thermal stresses (Jenniskens et al., 2012; Shober et al., 2024).

The disruption of small CM asteroids already in near-Earth space could explain the relatively high flux of short CRE age m-sized CM-type asteroids at Earth (McMullan et al., 2024; Shober et al., 2024), even if the delivery is

inefficient. However, the diversity in CRE ages and the level of aqueous and thermal alteration of the four CM2 chondrites tracked to date rule out the possibility that they all originated from a single disrupted NEA. Correlated mineralogy and cosmic-ray exposure ages (Nishiizumi & Caffee, 2012) points to this diversity among larger CM2 parent body NEA.

How large are these asteroids when they evolve from the main belt inwards? Observed 1-km sized C/P class asteroids that appear CM-type and still have a semi-major axis near the 3:1 and 5:2 resonances have relatively high 5–20° inclinations. Space weathering results in strong reddening (Thompson et al., 2019), so the spectral properties of D-class asteroids are not inconsistent with CM chondrites. However, D-class NEA from that region have  $i \sim 7^\circ$  (Brož, Vernazza, Marsset, Binzel, et al., 2024). This is also not in agreement with the low  $i < 3^\circ$  approach orbits of CM chondrites. Smaller source asteroids, say 10–100 m size, could arrive on lower inclined orbits if the source region is at low inclination and resonances had less time to pump up the inclination.

Previously suggested sources such as Polana (e.g., Jenniskens et al., 2012) and Veritas (e.g., Farley et al., 2006; Meier et al., 2016; Nesvorný et al., 2003) are at too high inclination to account for the observed orbital elements of CM chondrite falls. The precise orbit of Winchcombe with a semi-major axis just beyond the 3:1 mean-motion resonance suggests that this source is near the 5:2 mean-motion resonance or beyond.

Possible source asteroid families include the large Themis family ( $i = 1.1^\circ$ , red in Figure 1) and the small Marconia family ( $i = 2.6^\circ$ ) in the outer main belt, as well as the Astrid family ( $i = 0.7^\circ$ ) and the Misa family, or better the younger overlapping family named after 2000 EZ39 ( $i = 2.2^\circ$ ), in the central main belt. The 2000 EZ39 family has a steep size distribution and is rich in small asteroids, but does not have the 0.7  $\mu$  band (Bolin et al., 2018) that is a prominent feature of CM chondrites (Suttle et al., 2021). Little is known about the small Marconia family.

The low inclination of Maribo and Winchcombe points to the Astrid family ( $i = 0.7^\circ$ ), a small relatively compact family near the 5:2 resonance. Astrid itself has a hint of a 0.7  $\mu$  band (Tatsumi et al., 2024). However, this small family has a shallow size distribution and a relatively high age of  $135 \pm 15$ –20 Ma (Carruba, 2016). However, although the given CM chondrites come from somewhat larger (10–100 m) NEA, it will take these larger asteroids longer to evolve to the near-Earth space. Those asteroids would be too small to be detected efficiently in this part of the asteroid belt.

Alternatively, Themis ( $i = 1.1^\circ$ ) is one of the richest families and among the four earliest recognized families

(Hirayama, 1918). It is associated with 198-km sized asteroid (24) Themis, which would originally have had a diameter of 286 km (De Prá, Pinilla-Alonso, et al., 2020). The family has at least one young  $\leq 10$  Ma subfamily called Beagle with spectra similar to CM2 chondrites (Carruba, 2019; Fornasier et al., 2016; Nesvorný et al., 2015; Takir et al., 2015). The oldest CRE ages in CM chondrites range from 4 to 14 Ma (Krietsch et al., 2021; Meier et al., 2016).

About 13% of Themis family members have the 0.7  $\mu\text{m}$  band and near-UV absorption from charge transfer of interlayer iron in phyllosilicates (Florczak et al., 1999; Kaluna et al., 2016; Tatsumi et al., 2021, 2024). The Themis family is associated with active asteroids, with hydroxyl-bearing minerals at 3  $\mu\text{m}$  (Takir & Emery, 2012) and even with water ice (Campins et al., 2010). The spectrum is that of anhydrous IDPs (Marsset et al., 2016). The majority of unmelted micrometeorites has compositions similar to CM chondrites (Kurat et al., 1994) but are thought to be of Jupiter-family comet origin (Nesvorný et al., 2010). Indeed, Themis has been proposed as a possible source of some Jupiter-family comets from loss via the 2:1 resonance (Hsieh et al., 2020).

If Themis is the source of CM chondrites, then these asteroids would first pass the 7:3 resonance, before being delivered to near-Earth space via the 5:2 resonance. Indeed, small asteroids can cross the resonance for fast enough Yarkovsky drift rates (Xu & Zhou, 2020).

Some H chondrites contain clasts of CM carbonaceous chondrites (Bridges & Hutchison, 1997; Zolensky et al., 2016). Earlier, Rubin and Bottke (2009) proposed that the Baptistina family was the origin of these clasts, but if Koronis is the source of some H chondrites, then Themis being the source of CM carbonaceous chondrites would explain why a steady stream of CM fragments could mix with H chondrite regolith that has built up on the Koronis parent body over time. Both families are very old. Koronis broke about 1700 Ma ago, when Themis was already a debris field (age  $\sim 3000$  Ma). After the breakup of Koronis, the surfaces of Koronis family asteroids were also impacted by CM fragments, with collisions resulting in CM-clasts becoming part of the regolith breccia. Ipiranga is one of those H chondrites known to contain CM clasts (Zolensky & Le, 2024). We find that it has Fa and Fs compositions determined from infrared spectroscopy by Mitchell et al. (2020) that place it in the low-Fs pristine main belt group in Figure 7.

### **C1-Ungrouped (CM-Affinity) Meteorites and the Veritas Family**

Only one C1-ungrouped meteorite was tracked, Flensburg, and that case resulted in a semi-major axis that placed the asteroid squarely in the 5:2 resonance.

The meteorite has an ultra-short CRE age. The 5:2 resonance is capable of very rapid delivery of meteorites to Earth (Nesvorný et al., 2009). The meteorite has CM affinity. It is possible that it originated from a larger asteroid in the Themis family, which had the inclination pumped up by the 5:2 resonance. However, it is more likely that a small asteroid from the young 8.3-Myr old Veritas family (Tsiganis et al., 2007), a potential source of CM or CR chondrites (Brož, Vernazza, Marsset, DeMeo, et al., 2024), evolved into the inner solar system and then broke off the Flensburg meteoroid. Because Flensburg is an ungrouped meteorite, it is possible that this material is only a clast in an otherwise CM1/2-class material breccia, in which case the Veritas family is CM type.

### **CI Carbonaceous Chondrites and the Polana/Eulalia Families**

Delbo et al. (2023) showed that among all the primitive inner main belt families, the reflectance spectra of asteroid Bennu are the most similar to those of the Eulalia family and that of asteroid Ryugu most similar to those of the older Polana family. Both asteroids were sampled and proven to be CI chondrites (Delbo et al., 2023). This suggests that these families are CI type and a source of CI-like near Earth objects (Brož, Vernazza, Marsset, DeMeo, et al., 2024; Takir et al., 2024).

Further evidence that the inner main belt is a source of CI carbonaceous chondrites is that CI-like clasts (xenolithic fragments) are found in HEDs and ordinary chondrites (Zolensky et al., 1996) that are thought to have originated in the inner main belt. These clasts have hydrogen isotopes similar to those of common CI chondrites (Patzek et al., 2020). Of all H chondrites known to have CI or CM clasts listed by Zolensky and Le (2024), only four have recorded Fa and Fs numbers in the meteoritical bulletin: Carancas, DAG577, NWA 8369, and ZAG H3-6. All belong to the high-Fs group (Inner Main Belt H chondrites, Figure 7), and all have CI clasts.

An origin of CI chondrites in the inner main belt would suggest a higher flux at Earth than for CM chondrites. However, CI chondrites are rare in our collections. The difference is not at the source because the size-frequency distribution of Polana (SFD slope =  $-3.2$ , Table 5) is as steep as that of the Beagle cluster in the Themis family (SFD slope =  $-3.0$ ). Instead, Polana family asteroids may be less efficient at creating m-sized debris than Themis family asteroids when they come into the inner solar system.

### **CM Carbonaceous Chondrites and the Erigone Family**

The inner main belt has two different classes of primitive asteroids (Arredondo et al., 2021b). One group

of C-class families do not have or have only shallow, hydration bands (Polana, Eulalia, Clarissa, Svea) and are identified as CI ordinary chondrites (see above). The other group (Erigone, Sulamitis, Klio, and Chaldaea) contains hydration bands with a sharp low-wavelength slope typical of carbonaceous chondrites (Rivkin et al., 2022). NASA's *Lucy* mission is about to fly by asteroid (52246) Donaldjohanson on April 20, 2025, a possible member of the Erigone family.

H chondrite NWA 8369 has both CI and CM2 clasts, suggesting a second source of CM2 chondrites in the inner asteroid belt. Small CM and CI clasts are also found in HED chondrites (Zolensky et al., 1996). The CM clasts have hydrogen compositions similar to that of CM chondrites (Patzek et al., 2020). If the CI clasts are from Polana-group asteroids, based on their location in the inner main belt relative to Vesta (Figure 1), it is possible that the Erigone group, which contain the iron-rich phyllosilicates typical of CM chondrites (Tatsumi et al., 2024), is a source of CM chondrites in the inner main belt. That said, most of the Erigone group families are relatively young, having been derived from a population of larger CM asteroids in the inner main belt. Depending on the age of the H chondrite breccias, these CM clasts may have originated in older and now diffuse families in the inner main belt such as Nemausa (Table 5).

### CV/CO/CK and the Eos Family

So far, no CV, CO, or CK carbonaceous chondrite approach orbits have been measured. Similarities with asteroid spectra point to an origin in the Eos family (e.g., Bell, 1988; Gattacceca et al., 2020; Tanbakouei et al., 2021), a prominent family in the outer main belt (green in Figure 1). We note that there is a young ~2.9 Ma sub-family associated with asteroid (633) Zelima in the Eos family (Carruba & Ribeiro, 2020; Tsirvoulis, 2019), and CO and CV (and perhaps also CK) meteorites have a peak in the CRE age distribution at ~5.5 Ma (Eugster, 2006; Scherer & Schultz, 2000). If the low- $i$  7-Myr old H chondrites come from the Karin cluster, it is perhaps not unreasonable to propose that the ~5.5 Myr old CO/CV/CK meteorites are from the Zelima cluster. If so, the small Zelima meteoroids may arrive to us not via the 8J-3S-3A three-body resonance that they are next to or the or  $z_1$  secular resonance that they are in (Carruba & Ribeiro, 2020), but via the more efficient 5:2 or 3:1 mean-motion resonances that avoid the aphelion of their orbit evolving too close to Jupiter's orbit. They are predicted to arrive on  $a = 2.5\text{--}2.9$  AU and  $i \sim 10^\circ$  orbits. CV, CO, and CK chondrites survive the interplanetary medium better than CM chondrites. In addition to the ~5.5 Ma peak, CO chondrites have CRE peaks also at about 9, 17, 26 and 45 Ma (Eckart et al., 2024). Those collisions may have been

elsewhere in the Eos family. Some 1-km sized NEA of K and L class also appear to originate from the Eos family (Brož, Vernazza, Marsset, Binzel, et al., 2024).

### The Source of C2-Ungrouped Tagish Lake

Tagish Lake has CM, CI, and CR affinities but has isotopic signatures different from each of these (Schrader et al., 2024). The phyllosilicates are Mg-rich, unlike those detected in the reflectance spectra of most primitive asteroids in the inner main belt. The meteorites are fragile and may survive atmospheric entry even less efficiently than CI chondrites. Meteorites similar to Tagish Lake include Tarda, Wisconsin Range 91600, and Meteorite Hills 00432. The reflectance spectrum is that of a D-class asteroid (Hiroi et al., 2001).

Gatrelle et al. (2021) identified D-class NEA 2000 LC16 as a plausible parent body, while Hlobik and Tóth (2024) identified small NEO asteroids 2005 YU<sub>8</sub> ( $a = 2.01$  AU,  $i = 4.0^\circ$ ,  $H = 23.7$  magnitude) and 2016 AF<sub>166</sub> ( $a = 1.94$  AU,  $i = 3.1^\circ$ ,  $H = 25.4$  magnitude) as moving on similar orbits. However, the high ~7.8 Ma CRE age of Tagish Lake argues against it having originated from an asteroid already in an evolved NEA orbit.

The orbit of Tagish Lake suggests that it came from the inner main belt and was delivered by the  $v_6$  resonance (Brown et al., 2000). There are only a handful of asteroids of D-class known in the inner main belt (DeMeo et al., 2014). Asteroid (15112) Arelenewolfe has the lower inclination suggested by Tagish Lake ( $a = 2.30$  AU,  $i = 3.0^\circ$ ), but it is only 7 km in diameter. The largest D-class asteroid in the inner main belt is 63-km (336) Lacadiera (Rhoden et al., 2020) with orbital elements  $a = 2.25$  AU and  $i = 6.1^\circ$  (Table 6). Neither one has a known ~7.8 Ma family associated with it.

### Enstatite Achondrites and the Roxane Family

Aubrites are a good spectroscopic fit to the Hungaria family (Clark et al., 2004; Gaffey et al., 1992), a family with homogeneous high albedo E-class (Xe) spectra quite different from the non-family background in that high-inclined part of the asteroid belt (Lucas et al., 2019). A dynamical pathway from the family to Earth was identified by Čuk et al. (2014) that does not involve resonances, but rather Yarkovsky drifting across the orbit of Mars, resulting in high CRE ages. Aubrites as a group have CRE ages between 12 and 118 Ma (Lorenzetti et al., 2003).

However, the first documented aubrite Ribbeck (Table 2), known also as asteroid 2024 BX1 before the impact, has an orbit that points to a source in the inner main belt and delivery via  $v_6$  (CRE age of 70 Ma).

Located relatively close to  $v_6$ , asteroid (317) Roxane and nearby high albedo asteroids (the Roxane family) were proposed as a source of aubrites by Fornasier et al. (2008). The  $113 \times 67 \times 65$  km sized E-class asteroid (44) Nysa (Table 6) has a similar spectrum but is located closer to the 3:1 resonance.

There are also E-class asteroids scattered higher ( $i \sim 5^\circ$ ) in the inner main belt, most are among Flora family asteroids (Hamann et al., 2024). Perhaps not surprisingly, some aubrites contain LL-type ordinary chondrite clasts (Rubin, 2010). Visited by the *Rosetta* mission, asteroid (2867) Steins is one of the inner main belt E-class asteroids but in a higher inclined  $i \sim 9.5^\circ$  orbit.

Recently, we identified two pathways to Earth for high-albedo asteroids from their distribution in  $a$ - $i$  space (Hamann et al., 2024). One group of asteroids is found along a path from the Hungaria family (green in Figure 1) to  $a = 1$  AU,  $i = 0^\circ$  at Earth; another group is located along a path from the inner main belt to Earth. The two sources have slightly different spectra, with surfaces of inner main belt E-class asteroids being more contaminated by the ordinary chondrite material (Clark et al., 2004). Ribbeck has the weaker oldhamite band of (317) Roxane (Cantillo et al., 2024).

### Enstatite Chondrites and the Athor Family

It was recently proposed that the Athor family (Delbo et al., 2019), with (161) Athor being an M/Xc-class asteroid, has the right albedo and spectral characteristics to be a source of EL chondrites (Avdellidou et al., 2022). Indeed, the one EL ordinary chondrite, Neuschwanstein, with a CRE age of 48 Ma (Meier et al., 2022), arrived from the 3:1 resonance ( $a = 2.40 \pm 0.02$  AU,  $i = 11.41 \pm 0.03^\circ$ ), with the Athor family stretching across the inner main belt but centered on  $a = 2.38$  AU and  $i = 8.8^\circ$ . The Athor family, however, has a high dynamical age of  $\sim 3000$  Ma, and a 48-Ma cluster has not yet been identified in this family.

EH chondrite Raja arrived also from the inner main belt, from an evolved orbit with inclination  $i = 6.31 \pm 0.34^\circ$  (Zappatini, Gnos, et al., 2024) not unlike the  $8.8^\circ$  of the Athor family. No CRE age has been determined yet. Both EL and EH chondrites have CRE peaks at  $\sim 3$  Ma,  $\sim 8$  Ma and a broad peak at 20–50 Ma (Eugster, 2006; Wieler, 2002). A second EH3 meteorite fell near Ait Saoun in Morocco on August 6, 2024 (Chennaoui-Aoudejehane, Spilde, et al., 2024), but the fireball was recorded from only one camera station and no orbit has been derived yet. NEA of enstatite affinity appear to have a short semi-major axis and low-inclined orbits (Brož, Vernazza, Marsset, Binzel, et al., 2024).

### The Source of Irons and Stony-Irons

Not much can be said here about the origin of irons and stony-irons. There are about 13 different iron groups (Scott, 2020). One iron Ådalen (provisional name), of unknown classification pending analysis, had an evolved orbit  $a = 1.90 \pm 0.03$  AU and  $i = 15.22 \pm 0.14^\circ$  (Kyrylenko et al., 2023), suggesting it was delivered by the  $v_6$  resonance from the inner main belt. Iron asteroids are thought to be of M-class, but that is uncertain until asteroid 16 Psyche is visited by NASA's Psyche mission. Kilometer-sized NEAs of M-class mostly come in on highly evolved short  $a \sim 1$  AU and high  $i \sim 15$ – $30^\circ$  orbits, with some examples from high  $i$  and  $a \sim 3.2$  AU and from low  $i$  and  $a \sim 2.2$  AU (Brož, Vernazza, Marsset, Binzel, et al., 2024). The one observed iron meteorite orbit does not fall in any of these groups. Most M-class asteroids are found in the central, pristine, and outer main belt (DeMeo & Carry, 2014).

### The Source of Ureilites

The reflectance spectrum of polymict ureilite Almahata Sitta, recovered from asteroid 2008 TC3, is unknown among main belt asteroids (Jenniskens et al., 2010). Recent studies of space weathering of ureilite surfaces have shown that the meteorites will evolve a more reddish spectral slope over time (Goodrich et al., 2019). DeMeo et al. (2022) matched ureilites with L-class asteroids (not to be confused with L-chondrite type meteorites).

As a group, ureilites have a CRE age distribution starting at  $\sim 45$  Ma, smoothly increasing in number to shorter ages, with most between 1 and 20 Ma (David & Leya, 2019; Leya & Stephenson, 2019). There are no clear peaks in the distribution. The CRE age of 2008 TC3 was about 20 Ma, although individual chondrite clasts showed a range in CRE ages from 7 to 24 Ma (Riebe et al. 2017, 2022), in line with other ureilites having CRE ages lower than 45 Ma. This may reflect ongoing fragmentation of these asteroids from their source region to impact on Earth. The ureilites in 2008 TC3 were brittle and easily broken.

Here, we note that the space-weathered spectrum of 2008 TC3 is not unlike that of L-class (234) Barbara. That asteroid is the name type of the “Barbarians”, scattered asteroids in the inner main belt that have unusual polarimetric properties because they are a mineral assemblage composed of high albedo, high index of refraction inclusions with a small optical size scale embedded in a dark matrix material more closely related to C-complex asteroids (Masiero et al., 2023). Mahlke et al. (2023) suggested that the high albedo component was CAI inclusions and that these asteroids correspond to CO-

TABLE 9. Chronology of proposed asteroid-meteorite links in earlier reviews by Jenniskens (2014, 2018) and the links made here. Results are compared to 1-km sized NEA source regions proposed by Brož, Vernazza, Marsset, Binzel, et al. (2024) and Brož, Vernazza, Marsset, DeMeo, et al. (2024)<sup>a</sup> and Marsset et al. (2024).

Type (CRE age)	Meteoroids/meteorites:			1 km-sized NEA: 2024 (Brož et al.)
	2013	2018	2024 (this work)	
HED	<b>Vesta family</b>	<b>Vesta family</b>	<b>Vesta craters</b> (Table 7)	Vesta family
LL	<b>Flora family</b>	<b>Flora family</b>	<b>Flora family</b>	Flora family
LL shocked	—	—	Flora family/Baptistina family	—
LL + H breccia	—	—	Eunomia family	—
L/LL	—	—	Flora?	Juno family
H (7 Ma, $i < 5^\circ$ )	—	—	<b>Koronis family</b> —Karin cluster	—
H (12 Ma, $i < 5^\circ$ )	—	—	<b>Koronis family</b> —Koronis <sub>2</sub>	—
H (83 Ma, $i < 5^\circ$ )	—	—	<b>Koronis family</b> —Koronis <sub>3</sub>	—
H (35 Ma, $i < 10^\circ$ )	—	Low- <i>i</i> IMB	Massalia <sub>2</sub> –40 Ma cluster	—
H (6 Ma, $i > 10^\circ$ )	Phocaea family?	Phocaea family	Nele (=Iannini) family	—
H (18 Ma, $i > 10^\circ$ )	—	—	Maria family—Crescentia cluster?	Phocaea and Maria families
L	—	Low- <i>i</i> IMB	Hertha family	Massalia <sub>2</sub> cluster
L (450 Ma Ar-Ar)	Gefion family	Low- <i>i</i> , 3:1	Hertha family	Juno and Gefion families
L (45 Ma, 450 Ma Ar-Ar)	—	—	Hertha family—Hertha <sub>2</sub> cluster	—
CI <sup>b</sup>	—	—	<b>Polana/Eulalia family</b>	Polana, Euphrosyne, etc. families
CM (OMB)	—	—	Themis family—Beagle cluster	Adeona, Dora, etc. families
CM (IMB)	Eulalia family?	Sulamitis family	Erigone/Sulamitis families	—
C1-ung (Flensburg)	—	—	Veritas family	—
C2-ung (Tagish Lake)	—	—	Lacadiera crater?	—
CO/CV/CK (5.5 Ma)	—	—	Eos family—Zelima cluster	—
CO/CV/CK other	—	—	Eos family	Eos and Watsonia families
CR	—	—	—	Baptistina family
Ureilites	Polana family?	Polana family?	Brangäne family?	—
Aubrites	—	—	IMB; Roxane family?	Hungaria family and IMB
EL	—	—	Athor family?	—
Irons	—	—	?	—

Abbreviation: IMB, inner main belt.

Bold marks the more certain identifications.

<sup>a</sup>Including information listed on website (Brož, (2023): <https://sirrah.troja.mff.cuni.cz/~mira/meteomod/examples.html> (last accessed 11/1/2024).

<sup>b</sup>Based on asteroid taxonomy by Delbo et al. (2023) and samples returned from Bennu/Ryugu.

and CV-class meteorites. However, polymict ureilites are a mixture of low albedo (carbon rich ureilites) and high albedo materials of enstatite and ordinary chondrites. That mixture is intimate even at small scales and thus could be an alternative, especially if the asteroids are covered in a thin layer of fine-grained regolith.

The L-class asteroid family Brangäne in the central main belt at  $i \sim 10^\circ$  near the 3:1 resonance contains such Barbarians and represents a recent  $45 \pm 8$  Myr old (Brož, Vernazza, Marsset, Binzel, et al., 2024; Paolicchi et al., 2019; Spoto et al., 2015) cratering event among such asteroids. The family is rich in small asteroids. This possible link remains uncertain, also because the observed orbit of 2008 TC3 is highly evolved, with a short semi-major axis.

## CONCLUSIONS

Since the Jenniskens (2018) review, the number of documented meteorite falls from the observation of meteors has doubled to 75. The information from sample return missions and asteroid taxonomic studies has also increased. Taken together, it is now possible to assign more meteorite types to dominant asteroid families and even specific meteorites to some craters on Vesta. The chronology of our understanding, expressed at different levels of certainty, is summarized in Table 9 and Figure 14.

Compared to the 2018 review, there has been no change to the assignment of LL chondrites to the Flora family and delivery via the  $v_6$  resonance. This assignment

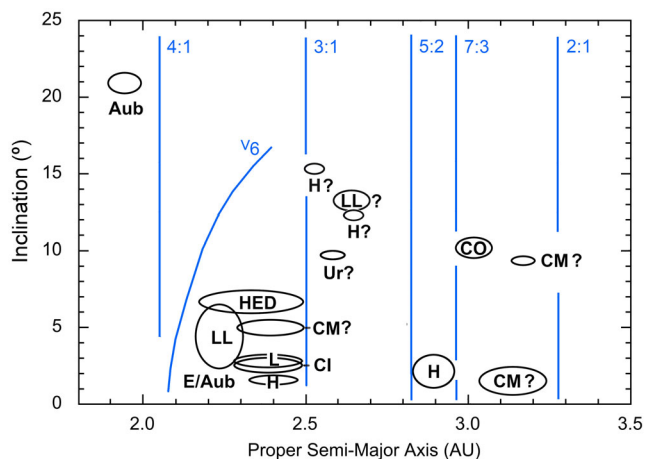


FIGURE 14. Schematic diagram showing the proposed origin regions of our meteorites in the main asteroid Belt.

is strengthened by recent studies showing that larger NEA also arrive from the same source, as did the 20 m-sized asteroid that caused the Chelyabinsk airburst.

We also confirm that HED meteorites likely originate from Vesta, not from the Vesta family but from Vesta itself. It is now shown that they can be linked to a small number of specific impact craters imaged in NASA's Dawn mission. They mostly arrive from the  $v_6$  resonance. In contrast, V-class NEA likely originate from the family, rather than from Vesta itself, arriving from both the  $v_6$  and 3:1 resonances.

Meteor observations have now established a source of H chondrites at low inclination beyond the 5:2 mean-motion resonance, three of which have the 7-Ma age at the peak of the H-chondrite CRE age distribution. These likely originated from the  $5.75 \pm 0.05$  Myr old Karin cluster in the Koronis family. Others appear to derive from the Koronis<sub>2</sub> cluster (age 10–15 Ma), while Ejby may have originated in the impact that resulted in the Koronis<sub>3</sub> cluster. If so, that cluster is  $83 \pm 11$  Myr old.

The Koronis family is not the only source of H chondrites. There is also a source of H-chondrites in the inner main belt with a ~35 Ma CRE peak. The Massalia family has a ~40 Myr old dynamical group and the source asteroid (20) Massalia appears to be an H chondrite. There is no other obvious source of H chondrites in the inner main belt.

The Hertha family is the most likely source of L chondrites, which arrive from a single source in the inner main belt. The Hertha family has near-IR reflectance spectra that are significantly different from, and plot in between, those of the Flora family (LL) and Massalia family (H) members. The 468-Ma collision that caused an unusually high flux of L chondrites on Earth shortly afterwards, and that reset the Ar-Ar age on many

shocked L chondrites, requires an unusual collision. When the Hertha family formed from a collision with X-class (135) Hertha, it created a large debris field of S-class asteroids. This Hertha family was formed with high ejecta speeds and left the parent body covered in the shock-blackened material. In this scenario, the Hertha<sub>2</sub> family represents shock-blackened L chondrites from a later collision on (135) Hertha.

Primitive families in the inner main belt fall in two groups. One group is a source of CI carbonaceous chondrites, as shown by the sample return missions from Ryugu and Bennu. Those are thought to have arrived from the Eulalia and Polana families. This excludes these families as a source for ureilites or CM carbonaceous chondrites, as proposed before. However, the Erigone group (including Sulamitis) may be the source of CM clasts in some ordinary chondrites and HED achondrites that originated from the inner main belt.

Another source of CM chondrites exists in the outer main belt. The CM chondrites observed at Earth so far originated from a surprisingly low- $i$  source and lower in inclination ( $i < 3^\circ$ ) than most candidate source regions. The most precisely measured orbit of Winchcombe points to it having evolved from the 5:2 mean-motion resonance. We cannot completely exclude a role for the Astrid family, but a more likely source is the large Themis family in the outer main belt, in particular, the <10 Myr old Beagle cluster. The oldest CM chondrites have ages of 4–14 Ma. That would explain the CM chondrite clasts found in brecciated H chondrites.

The orbit of Flensburg points to a link between C1-ungrouped (CM-affiliated) carbonaceous chondrites and the Veritas family. It is possible that CO/CV- and CK-class carbonaceous chondrites originate from Eos, in particular the Zelima cluster of the same dynamical age as one of the CRE age peaks of these meteorite types.

We have now entered an age where meteorites can be used as geological hand specimens of selected regions in the asteroid belt, but much work is still required to expand the current reach. Some of our proposed associations in Table 9 and Figure 14 differ from those suggested in the recent literature and require more work. Notably, our suggestions differ from the recent work of Brož, Vernazza, Marsset, Binzel, et al. (2024) and Brož, Vernazza, Marsset, DeMeo, et al. (2024) and Marsset et al. (2024) in regard to the origin of L, H, and CM chondrites.

Future tracking of meteorite orbits has the potential to set firmer constraints on the identity of the source regions and the age of young asteroid families. In addition, the CRE age and Ar-Ar resetting ages still need to be measured for 26 of the meteorites with documented orbits, to bring to light the dynamical evolution of small asteroids and meteoroids from their source regions to Earth.

**Acknowledgments**—We thank reviewers Jiří Borovička and an anonymous referee for improving the content of the manuscript, and we thank Kees Welten for proof reading. The meteorite characterization required for this work is the product of laboratory work by numerous researchers and teams. We especially thank Henner Busemann, My Riebe, Matthias M. Meier, Kees Welten, Marc Caffee, and others for their work on CRE ages. We thank Takahiro Hiroi for assistance with Table 3. Welten provided the bulk wt% metal and composition for *Annama* reported in Table 2. The meteor data are collected by network and camera operators all over the world. The investigation described here was performed as part of efforts to develop a Global Fireball Observatory, with support by P. Bland, E. Samson, M. Towner, and M. Cupák at Curtin University. The *NASA Meteorite Tracking and Recovery Network* in California and Nevada operates as part of the Global Fireball Observatory, with support by Jim Albers, Tom Herring (WNC/Jack C. Davis Observatory), Jon Richards, Kostas Chloros (Lick Observatory), Lance Ginner, Jim Collins, Alexander Pollak and Wael Farrah (Allan Telescope Array), John Kenney (CUI), Rita Pujari and Natalie Swingle (GBCNV), Emory and Eva La Rue, Amina Anderson, Rosana Romer-Correa, Pamela Such and Leslie Kuiper, Robert Lunsford, Jason Utas, Eric McLaughlin (Rancho Mirage Observatory), Ryan Dorsey (Lewis Center for Educational Research), Sean Spratt and Michael Lewis, Frederick Ringwald (CSU Fresno), and Sam Miller (Sierra Remote Observatories). The CAMS meteoroid orbit survey in California is supported by Jim Albers, Dave Samuels, Bryant Grigsby, Kostas Chloros, Eric Eglund, and Tim Beck. The work on this paper was supported by NASA grant 80NSSC18K0854 “A meteorite-type dependent orbital element survey of small impacting NEO” and by the NASA Ames Research Center’s Asteroid Threat Assessment Project (ATAP).

**Conflict of Interest**—The authors operate the CAMS meteoroid orbit survey and the Global Fireball Observatory program.

**Data Availability Statement**—Data sharing not applicable to this article as no datasets were generated or analysed during the current study.

**Editorial Handling**—Dr. Josep M. Trigo-Rodríguez

## REFERENCES

- Aljbaae, S., Carruba, V., Masiero, J. R., Domingos, R. C., and Huaman, M. 2017. The Maria Asteroid Family. *Monthly Notices of the Royal Astronomical Society* 471: 4820–26.
- Aljbaae, S., Souchay, J., Prado, A. F. B. A., and Chanut, T. G. G. 2019. A Dynamical Study of the Gefion Asteroid Family. *Astronomy & Astrophysics* 622: 6 id.A39.
- Amaral, L. S., Trindade, L. S., Bella, C. A. P. B., Zurita, M. L. P. V., Poltronieri, R. C., Silva, G. G., Faria, C. J. L., Jung, C. F., and Koukal, J. A. 2017. Proceedings of the International Meteor Conference, Petnica, Serbia, 21–24 September 2017, edited by M. Gyssens, and J.-L. Rault, p. 171–75. Mechelen: International Meteor Organization.
- Anderson, S. L., Benedix, G. K., Godel, B., Alosius, R. M. L., Krietsch, D., Busemann, H., Maden, C., et al. 2024. The Arpu Kvilpu Meteorite: In-Depth Characterization of an H5 Chondrite Delivered from a Jupiter Family Comet Orbit. *Meteoritics & Planetary Science* 59: 3087–3110.
- Anderson, S. L., Towner, M. C., Fairweather, J., Bland, P. A., Devillepoix, H. A. R., Sansom, E. K., Cupak, M., Shober, P. M., and Benedix, G. K. 2022. Successful Recovery of an Observed Meteorite Fall Using Drones and Machine Learning. *The Astrophysical Journal Letters* 930: 7 L25.
- Andrade, M., Docobo, J. A., Garcia-Guinea, J., Campo, P. P., Tapia, M., Sánchez-Muoz, L., Villasante-Marcos, V., et al. 2022. The Traspena Meteorite: Heliocentric Orbit, Atmospheric Trajectory, Strewn Field, and Petrography of a New L5 Ordinary Chondrite. *Monthly Notices of the Royal Astronomical Society* 518: 3850–76.
- Antier, K. 2023. Bolide du 10 Septembre, 00h13. Online at Vigie Ciel/FRIPON website. [cited 2023 September]. Available from: <https://www.vigie-ciel.org/2023/09/10/bolide-du-10-septembre-00h13/>.
- Arredondo, A., Campins, H., Pinilla-Alonso, N., de León, J., Lorenzi, V., and Morate, D. 2021. Near-Infrared Spectroscopy of the Sulamitis Asteroid Family: Surprising Similarities in the Inner Belt Primitive Asteroid Population. *Icarus* 358: 114210.
- Arredondo, A., Campins, H., Pinilla-Alonso, N., de León, J., Lorenzi, V., Morate, D., Rizo, J. L., and De Prá, M. 2021. Spectral Diversity of the Inner Belt Primitive Asteroid Background Population. *Icarus* 368: 114619.
- Arredondo, A., Lorenzi, V., Pinilla-Alonso, N., Campins, H., Malfavan, A., de León, J., and Morate, D. 2020. Near-Infrared Spectroscopy of the Klio Primitive Inner-Belt Asteroid Family. *Icarus* 335: 113427.
- Avdellidou, C., Delbo, M., Morbidelli, A., Walsh, K. J., Munaibari, E., Bourdelle de Micas, J., Devogèle, M., Fornasier, S., Gounelle, M., and van Belle, G. 2022. Athor Asteroid Family as the Source of the EL Enstatite Meteorites. *Astronomy & Astrophysics* 665: 13 L9.
- Bagolia, C., Bhandari, N., Sinha, N., Goswami, J. N., Lal, D., and Lorin, J. C. 1980. Multiple Fall of Příbram Meteorites Photographed. XII—Pre-Atmospheric Size of the Příbram Meteorite Based on Studies of Fossil Cosmic Ray Tracks and Spallation Products. *Bulletin of the Astronomical Institute of Czechoslovakia* 31: 51–58.
- Balossi, R., Tanga, P., Sergeev, A., Cellino, A., and Spoto, F. 2024. Gaia DR3 Asteroid Reflectance Spectra: L-Type Families, Memberships, and Ages. Applications of Gaia Spectra. *Astronomy & Astrophysics* 688: 14 A221.
- Barghini, D., Carbognani, A., et al. 2023. Analisi dati del bolide di San Valentino. PRISMA Days 2023, Prato, 17–18 November 2023 [cited 2024 September 15]. Available from: [https://indico.ict.inaf.it/event/2601/contributions/16309/attachments/7493/15483/01.Analisi\\_Bolide\\_Matera.pdf](https://indico.ict.inaf.it/event/2601/contributions/16309/attachments/7493/15483/01.Analisi_Bolide_Matera.pdf).

- Barghini, D., Carbognani, A., Gardiol, D., Bertocco, S., Di Carlo, M., Di Martino, M., Falco, C., et al. 2024. The Recovery of the Matera H5 Ordinary Chondrite Thanks to the Observations of the PRISMA Fireball Network. *Europianet Science Congress 2024*, id. EPSC2024-449.
- Bell, J. F. 1988. A Probable Asteroidal Parent Body for the CO or CV Chondrites. *Meteoritics* 23: 256–57.
- Benedix, G. K., Bland, P. A., Friedrich, J. M., Mittlefehldt, D. W., Sanborn, M. E., Yin, Q.-Z., Greenwood, R. C., et al. 2017. Bunburra Rockhole: Exploring the Geology of a New Differentiated Asteroid. *Geochimica et Cosmochimica Acta* 208: 145–159.
- Betlem, H., ter Kuile, C. R., de Lignie, M., van't Leven, J., Jobse, K., Miskotte, K., and Jenniskens, P. 1998. Precision Meteor Orbits Obtained by the Dutch Meteor Society—Photographic Meteor Survey (1981–1993). *Astronomy & Astrophysics, Supplement Series* 128: 179–185.
- Bischoff, A., Alexander, C. M. O'D., Barrat, J.-A., Burkhardt, C., Busemann, H., Degering, D., Di Rocco, T., et al. 2021. The Old, Unique C1 Chondrite Flensburg—Insight into the First Processes of Aqueous Alteration, Brecciation, and the Diversity of Water-Bearing Parent Bodies and Lithologies. *Geochimica et Cosmochimica Acta* 293: 142–186.
- Bischoff, A., Barrat, J.-A., Berndt, J., Borovička, J., Burkhardt, C., Busemann, H., Hakenmüller, J., et al. 2019. The Renchen L5–6 Chondrite Breccia. *Geochemistry* 79: 125525.
- Bischoff, A., Patzek, M., Alosius, R. M. L., Barrat, J.-A., Berndt, J., Busemann, H., Degering, D., et al. 2024. The Anomalous Polymict Ordinary Chondrite Breccia of Elmshorn (H3–6)—Late Reaccretion after Collision between Two Ordinary Chondrite Parent Bodies, Complete Disruption, and Mixing Possibly about 2.8 Gyr Ago. *Meteoritics & Planetary Science* 59: 2321–56.
- Bischoff, A., Patzek, M., Barrat, J.-A., Berndt, J., Busemann, H., Degering, D., Di Rocco, T., et al. 2024. Cosmic Pears from the Havelland (Germany): Ribbeck, the Twelfth Recorded Aubrite Fall in History. *Meteoritics & Planetary Science* 59: 35 14245.
- Bischoff, A., Patzek, M., Di Rocco, T., Pack, A., Stojic, A., Berndt, J., and Peters, S. 2023. Saint-Pierre-le-Viger (L5–6) from asteroid 2023 CX1 Recovered in the Normandy, France—220 Years after the Historic Fall of L'Aigle (L6 Breccia) in the Neighborhood. *Meteoritics & Planetary Science* 58: 1385–98.
- Bischoff, A., Patzek, M., Peters, S. T. M., Barrat, J.-A., Di Rocco, T., Pack, A., Ebert, S., Jansen, C. A., and Kmiecik, K. 2022. The Chondrite Breccia of Antonin (L4–5)—A New Meteorite Fall from Poland with a Heterogeneous Distribution of Metal. *Meteoritics & Planetary Science* 57: 2127–42.
- Bland, P. A., Spurný, P., Bevan, A. W. R., Howard, K. T., Towner, M. C., and Benedix, G. K. 2011. The Australian Desert Fireball Network: A New Era for Planetary Science. *Australian Journal of Earth Sciences* 59: 177–187.
- Bland, P. A., Spurný, P., Towner, M. C., Bevan, A. W. R., Singleton, A. T., Bottke, W. F., Greenwood, R. C., et al. 2009. An Anomalous Basaltic Meteorite from the Innermost Main Belt. *Science* 325: 1525–27.
- Bland, P. A., Towner, M. C., Sansom, E. K., Devillepoix, H., Howie, R. M., Paxman, J. P., Cupák, M., et al. 2016. Fall and Recovery of the Murrili Meteorite, and an Update on the Desert Fireball Network 79th Annual Meeting of the Meteoritical Society (LPI Contrib. No. 1921), id.6265.
- Bogard, D. D., Clark, R. S., Keith, J. E., and Reynolds, M. A. 1971. Noble Gases and Radionuclides in Lost City and Other Recently Fallen Meteorites. *Journal of Geophysical Research* 76: 4076–83.
- Bolin, B. T., Morbidelli, A., and Walsh, K. J. 2018. Size-Dependent Modification of Asteroid Family Yarkovsky V-Shapes. *Astronomy & Astrophysics* 611: 27 A82.
- Borovička, J., Bettonvil, F., Baumgarten, G., Strunk, J., Hankey, M., Spurný, P., and Heinlein, D. 2021. Trajectory and Orbit of the Unique Carbonaceous Meteorite Flensburg. *Meteoritics & Planetary Science* 56: 425–439.
- Borovička, J., Popova, O., and Spurný, P. 2019. The Maribo CM2 Meteorite Fall—Survival of Weak Material at High Entry Speed. *Meteoritics & Planetary Science* 54: 1024–41.
- Borovička, J., Spurný, P., and Shrubny, L. 2020. Two Strengths of Ordinary Chondritic Meteoroids as Derived from their Atmospheric Fragmentation Modeling. *The Astronomical Journal* 160: 42–57.
- Borovička, J., Spurný, P., Shrubny, L., Štork, R., Kotková, L., Fuchs, J., Keclíková, J., et al. 2022. Data on 824 Fireballs Observed by the Digital Cameras of the European Fireball Network in 2017–2018. I. Description of the Network, Data Reduction Procedures, and the Catalog. *Astronomy & Astrophysics* 667: 20 A157.
- Borovička, J., Spurný, P., and Brown, P. 2015. Small near-Earth Asteroids as a Source of Meteorites. In *Asteroids IV*, edited by P. Michel, F. E. DeMeo, and W. F. Bottke, Jr., 257–280. Tucson AZ: University of Arizona Press.
- Borovička, J., Spurný, P., Brown, P., Wiegert, P., Kalenda, P., Clark, D., and Shrubny, L. 2013. The Trajectory, Structure and Origin of the Chelyabinsk Asteroidal Impactor. *Nature* 503: 235–37.
- Borovička, J., Spurný, P., Kalenda, P., and Tagliaferri, E. 2003. The Morávka Meteorite Fall: 1 Description of the Events and Determination of the Fireball Trajectory and Orbit from Video Records. *Meteoritics & Planetary Science* 38: 975–987.
- Borovička, J., Spurný, P., Šegon, D., Andreić, Ž., Kac, J., Korlević, K., Atanackov, J., et al. 2015. The Instrumentally Recorded Fall of the Križevci Meteorite, Croatia, February 4, 2011. *Meteoritics & Planetary Science* 50: 1244–59.
- Borovička, J., Tóth, J., Igaz, A., Spurný, P., Kalenda, P., Haloda, J., Svoreá, J., et al. 2013. The Košice Meteorite Fall: Atmospheric Trajectory, Fragmentation, and Orbit. *Meteoritics & Planetary Science* 48: 1757–79.
- Borovička, J., Weber, H. W., Jopek, T., Jakes, P., Randa, Z., Brown, P. G., ReVelle, D. O., et al. 2003. The Morávka Meteorite Fall: 3. Meteoroid Initial Size, History, Structure, and Composition. *Meteoritics & Planetary Science* 38: 1005–21.
- Bottke, W. F., Morbidelli, A., Jedicke, R., Petit, J.-M., Levison, H. F., Michel, P., and Metcalfe, T. S. 2002. Debaised Orbital and Absolute Magnitude Distribution of the Near-Earth Objects. *Icarus* 146: 399–433.
- Bottke, W. F., Nesvorný, D., Grimm, R. E., Morbidelli, A., and O'Brien, D. P. 2006. Iron Meteorites as Remnants of Planetesimals Formed in the Terrestrial Planet Region. *Nature* 439: 821–24.
- Bottke, W. F., Vokrouhlický, D., Rubincam, D. P., and Nesvorný, D. 2006. The Yarkovsky and Yorp Effects:

- Implications for Asteroid Dynamics. *Annual Review of Earth and Planetary Sciences* 34: 157–191.
- Bottke, W., Vokrouhlický, D., Nesvorný, D., and Shrubny, L. 2010. (6) Hebe Really is the H Chondrite Parent Body. *Bulletin of the American Astronomical Society* 42: 1051. AAS DPS meeting #42, id. 46.06.
- Bourdelle de Micas, J., Fornasier, S., Avdellidou, C., Delbo, M., van Belle, G. T., Ochner, P., Grundy, W., and Moskovitz, N. 2022. Composition of Inner Main-Belt Planetesimals. *Astronomy and Astrophysics* 665: 23 A83.
- Bourdelle de Micas, J., Fornasier, S., Delbo, M., Ferrone, S., van Belle, G., Ochner, P., and Avdellidou, C. 2024. Compositional Characterization of Primordial S-Type Asteroid Family of the Inner Main Belt. *Astronomy & Astrophysics* 682: 24 A64.
- Branch, P., Hankey, M., and Garvie, L. 2022. Junction City. *Meteoritical Bulletin* 113.
- Brandon, A. D., Puchtel, I. S., Humayum, M., and Zolensky, M. 2005. Osmium Isotope Evidence for an s-Process Carrier in Primitive Chondrites. *36th Lunar and Planetary Science Conference*, abstract #1396.
- Bridges, J. C., and Hutchison, R. 1997. A Survey of Clasts and Large Chondrules in Ordinary Chondrites. *Meteoritics & Planetary Science* 32: 389–394.
- Brown, P. G., Hildebrand, A. R., Zolensky, M. E., Grady, M., Clayton, R. N., Mayeda, T. K., Tagliaferri, E., et al. 2000. The Fall, Recovery, Orbit, and Composition of the Tagish Lake Meteorite: A New Type of Carbonaceous Chondrite. *Science* 290: 320–25.
- Brown, P. G., McCausland, P. J. A., Hildebrand, A. R., Hanton, L. T. J., Eckart, L. M., Busemann, H., Krietsch, D., et al. 2023. The Golden Meteorite Fall: Fireball Trajectory, Orbit, and Meteorite Characterization. *Meteoritics & Planetary Science* 58: 1773–1807.
- Brown, P. G., Vida, D., Moser, D. E., Granvik, M., Koshak, W. J., Chu, D., Steckloff, J., et al. 2019. The Hamburg Meteorite Fall: Fireball Trajectory, Orbit, and Dynamics. *Meteoritics & Planetary Science* 54: 2027–45.
- Brown, P., Ceplecha, Z., Hawkes, R. L., Wetherill, G., Beech, M., and Mossman, K. 1994. The Orbit and Atmospheric Trajectory of the Peekskill Meteorite from Video Records. *Nature* 367: 624–26.
- Brown, P., McCausland, P. J. A., Fries, M., Silber, E., Edwards, W. N., Wong, D. K., Weryk, R. J., Fries, J., and Krzeminski, Z. 2011. The Fall of the Grimsby Meteorite—I: Fireball Dynamics and Orbit from Radar, Video, and Infrasonic Records. *Meteoritics & Planetary Science* 46: 339–363.
- Brown, P., Pack, D., Edwards, W. N., ReVelle, D. O., Yoo, B. B., Spalding, R. E., and Tagliaferri, E. 2004. The Orbit, Atmospheric Dynamics, and Initial Mass of the Park Forest Meteorite. *Meteoritics & Planetary Science* 39: 1781–96.
- Brož, M. 2023. METEOMOD: An Advanced Orbital Distribution Model for Meteoroids <https://sirrah.troja.mff.cuni.cz/~mira/meteoromod/meteoromod.html>.
- Brož, M., Vernazza, P., Marsset, M., Binzel, R. P., DeMeo, F. E., Birian, M., Colas, F., et al. 2024. Source Regions of Carbonaceous Meteorites and near-Earth Objects. *Astronomy & Astrophysics* 689: 42 A183.
- Brož, M., Vernazza, P., Marsset, M., DeMeo, F. E., Binzel, R. P., Vokrouhlický, D., and Nesvorný, D. 2024. Young Asteroid Families as the Primary Sources of Meteorites. *Nature* 634: 566–571.
- Burbine, T. H., Khanani, I., Kumawat, D., Hussain, A., Wallace, S. M., and Dyar, M. D. 2024. Testing the Bus-DeMeo Asteroid Taxonomy Using Meteorite Spectra. *The Planetary Science Journal* 5: 12 194.
- Burbine, T. H., McCoy, T. J., Meibom, A., Gladman, B., and Keil, K. 2002. Meteorite Parent Bodies: Their Number and Identification. In *Asteroids III*, 653–667. Tucson, AZ: University of Arizona Press.
- Bus, S. J., Binzel, R. P., Sunshine, J., Burbine, T. H., and McCoy, T. J. 2002. Near-Infrared Spectroscopy of Henan and Watsonia Family Asteroids. *Bulletin of the American Astronomical Society* 34: 859.
- Campins, H., Hargrove, K., Pinilla-Alonso, N., Howell, E. S., Kelley, M. S., Licandro, J., Mothé-Diniz, T., Fernández, Y., and Ziffer, J. 2010. Water Ice Andorganics on the Surface of the Asteroid 24 Themis. *Nature* 464: 1320–21.
- Cantillo, D. C., Ridenhour, K. I., Battle, A., Joyce, T., Breceda, J. N., Perason, N., and Reddy, V. 2024. Laboratory Spectral Characterization of Ribbeck Aubrite: Meteorite Sample of Earth-Impacting Near-Earth Asteroid 2024 BX1. *Planetary Science Journal* 5: 14 138.
- Carbognani, A., and Fenucci, M. 2023. Identifying Parent Bodies of Meteorites among near-Earth Asteroids. *Monthly Notices of the Royal Astronomical Society* 525: 1705–25.
- Carruba, V. 2009. The (Not So) Peculiar Case of the Padua Family. *Monthly Notices of the Royal Astronomical Society* 395: 358–377.
- Carruba, V. 2016. On the Astrid Asteroid Family. *Monthly Notices of the Royal Astronomical Society* 461: 1605–13.
- Carruba, V. 2019. On the Age of the Beagle Secondary Asteroid Family. *Planetary and Space Science* 166: 90–100.
- Carruba, V., Aljbaae, S., and Winter, O. C. 2015. On the Erigone Family and the z2 Secular Resonance. *Monthly Notices of the Royal Astronomical Society* 455: 2279–88.
- Carruba, V., Aljbaae, S., Farena, A. L., Barletta, W., Lucchini, A., Martins, B., and Furlaneto, P. 2020. Spin Pairs in the Koronis Asteroid Family. *Planetary and Space Science* 193: 105083.
- Carruba, V., Aljbaae, S., Knezevic, Z., Mahlke, M., Masiero, J. R., Roig, F., Domingos, R. C., et al. 2024. On the Identification of the First Young Asteroid Families in g-Type Non-linear Secular Resonances. *Monthly Notices of the Royal Astronomical Society* 528: 796–814.
- Carruba, V., and Barletta, W. 2019. The Influence of Ceres on the Dynamical Evolution of the Zdenekhorský/Nemesis Asteroid Family. *Planetary and Space Science* 165: 10–18.
- Carruba, V., and Nesvorný, D. 2016. Constraints on the Original Ejection Velocity Fields of the Asteroid Families. *Monthly Notices of the Royal Astronomical Society* 457: 1332–38.
- Carruba, V., and Ribeiro, J. V. 2020. The Zelima Asteroid Family: Resonant Configuration and Rotational Fission Clusters. *Planetary and Space Science* 182: 104810.
- Carruba, V., Burns, J. A., Bottke, W., and Nesvorný, D. 2003. Orbital Evolution of the Gefion and Adeona Asteroid Families: Close Encounters with Massive Asteroids and the Yarkovsky Effect. *Icarus* 162: 308–327.
- Carruba, V., Domingos, R. C., Huaman, M. E., dos Santos, C. R., and Souami, D. 2014. Dynamical Evolution and Chronology of the Hygiea Asteroid Family. *Monthly Notices of the Royal Astronomical Society* 437: 2279–90.
- Carruba, V., Domingos, R. C., Nesvorný, D., Roig, F., Huaman, M. E., and Souami, D. 2013. A Multidomain

- Approach to Asteroid Families' Identification. *Monthly Notices of the Royal Astronomical Society* 433: 2075–96.
- Carruba, V., Machuca, J. F., and Gasparino, H. P. 2011. Dynamical Erosion of Asteroid Groups in the Region of the Pallas Family. *Monthly Notices of the Royal Astronomical Society* 412: 2052–62.
- Carruba, V., Novaković, B., and Aljbaae, S. 2017. The Hoffmeister Asteroid Family. *Monthly Notices of the Royal Astronomical Society* 465: 4099–4105.
- Carruba, V., Vokrouhlický, D., Nesvorný, D., and Aljbaae, S. 2018. On the Age of the Nele Asteroid Family. *Monthly Notices of the Royal Astronomical Society* 455: 1308–17.
- Cartwright, J. A., Herzog, G. F., Hermann, S., Shankar, N., McCausland, P. J. A., and Ott, U. 2011. The Grimsby H Chondrite: Combined Noble Gas and Radionuclide Analysis. *42nd Lunar and Planetary Science Conference*, abstract #2686.
- Cartwright, J. A., Ott, U., Mittlefehldt, D. W., Herrin, J. S., Herrmann, S., Mertzman, S. A., Mertzman, K. R., Peng, Z. X., and Quinn, J. E. 2013. The Quest for Regolithic Howardites. Part 1: Two Trends Uncovered Using Noble Gases. *Geochimica et Cosmochimica Acta* 105: 395–421.
- Ceballos, I. Y., Orihuela, J., Goncalves, S. G., Zurita, M., Cardozo, M. D., and Delgado, M. H. 2021. Meteorite and Bright Fireball Records from Cuba. *Mineralia Slovaca* 53: 131–145.
- Celino, A., Bagnulo, S., Tanga, P., Novaković, B., and Delbò, M. 2014. A Successful Search for Hidden Barbarians in the Watsonia Asteroid Family. *Monthly Notices of the Royal Astronomical Society* 439: L75–L79.
- Celino, A., Zappalà, V., Doressoundiram, A., Di Martino, M., Bendjaya, P., Dotto, E., and Migliorini, F. 2001. The Puzzling Case of the Nysa-Polana Family. *Icarus* 152: 225–237.
- Cellino, A., Bagnulo, S., Tanga, P., Devogèle, M., Bendjaya, P., Reilly, E., Rivet, J.-P., and Spoto, F. 2019. Brangäne: A New Family of Barbarian Asteroids. *Monthly Notices of the Royal Astronomical Society* 485: 570–76.
- Ceplecha, Z. 1961. Multiple Fall of Příbram Meteorites Photographed. *Bulletin of the Astronomical Institute of Czechoslovakia* 12: 21–47.
- Ceplecha, Z. 1977. Meteoroid Populations and Orbits. In *Comets, Asteroids, Meteorites: Interrelations, Evolution and Orbits*, vol. 39, 143–152. IAU Colloquium.
- Ceplecha, Z. 1996. Luminous Efficiency Based on Photographic Observations of the Lost City Fireball and Implications for the Influx of Interplanetary Bodies onto Earth. *Astronomy & Astrophysics* 311: 329–332.
- Ceplecha, Z., and ReVelle, D. O. 2005. Fragmentation Model of Meteoroid Motion, Mass Loss, and Radiation in the Atmosphere. *Meteoritics & Planetary Science* 40: 35–54.
- Ceplecha, Z., Borovička, J., Elford, G. W., ReVelle, D. O., Hawkes, R. L., Porubcan, V., and Simek, M. 1998. Meteor Phenomena and Bodies. *Space Science Reviews* 84: 327–471.
- Chapman, C. R., Enke, B., Merline, W. J., Nesvorný, D., Tamblyn, P., and Young, E. F. 2009. Reflectance Spectra of Members of Very Young Asteroid Families. *40th Lunar and Planetary Science Conference*, abstract #2258.
- Chennaoui-Aoudjehane, H., Agee, C. B., Devillepoix, H., Bouvier, A., Benkhaldoun, Z., and Guennoun, M. 2024. Taghzout Meteorite: The First Recovered Fall in Morocco Detected by MOFID Camera Network. 86th Annual Meeting of the Meteoritical Society 2024 (LPI Contribution No. 3036), id. 6030.
- Chennaoui-Aoudjehane, H., Ross, A., and Agee, C. 2024. Taghzout. *Meteoritical Bulletin* 113.
- Chennaoui-Aoudjehane, S. M., Agee, C., and Ziegler, K. 2024. Ait Saoun. *Meteoritical Bulletin* 113.
- Clark, B. E., Bus, S. J., Rivkin, A. S., McConnochie, T., Sanders, J., Shah, S., Hiroi, T., and Shepard, M. 2004. E-Type Asteroid Spectroscopy and Compositional Modeling. *Journal of Geophysical Research, Planets* 109: E02001.
- Cloutis, E., and Gaffey, M. J. 1993. Accessory Phases in Aubrites: Spectral Properties and Implications for Asteroid 44 Nysa. *Earth, Moon, and Planets* 63: 227–243.
- Colas, F. 2023. FRIPON Project Website. [cited 2024 September 1]. Available from: <https://fireball.fripon.org/displaymultiple.php?id=21175>.
- Colas, F., Zanda, B., Bouley, S., Jeanne, S., Malgoyre, A., et al. 2020. FRIPON: A Worldwide Network to Track Incoming Meteoroids. *Astronomy & Astrophysics* 644: A53: 23.
- Consolmagno, G. J., and Drake, M. J. 1977. Composition and Evolution of the Eucrite Parent Body: Evidence from Rare Earth Elements. *Geochimica et Cosmochimica Acta* 41: 1271–82.
- Čuk, M., Gadman, B. J., and Nesvorný, D. 2014. Hungaria Asteroid Family as the Source of Aubrite Meteorites. *Icarus* 239: 154–59.
- David, J.-C., and Leya, I. 2019. Spallation, Cosmic Rays, Meteorites, and Planetology. *Progress in Particle and Nuclear Physics* 109: 103711.
- De León, J., Campins, H., Tsiganis, K., Morbidelli, A., and Licandro, J. 2010. Origin of the Near-Earth Asteroid Phaethon and the Geminids Meteor Showers. *Astronomy & Astrophysics* 513: A26: 7.
- De Prá, M. N., Licandro, J., Pinilla-Alonso, N., Lorenzi, V., Rondón, E., Carvano, J., Morate, D., and De León, J. 2020. The Spectroscopic Properties of the Lixiaohua Family, Cradle of Main Belt Comets. *Icarus* 338: 113473.
- De Prá, M. N., Pinilla-Alonso, N., Carvano, J., Licandro, J., Morate, D., Lorenzi, V., de León, J., Campins, H., and Mothé-Diniz, T. 2020. A Comparative Analysis of the Outer-Belt Primitive Families. *Astronomy & Astrophysics* 643: 16 A102.
- Delbo, M., Avdellidou, C., and Morbidelli, A. 2019. Ancient and Primordial Collisional Families as the Main Sources of X-Type Asteroids of the Inner Main Belt. *Astronomy & Astrophysics* 624: 21 A69.
- Delbo, M., Avdellidou, C., and Walsh, K. J. 2023. Gaia View of Primitive Inner-Belt Asteroid Families. Searching for the Origins of the Asteroids Bennu and Ryugu. *Astronomy & Astrophysics* 680: 8 A10.
- Delbo, M., Walsh, K., Bolin, B., Avdellidou, C., and Morbidelli, A. 2017. Identification of a Primordial Asteroid Family Constrains the Original Planetesimal Population. *Science* 357: 1026–29.
- DeMeo, F. E., Alexander, C. M. O'D., Walsh, K. J., Chapman, C. R., and Binzel, R. P. 2015. The Compositional Structure of the Asteroid Belt. In *Asteroids IV*, edited by P. Michel, F. E. DeMeo, and W. F. Bottke, 13–42. Tucson, AZ: University of Arizona Press.
- DeMeo, F. E., and Carry, B. 2014. Solar System Evolution from Compositional Mapping of the Asteroid Belt. *Nature* 505: 629–634.
- DeMeo, F. E., Binzel, R. P., Carry, B., Polishook, D., and Moskovitz, N. A. 2014. Unexpected D-Type Interlopers in the Inner Main Belt. *Icarus* 229: 392–99.

- DeMeo, F. E., Burt, B. J., Marsset, M., Polishook, D., Burbine, T. H., Carry, B., Binzel, R. P., et al. 2022. Connecting Asteroids and Meteorites with Visible and Near-Infrared Spectroscopy. *Icarus* 380: 114971.
- Dermott, S. F., Christou, A. A., Li, D., Kehoe, T. J. J., and Robinson, J. M. 2018. The Common Origin of Family and Non-Family Asteroids. *Nature Astronomy* 2: 549–554.
- Dermott, S. F., Li, D., Christou, A. A., Kehoe, T. J. J., Murray, C. D., and Robinson, J. M. 2021. Dynamical Evolution of the Inner Asteroid Belt. *Monthly Notices of the Royal Astronomical Society* 505: 1917–39.
- Devillepoix, H. 2020. Puli Ilkaringuru. *Meteoritical Bulletin* 112.
- Devillepoix, H. 2022. How Satellites, Radar and Drones Are Tracking Meteorites and Aiding Earth's Asteroid Defense. *The Conversation*. [cited 2022 November 21]. Available from: <https://theconversation.com/how-satellites-radar-and-drones-are-tracking-meteorites-and-aiding-earths-asteroid-defence-194997>.
- Devillepoix, H. A. R. 2024. Meteorites Recovered Desert Fireball Network. [cited 2024 September 1]. Available from: <https://dfn.gfo.rocks/meteorites.html>.
- Devillepoix, H. A. R., Cupák, M., Bland, P. A., Samson, E. K., Towner, M. C., Howie, R. M., Hartig, B. A. D., et al. 2020. A Global Fireball Observatory. *Planetary and Space Science* 191: 105036.
- Devillepoix, H. A. R., Sansom, E. K., Bland, P. A., Towner, M. C., Cupák, M., Howie, R. M., Jansen-Sturgeon, T., et al. 2018. The Dingle Dell Meteorite: A Halloween Treat from the Main Belt. *Meteoritics & Planetary Science* 53: 2212–27.
- Devillepoix, H. A. R., Sansom, E. K., Shober, P., Anderson, S. L., Downer, M. C., Lagain, A., Cupák, M., et al. 2022. Trajectory, Recovery, and Orbital History of the Madura Cave Meteorite. *Meteoritics & Planetary Science* 57: 1328–38.
- Dionnet, Z., Aléon-Toppani, A., Brunetto, R., Rubino, S., Suttle, M. D., Lantz, C., Avdellidou, C., et al. 2022. Multiscale Correlated Analysis of the Aguas Zarcas CM Chondrite. *Meteoritics & Planetary Science* 57: 965–988.
- Distel, A., Wittmann, A., and Garvie, L. 2023. Mvskoke Merkv. *Meteoritical Bulletin* 113.
- Dunn, T. L., Burbine, T. H., Bottke, W. F., and Clark, J. P. 2013. Mineralogies and Source Regions of Near-Earth Asteroids. *Icarus* 222: 273–282.
- Dykhuis, M. J., and Greenberg, R. 2015. Collisional Family Structure within the Nysa-Polana Complex. *Icarus* 252: 199–211.
- Dyl, K. A., Benedix, G. K., Bland, P. A., Friedrich, J. M., Spurný, P., Towner, M. C., O'Keefe, M. C., et al. 2016. Characterization of Mason Gully (H5): The Second Recovered Fall from the Desert Fireball Network. *Meteoritics & Planetary Science* 51: 596–613.
- Eckart, L. M., Mertens, C. A. K., Busemann, H., Maden, C., Righter, K., and Alexander, C. M. O'D. 2024. Noble Gases in CO Chondrites: Primordial Components, Effects of Parent Body Thermal Alteration, and Cosmic Ray Exposure Ages. *86th Annual Meeting of the Meteoritical Society* (LPI Contribution No. 3036), id.6208.
- Ehlert, S., and Blaauw Erskine, R. 2020. Measuring Fluxes of Meteor Showers with the NASA all-Sky Fireball Network. *Planetary and Space Science* 188: 104938.
- Eloy, P.-A., Trigo-Rodríguez, J. M., Rimola, A., et al. 2021. 25 Years of the Spanish Meteor Network (SPMN) and the 2020 Ursid Meteor Activity. *eMeteorNews* 6: 390–96.
- Erasmus, N., McNeill, A., Mommert, M., Trilling, D. E., Sickafoose, A. A., and Paterson, K. 2019. A taxonomic study of asteroid families from KMTNET-SAAO multiband photometry. *The Astrophysical Journal Supplement Series* 242: 15: 12.
- Eugster, O. 2003. Cosmic-Ray Exposure Ages of Meteorites and Lunar Rocks and their Significance. *Geochemistry* 63: 3–30.
- Eugster, O. 2006. Irradiation Records, Cosmic-Ray Exposure Ages, and Transfer Times of Meteorites. In *Meteorites and the Early Solar System II*, edited by D. S. Lauretta, and H. Y. McSween, Jr., p. 829–851. Tucson, AZ: University of Arizona Press.
- Eugster, O., and Michel, T. 1995. Common Asteroid Break-up Events of Eucrites, Diogenites, and Howardites and Cosmic-Ray Production Rtes for Noble Gases in Achondrites. *Geochimica et Cosmochimica Acta* 59: 177–199.
- Farinella, P., Froeschlé, C., and Gonczi, R. 1994. Meteorite Delivery and Transport. In *Asteroids, Comets, Meteors 1993*, edited by A. Milani, M. Di Martino, and A. Cellino, 205. Dordrecht: Elsevier.
- Farley, K. A., Vokrouhlický, D., Bottke, W. F., and Nesvorný, D. 2006. A Late Miocene Dust Shower from the Break-Up of an Asteroid in the Main Belt. *Nature* 439: 295–97.
- Farnocchia, D., Jenniskens, P., Robertson, D. K., Chesley, S. R., Dimare, L., and Chodas, P. W. 2017. The Impact Trajectory of Asteroid 2008 TC3. *Icarus* 294: 218–226.
- Ferrière, L., Roszjar, J., and Povinec, P. P. 2022. The Kindberg L6 Ordinary Chondrite Fall and Recovery in Austria—A Case Study of Citizen Science. 85th Annual Meeting of the Meteoritical Society (LPI Contribution No. 2695), id. 6116.
- Ferrone, S., Delbo, M., Avdellidou, C., Melikyan, R., Morbidelli, A., Walsh, K., and Deienno, R. 2023. Identification of a 4.3 Billion Year Old Asteroid Family and Planetesimal Population in the Inner Main Belt. *Astronomy & Astrophysics* 676: A5: 20.
- Ferus, M., Petera, L., Koukal, J., Lenza, L., Drtinova, B., Haloda, J., Matysek, D., et al. 2020. Elemental Composition, Mineralogy and Orbital Parameters of the Poranga Meteorite. *Icarus* 341: 113670.
- Fieber-Beyer, S. K., and Gaffey, M. J. 2020. The Family of (6) Hebe. *The Planetary Science Journal* 1: 68.
- Fieber-Beyer, S. K., Gaffey, M. J., Kelley, M. S., Reddy, V., Reynolds, C. M., and Hicks, T. 2011. The Maria Asteroid Family: Genetic Relationships and a Plausible Source of Mesosiderites near the 3:1 Kirkwood Gap. *Icarus* 213: 524–537.
- Florczak, M., Lazzaro, D., Mothé-Diniz, T., Angeli, C. A., and Betzler, A. S. 1999. A Spectroscopic Study of the Themis Family. *Astronomy & Astrophysics, Supplement Series* 134: 463–471.
- Flynn, G. J., Consolmagno, G. J., Brown, P., and Macke, R. J. 2017. Physical Properties of the Stone Meteorites: Implications for the Properties of their Parent Bodies. *Chemie der Erde-Geochemistry* 78: 269–298.
- Foglia, S., and Masi, G. 2004. New Clusters For Highly Inclined Main-Belt Asteroids. *The Minor Planet Bulletin* 31: 100–102.
- Fornasier, S., Lantz, C., Perna, D., Campins, H., Barucci, M. A., and Nesvorný, D. 2016. Spectral Variability on Primitive Asteroids of the Themis and Beagle Families:

- Space Weathering Effects or Parent Body Heterogeneity? *Icarus* 269: 1–14.
- Fornasier, S., Migliorini, A., Dotto, E., and Barucci, M. A. 2008. Visible and near Infrared Spectroscopic Investigation of E-Type Asteroids, Including 2867 Steins, a Target of the Rosetta Mission. *Icarus* 196: 119–134.
- Fries, M., and Fries, J. 2010. Doppler Weather Radar as a Meteorite Recovery Tool. *Meteoritics & Planetary Science* 45: 1476–87.
- Gaffey, M. J., and Fieber-Beyer, S. K. 2019. Is the (20) Massalia Family the Source of the L-Chondrites? *50th Lunar and Planetary Science Conference* (LPI Contribution No. 2132), abstract #1441.
- Gaffey, M. J., and Gilbert, S. L. 1998. Asteroid 6 Hebe: The Probable Parent Body of the H-Type Ordinary Chondrites and the IIE Iron Meteorites. *Meteoritics & Planetary Science* 33: 1281–95.
- Gaffey, M. J., Reed, K. L., and Kelley, M. S. 1992. Relationship of E-Type Apollo Asteroid 3103 (1982 BB) to the Enstatite Achondrite Meteorites and the Hungaria Asteroids. *Icarus* 100: 95–109.
- Galinier, M., Delbo, M., Avdellidou, C., and Galluccio, L. 2024. Discovery of the First Olivine-Dominated A-Type Asteroid Family. *Astronomy & Astrophysics* 683: 10 L3.
- Gardioli, D., Barghini, D., Buzzoni, A., Carbognani, A., Di Carlo, M., Di Martino, M., Knapic, C., et al. 2021. Cavezzo, the First Italian Meteorite Recovered by the PRISMA Fireball Network. Orbit, Trajectory and Strewnfield. *Monthly Notices of the Royal Astronomical Society* 501: 1215–27.
- Garvie, L. A. J. 2021. Mineralogy of the 2019 Aguas Zarcas (CM2) Carbonaceous Chondrite Meteorite Fall. *American Mineralogist* 160: 1900–1916.
- Gatrelle, G. M., Hardersen, P. S., Izawa, M. R. M., and Nowinski, M. C. 2021. Round up the Usual Suspects: Near-Earth Asteroid 17274 (2000 LC16) a Plausible D-Type Parent Body of the Tagish Lake Meteorite. *Icarus* 361: 114349.
- Gattacceca, J., Bonal, L., Sonzogni, C., and Longerey, J. 2020. CV Chondrites; More than One Parent Body. *Earth and Planetary Science Letters* 547: 116467.
- Gil-Hutton, R. 2006. Identification of Families among Highly Inclined Asteroids. *Icarus* 183: 93–100.
- Glass, I. S., and Cooper, T. 2024. News Note: Bright Bolide and Meteorite Fall on 25 August 2024. *Monthly Notes of the Astronomical Society of South Africa* 83: 82–83.
- Gomez Barrientos, J., de Kleer, K., Ehlmann, B. L., Tissot, F. L. H., and Mueller, J. 2024. The Surface Composition of L-Type Asteroids from JWST Spectroscopy. *The Astrophysical Journal Letters* 967: 8 L11.
- Goodrich, C. A., Gillis-Davis, J., Cloutis, E., Applin, D., Takir, D., Hibbitts, C., Christoffersen, R., Fries, M., Klima, R., and Decker, S. 2019. Effects of Space Weathering: On Reflectance Spectra of Ureilites: First Studies. *49th Lunar and Planetary Science Conference* (LPI Contribution No. 2083), abstract #1579.
- Graf, T., and Marti, K. 1995. Collisional History of H Chondrites. *Journal of Geophysical Research* 100: 21247–64.
- Graf, T., Marti, K., Xue, S., Herzog, G. F., Klein, J., Middleton, R., Metzler, K., et al. 1997. Exposure History of the Peekskill (H6) Meteorite. *Meteoritics & Planetary Science* 32: 25–30.
- Granvik, M., and Brown, P. 2018. Identification of Meteorite Source Regions in the Solar System. *Icarus* 311: 271–287.
- Granvik, M., Morbidelli, A., Jedicke, R., Bolin, B., Bottke, W. F., Beshore, E., Vokrouhlický, D., Delbò, M., and Patrick, M. 2016. Super-Catastrophic Disruption of Asteroids at Small Perihelion Distances. *Nature* 530: 303–6.
- Granvik, M., Morbidelli, A., Jedicke, R., Bolin, B., Bottke, W. F., Beshore, E., Vokrouhlický, D., Nesvorný, D., and Michel, P. 2018. Debaised Orbit and Absolute-Magnitude Distributions for Near-Earth Objects. *Icarus* 312: 181–207.
- Greenwood, R. C., Burbine, T. H., and Franchi, I. A. 2020. Linking Asteroids and Meteorites to the Primordial Planetesimal Population. *Geochimica et Cosmochimica Acta* 277: 377–406.
- Gritsevich, M., Moilanen, J., Visuri, J., Meier, M. M. M., Maden, C., Oberst, J., Heinlein, D., et al. 2024. The Fireball of November 24, 1970, as the most Probable Source of the Ischgl Meteorite. *Meteoritics & Planetary Science* 59: 1658–91.
- Guennoun, M., Devillepoix, H. A. R., Cupak, M., Benkhaldoun, Z., Chennaoui-Aoudjehane, H., and Bouvier, A. 2024. Fall Area Calculations and Association of Meteor Orbits with Parent Bodies: A Case Study Using the MOFID Network for Taghzout Meteorite Fall Morocco. 86th Annual Meeting of the Meteoritical Society, 28 July–2 August, Brussels, Belgium (LPI Contrib. No. 3036), id 6215.
- Haack, H., Grau, T., Bischoff, A., Horstmann, M., Wasson, J., Sorensen, A., Laubenstein, M., et al. 2012. Maribo—A New CM Fall from Denmark. *Meteoritics & Planetary Science* 47: 30–50.
- Haack, H., Michelsen, R., Stober, G., Keuer, D., and Singer, W. 2010. The Maribo CM2 Fall: Radar Based Orbit Determination of an Unusually Fast Fireball. Meteoritical Society Meeting 2010, New York, July 26–30, abstract #5085.
- Haack, H., Sørensen, A. N., Bischoff, A., Patzek, M., Barrat, J.-A., Midtskogen, S., Stempels, E., et al. 2019. Ejby – A New H5/6 Ordinary Chondrite Fall in Copenhagen, Denmark. *Meteoritics & Planetary Science* 54: 1853–69.
- Halliday, I., Blackwell, A. T., and Griffin, A. A. 1978. The Innisfree Meteorite and the Canadian Camera Network. *Journal of the Royal Astronomical Society of Canada* 72: 15–39.
- Halliday, I., Griffin, A. A., and Blackwell, A. T. 1996. Detailed Data for 259 Fireballs from the Canadian Camera Network and Inferences Concerning the Influx of Large Meteoroids. *Meteoritics & Planetary Science* 31: 185–217.
- Hamann, C., Greshake, A., Hecht, L., Jenniskens, P., Kaufmann, F., Luther, R., Van den Neucker, A., et al. 2024. Initial Analysis of the Ribbeck Aubrite Recovered from Asteroid 2024 BX1. 86th Annual meeting of the Meteoritical Society. 28 July–2 August, Brussels, Belgium, LPI Contribution no. 3036, abstract #6418.
- Hankey, M., and Branch, P. 2025. Trajectory, Orbit and Strewnfield of the Junction City Meteorite. *Meteoritics & Planetary Science* (in preparation).
- Hankey, M., Molau, S., and Perlerin, V. 2023. ALLSKY7 History, Status and Updates. In *Proceedings of the International Meteor Conference, Porosio, Hungary, 29 September–2 October 2022*, edited by U. Pájer, A. Keresturi, C. Steyaert, J. Rendtel, R. Rudawska, C. Verbeeck, M. Gyssens, and F. Ocana, 139–141. Potsdam: International Meteor Organization.
- Hankey, M., Perlerin, V., Lunsford, R., and Meisel, D. 2013. American Meteor Society Online Fireball Report. In

- Proceedings of the International Meteor Conference, Poznan, Poland, 22–25 August 2013*, edited by M. Gyssens, P. Roggemans, and P. Zoladek, 115–19. Mechelen: International Meteor Organization.
- Hankey, M., Spurný, P., and Shrbený, L. 2025. The Trajectory, Orbit and Strenwfield of the Elmshorn Meteorite. *Meteoritics & Planetary Science* (in preparation).
- Hanuš, J., Marsset, M., Vernazza, P., Viikinkoski, M., Drouard, A., Brož, M., Carry, B., et al. 2019. The Shape of (7) Iris as Evidence of an Ancient Large Impact? *Astronomy & Astrophysics* 624: A121.
- Harvison, B., De Prá, M., Pinilla-Alonso, N., et al. 2024. PRIMASS Near-Infrared Study of the Erigone Collisional Family. *Icarus* 412: 115973.
- Heck, P. R., Greer, J., Boesenberg, J. S., Bouvier, A., Caffee, M. W., Cassata, W. S., Corrigan, C., et al. 2020. The Fall, Recovery, Classification, and Initial Characterization of the Hamburg, Michigan H4 chondrite. *Meteoritics & Planetary Science* 55: 2341–59.
- Heinlein, D., Patzek, M., and Bischoff, A. 2020. Flensburg. *Meteoritical Bulletin* 108.
- Heinlein, D., Patzek, M., and Bischoff, A. 2024. Elmshorn. *Meteoritical Bulletin* 112.
- Hergenrother, C. W., Larson, S. M., and Spahr, T. B. 1996. The Hansa Family: A New High-Inclination Asteroid Family. *Bulletin of the American Astronomical Society* 28: 1097 AAS DPS meeting #28, id.10.07.
- Hernandez, J., Natheus, A., Hiesinger, H., Goetz, W., Hoffmann, M., Schmedemann, N., Thangjam, G., Mengel, K., and Sarkar, R. 2022. Geology and Colour of Kupalo Crater on Ceres. *Planetary and Space Science* 220: 105583.
- Herzog, G. F., and Caffee, M. W. 2014. Cosmic Ray Exposure Ages of Meteorites. In *Treatise on Geochemistry*, 2nd ed., 419–454. Amsterdam: Elsevier.
- Hildebrand, A. R., Hanton, L. T. J., Ciceri, F., Nowell, R., Lyytinen, E., Silber, E. A., Brown, P. G., et al. 2018. Characteristics of a Well Recorded, Bright, Meteorite-Dropping Fireball, British Columbia, Canada, September 4, 2017. *49th Lunar and Planetary Science Conference* (LPI Contribution No. 2083), abstract #3006.
- Hildebrand, A. R., McCausland, P. J. A., Brown, P. G., Longstaffe, F. J., Russell, S. D. J., Tagliaferri, E., Wacker, J. F., and Mazur, M. J. 2006. The Fall and Recovery of the Tagish Lake Meteorite. *Meteoritics & Planetary Science* 41: 407–431.
- Hirayama, K. 1918. Groups of Asteroids of Common Origin. *Astronomical Journal* 31: 185–88.
- Hiroi, T., Zolensky, M. E., and Pieters, C. M. 2001. The Tagish Lake Meteorite: A Possible Sample from a D-Type Asteroid. *Science* 293: 2234–36.
- Hlobik, F., and Tóth, J. 2024. Orbital Evolution and Possible Parent Asteroids of 40 Instrumentally Observed Meteorites. *Planetary and Space Science* 240: 105827.
- Hsieh, H. H., Novaković, B., Walsh, K. J., and Schörghofer, N. 2020. Potential Themis-Family Asteroid Contribution to the Jupiter-Family Comet Population. *The Astronomical Journal* 159: 179, 10 pp.
- Huaman, M., Carruba, V., Domingos, R. C., and Aljbaae, S. 2017. The Asteroid Population in g-Type Non-linear Secular Resonances. *Monthly Notices of the Royal Astronomical Society* 468: 4982–91.
- Huaman, M., Roig, F., Carruba, V., De Cássia Domingos, R., and Aljbaae, S. 2018. The Resonant Population of Asteroids in Liberating States of the v6 Linear Secular Resonance. *Monthly Notices of the Royal Astronomical Society* 481: 1707–17.
- Hyden, J., Thomas, C., Harvison, B., Lucas, M., Trilling, D., Moskovitz, N., and Lim, L. 2020. Spectral Analysis of the Massalia Asteroid Family. *Bulletin of the American Astronomical Society* 52: 429.
- Jenniskens, P. 2014. Recent Documented Meteorite Falls, a Review of Meteorite—Asteroid Links. In *Meteoroids 2013, Proceedings of the Astronomical Conference, A.M. University, Poznan, Poland, August 26–30, 2013*, edited by T. Jopek, F. J. M. Rietmeijer, J. Watanabe, and I. P. Williams, 57–68. Poznan: A. M. University Press.
- Jenniskens, P. 2018. Review of Asteroid-Family and Meteorite-Type Links. *Astronomy in Focus, Proceedings of the IAU* 14: 9–12.
- Jenniskens, P., Albers, J., Tillier, C. E., Edgington, S. F., Longenbaugh, R. S., Goodman, S. J., Rudlosky, S. D., et al. 2018. Detection of Meteoroid Impacts by the Geostationary Lightning Mapper on the GOES-16 Satellite. *Meteoritics & Planetary Science* 53: 2445–69.
- Jenniskens, P., Fries, M. D., Yin, Q.-Z., Zolensky, M., Kort, A. N., Sandford, S. A., Sears, D., et al. 2012. Radar-Enabled Recovery of the Sutter's Mill Meteorite, a Carbonaceous Chondrite Regolith Breccia. *Science* 338: 1583–87.
- Jenniskens, P., Gabadirwe, M., Yin, Q.-Z., Proyer, A., Oliver, M., Kohout, T., Franchi, F., Givson, R., et al. 2021. The Impact and Recovery of Asteroid 2018 LA. *Meteoritics & Planetary Science* 56: 844–893.
- Jenniskens, P., Gural, P. S., Dynneson, L., Grigsby, B. J., Newman, K. E., Borden, M., Koop, M., and Holman, D. 2011. CAMS: Cameras for Allsky Meteor Surveillance to Establish Minor Meteor Showers. *Icarus* 216: 40–61.
- Jenniskens, P., Moskovitz, N., Garvie, L. A. J., Yin, Q.-Z., Howell, J. A., Free, D. L., Albers, J., et al. 2020. Orbit and Origin of the Dishcii'bikoh (Arizona) LL7 Chondrite. *Meteoritics & Planetary Science* 55: 535–557.
- Jenniskens, P., Robertson, D., Goodrich, C. A., Shaddad, M. H., Kudoda, A., Fioretti, A. M., and Zolensky, M. E. 2022. Bolide Fragmentation: What Parts of Asteroid 2008TC3 Survived to the Ground? *Meteoritics & Planetary Science* 57: 1641–64.
- Jenniskens, P., Rubin, A. E., Yin, Q.-Z., Sears, D. W. G., Sandford, S. A., Zolensky, M. E., Krot, A. N., et al. 2014. Fall, Recovery and Characterization of the Novato L6 Chondrite Breccia. *Meteoritics & Planetary Science* 49: 1388–1424.
- Jenniskens, P., Shaddad, M. H., Numan, D., Elsir, S., Kudoda, A. M., Zolensky, M. E., Le, L., et al. 2009. The Impact and Recovery of Asteroid 2008 TC3. *Nature* 458: 485–88.
- Jenniskens, P., Soto, G. J., Goncalves Silva, G., et al. 2024. Orbit, Meteoroid Size, and Cosmic-Ray Exposure History of the Aguas Zarcas CM2 Breccia. *Meteoritics & Planetary Science* (submitted).
- Jenniskens, P., Utas, J., Yin, Q.-Z., Matson, R. D., Fries, M., Howell, J. A., Free, D., et al. 2019. The Creston, California, Meteorite Fall and the Origin of L Chondrites. *Meteoritics & Planetary Science* 54: 699–720.
- Jenniskens, P., Vaubaillon, J., Binzel, R. P., DeMeo, F. E., Nesvorný, D., Bottke, W. F., Fitzsimmons, A., et al. 2010. Almahata Sitta (= Asteroid 2008 TC3) and the Search for

- the Ureilite Parent Body. *Meteoritics & Planetary Science* 45: 1590–1617.
- Kac, J. 2005. A<sup>3</sup>N—Alpe-Adria all-Sky Network. In *Proceedings of the International Meteor Conference, Held in Oostmalle, Belgium 15–18 September*, edited by L. Bastiaens, J. Verbert, J.-M. Wislez, and C. Verbeeck, 167–170. Mechelen: International Meteor Organization.
- Kaluna, H. M., Masiero, J. R., and Meech, K. J. 2016. Space Weathering Trends Among Carbonaceous Asteroids. *Icarus* 264: 62–71.
- Kanamori, T. 2009. A Meteor Shower Catalog Based on Video Observations in 2007–2008. *Journal of the International Meteor Organization* 37: 55–62.
- Kanamori, T. 2020. Meteorite Recovery in Chiba Prefecture Japan. In *CBET 4810*, edited by D. W. E. Green, 1. Cambridge, MA: Central Bureau for Astronomical Telegrams.
- Karner, J. K., Fries, M. D., Hutson, M. L., Ruzicka, A. M., Sheikh, D., and Terlaga, M. 2022. The Fall and Recovery of the Great Salt Lake Meteorite. 86th Annual Meeting of the Meteoritical Society (LPI Contribution No. 2990), id. 6307.
- Kartashova, A., Golubaev, A., Mozgova, A., Chuvashov, I., Bolgova, G., Glazachev, D., and Efremov, V. 2020. Investigation of the Ozerki Meteoroid Parameters. *Planetary and Space Science* 193: 105034.
- Kelley, M. S., Vilas, F., Gaffey, M. J., and Abell, P. A. 2003. Quantified Mineralogical Evidence for a Common Origin of 1929 Kollaa with 4 Vesta and the HED Meteorites. *Icarus* 165: 215–18.
- Kerraouch, I., Kebukawa, Y., Bischoff, A., Zolensky, M. E., Wölfer, E., Hellmann, J. L., Ito, M., et al. 2022. Heterogeneous Nature of the Carbonaceous Chondrite Breccia Aguas Zarcas—Cosmochemical Characterization and Origin of New Carbonaceous Chondrite Lithologies. *Geochimica et Cosmochimica Acta* 334: 155–186.
- King, A. J., Daly, L., Row, J., Joy, K., et al. 2022. The Winchcombe Meteorite, a Unique and Pristine Witness from the Outer Solar System. *Science Advances* 8: 17. doi.10.1126/sciadv.abc3925
- Kita, N. T., Welten, K. C., Valley, J. W., Spicuzza, M. J., Nakashima, D., Tenner, T. J., Ushikubo, T., et al. 2013. Fall, Classification, and Exposure History of the Mifflin L5 Chondrite. *Meteoritics & Planetary Science* 48: 641–655.
- Kneissl, T., Schmedemann, N., Reddy, V., Williams, D. A., Walter, S. H. G., Neesemann, A., Michael, G. G., et al. 2014. Morphology and Formation Ages of Mid-Sized Post-Rheasilvia Craters—Geology of Quadrangle Tuccia, Vesta. *Icarus* 244: 133–157.
- Kohout, T., Meier, M. M. M., Maden, C., Busemann, H., Welten, K. C., Laubenstein, M., Caffee, M. W., Gritsevich, M., and Grokhovsky, V. 2016. Pre-Entry Size and Cosmic History of the Annama Meteorite. 79th Annual Meeting of the Meteoritical Society (LPI Contr. 1921), id. 6316.
- Kövágó, G. 2021. Possible Meteorite Fall in Austria. *eMeteorNews* 6: 87–89.
- Kozubal, M., Gasdia, F. W., Dantowitz, R. F., Scheirich, P., and Harris, A. W. 2011. Photometric Observations of Earth-Impacting Asteroid 2008 TC3. *Meteoritics & Planetary Science* 46: 534–542.
- Krietsch, D., Busemann, H., Riebe, M. E. I., King, A. J., Alexander, C. M. O'D., and Maden, C. 2021. Noble Gases in CM Carbonaceous Chondrites: Effect of Parent Body Aqueous and Thermal Alteration and Cosmic Ray Exposure Ages. *Geochimica et Cosmochimica Acta* 310: 240–280.
- Krohn, K., Jaumann, R., Elbeshausen, D., Kneissl, T., Schmedemann, N., Wagner, R., Voigt, J., et al. 2014. Asymmetric Craters on Vesta: Impact on Sloping Surfaces. *Planetary and Space Science* 103: 36–56.
- Krzyszowska, A. M., Tyminski, Z., Allen, N. M., Busemann, H., Maden, C., Stachowicz, M., Kusiak, M. A., Lee, S., and Yi, K. 2024. Collisional History of L Chondrite Antonin Interred from K-Ar, U,Th-He and Phosphate U-Pb Dating. 86th Annual Meeting of the Meteoritical Society 2024 (LPI Contrib. No. 3036), id. 6168.
- Krzyszowska, A. M., Tyminski, Z., Kmiecik, K., Shrubny, L., Spurny, P., and Borovicka, J. 2022. The Antonin L5 Chondrite Fall (Poland): Mineralogy and Petrology of Meteorite, Bolide Trajectory and Meteoroid Orbit. 85th Annual Meeting of the Meteoritical Society 2024. (LPI Contrib. No. 2695), id. 6144.
- Kurat, G., Koeberl, C., Presper, T., Brandstätter, F., and Maurette, M. 1994. Petrology and Geochemistry of Antarctic Micrometeorites. *Geochimica et Cosmochimica Acta* 58: 3879–3904.
- Kyrylenko, I., Golubov, O., Slyusarev, I., Visuri, J., Gritsevich, M., Krugly, Y. N., Belskaya, I., and Shevchenko, V. G. 2023. The First Instrumentally Documented Fall of an Iron Meteorite: Orbit and Possible Origin. *The Astrophysical Journal* 953: 10 20.
- Leya, I., and Stephenson, P. C. 2019. Cosmic Ray Exposure Ages for Ureilites—New Data and a Literature Study. *Meteoritics & Planetary Science* 54: 1521–32.
- Li, B., Xu, Z., Li, Y., Liao, S., Hu, S., Xu, W., and Zhao, H.-B. 2025. The Fall and Origins of the Meteoroid Tanxi. *Research in Astronomy and Astrophysics* (submitted).
- Liao, S., and Schmitz, B. 2023. The Mid-Ordovician Meteorite Flux to Earth Shortly before Breakup of the L-Chondrite Parent Body. *Icarus* 389: 115285.
- Lindsay, S. S., Marchis, F., Emery, J. P., Enriquez, J. E., and Assafin, M. 2015. Composition, Mineralogy, and Porosity of Multiple Asteroid Systems from Visible and near-Infrared Spectral Data. *Icarus (New York, N.Y.)* 247: 53–70.
- Lindskog, A., Costa, M. M., Rasmussen, C. M. O., Connelly, J. N., and Eriksson, M. E. 2017. Refined Ordovician Timescale Reveals no Link between Asteroid Breakup and Biodiversification. *Nature Communications* 8: 14066.
- Llorca, J., Trigo-Rodríguez, J. M., Ortiz, J. L., Docobo, J. A., García-Guinea, J., Catro-Tirado, A. J., Rubin, A. E., et al. 2005. The Villalbeto de la Peña Meteorite Fall: I. Fireball Energy, Meteorite Recovery, Strewn Field, and Petrography. *Meteoritics & Planetary Science* 40: 795–804.
- Lorenzetti, S., Eugster, O., Busemann, H., Marti, K., Burbine, T. H., and McCoy, T. 2003. History and Origin of Aubrites. *Geochimica et Cosmochimica Acta* 67: 557–571.
- Lowry, V. C., Vokrouhlický, D., Nesvorný, D., and Campins, H. 2020. Clarissa Family Age from the Yarkovsky Effect Chronology. *The Astronomical Journal* 160: 12 127.
- Lucas, M., Emery, J. P., MacLennan, E. M., Pinilla-Alonso, N., Cartwright, R. J., Lindsay, S. S., Reddy, V., Sanchez, J. A., Thomas, C. A., and Lorenzi, V. 2019. Hungaria Asteroid Region Telescopic Spectral Survey (HARTSS) II: Spectral Homogeneity among Hungaria Family Asteroids. *Icarus* 322: 227–250.
- MacLennan, E., and Granvik, M. 2024. Thermal Decomposition as the Activity Driver of near-Earth Asteroid (3200) Phaethon. *Nature Astronomy* 8: 60–68.

- Madiedo, J. M. 2022. Advances in the Framework of the Southwestern Europe Meteor Network: Machine Learning Applied to the Study of Meteor Events. *53rd Lunar and Planetary Science Conference* (LPI Contribution No. 2549), abstract #1976.
- Mahlke, M., Eschrig, J., Carry, B., Bonal, L., and Beck, P. 2023. Spectral Analogues of Barbarian Asteroids among CO and CV Chondrites. *Astronomy & Astrophysics* 676: 13 A94.
- Marchi, S., McSween, H. Y., O'Brien, D. P., Schenk, P., DeSanctis, M. C., Gaskell, R., Jaumann, R., et al. 2012. The Violent Collisional History of Asteroid 4 Vesta. *Science* 336: 690–92.
- Marsset, M., Brož, M., Vernazza, P., Drouard, A., et al. 2020. The Violent Collision History of Aqueously Evolved (2) Pallas. *Nature Astronomy* 4: 569–576.
- Marsset, M., Carry, B., Dumas, C., Hanuš, J., Viikinkoski, M., Vernazza, P., Müller, T. G., et al. 2017. 3D Shape of Asteroid (6) Hebe from VLT/SPHERE Imaging: Implications for the Origin of Ordinary H Chondrites. *Astronomy & Astrophysics* 604: 12 A64.
- Marsset, M., Vernazza, P., Birlan, M., DeMeo, F., Binzel, R. P., Dumas, C., Milli, J., and Popescu, M. 2016. Compositional Characterisation of the Themis Family. *Astronomy & Astrophysics* 586: A15: 9.
- Marsset, M., Vernazza, P., Brož, M., Thomas, C. A., DeMeo, F. E., Burt, B., Binzel, R. P., et al. 2024. The Massalia Astroid Family as the Origin of Ordinary L Chondrites. *Nature* 634: 561–65.
- Masiero, J. R., DeMeo, F., Kasuga, T., and Parker, A. H. 2015. Asteroid Family Physical Properties. In *Asteroids IV*, edited by P. Michel, F. E. DeMeo, and W. F. Bottke, 323–340. Tucson: University of Arizona Press.
- Masiero, J. R., Devogèle, M., Marcias, I., Castenada Jaimés, J., and Celline, A. 2023. The Increasingly Strange Polarimetric Behavior of the Barbarian Asteroids. *The Planetary Science Journal* 4: id93: 7.
- Masiero, J. R., Mainzer, A. K., Bauer, J. M., Grav, T., Nugent, C. R., and Stevenson, R. 2013. Asteroid Family Identification Using the Hierarchical Clustering Method and WISE/NEOWISE Physical Properties. *Astrophysical Journal* 770: 7: 22.
- Matson, R., Cooke, W., Hankey, M., Clary, S., Scott, T., Garvie, L., Wittmann, A., and Schrader, D. 2024. La Posa Plain. *Meteoritical Bulletin* 113.
- McCord, T. B., Adams, J. B., and Johnson, T. V. 1970. Asteroid Vesta: Spectral Reflectivity and Compositional Implications. *Science* 168: 1445–47.
- McCrosky, R. E., Posen, A., Schwartz, G., and Shao, C.-Y. 1971. Lost City Meteorite—Its Recovery and a Comparison with Other Fireballs. *Journal of Geophysical Research* 76: 4090–4180.
- McGraw, A. M., Reddy, V., and Sanchez, J. A. 2022. Spectroscopic Characterization of the Gefion Asteroid Family: Implications for L-Chondrite Link. *Monthly Notices of the Royal Astronomical Society* 515: 5211–18.
- McMullan, S., Denis, V., Devillepoix, H. A. R., Rowe, J., Daly, L., King, A. J., Cupák, M., et al. 2024. The Winchcombe Fireball—That Lucky Survivor. *Meteoritics & Planetary Science* 59: 927–947.
- Meibom, A., and Clark, B. E. 1999. Evidence for the Insignificance of Ordinary Chondritic Material in the Asteroid Belt. *Meteoritics & Planetary Science* 34: 7–24.
- Meier, M. M. M. 2017. Meteoriteorbits.Info—Tracking all Known Meteorites with Photographic Orbits. *48th Lunar and Planetary Science Conference* (LPI Contribution No. 1964), abstract #1178.
- Meier, M. M. M., Grimm, S., Maden, C., and Busemann, H. 2016. Do We Have Meteorites from the Veritas Asteroid Break-Up Event 8 ma Ago?.
- Meier, M. M. M., Gritsevich, M., Welten, K. C., Lyytinen, E., Plant, A. A., Maden, C., and Busemann, H. 2020. Orbit, Meteoroid Size and Cosmic History of the Osceola (L6) Meteorite. 14th Europlanet Science Congress 2020. Virtual Meeting, Id. EPSC2020-730.
- Meier, M. M. M., Maden, C., and Busemann, H. 2022. Are Příbram, Neuschwanstein and Benešov Fragments of the Same near-Earth Asteroid? A Re-Evaluation in the Light of Almahata Sitta 85th Annual Meeting of the Meteoritical Society 2022 (LPI Contrib. No. 2695), id.6453.
- Meier, M. M. M., Welten, K. C., Caffee, M. W., Marty, B., Zimmermann, L., Bland, P. A., Spurny, P., Ferriere, L., Maden, C., and Busemann, H. 2019. Cosmic Histories of Six Meteorites with Known Orbits. *Developments in Noble Gas Understanding and Expertise (DINGUE VI) Workshop*, held 15–17 August 2019, ETH Zürich, Switzerland. Abstract #30.
- Meier, M. M. M., Welten, K. C., Riebe, M. E. I., Caffee, M. W., Gritsevich, M., Maden, C., and Busemann, H. 2017. Park Forest (L5) and the Asteroidal Source of Shocked L Chondrites. *Meteoritics & Planetary Science* 52: 1561–76.
- Migliorini, F., Manara, A., Cellino, A., de Martino, M., and Zappala, V. 1997. Iris: A Possible Source of Ordinary Chondrites? *Astronomy & Astrophysics* 321: 652–59.
- Milani, A., Cellino, A., Knežević, Z., Novaković, B., Spoto, F., and Paolicchi, P. 2014. Asteroid Families Classification: Exploiting Very Large Datasets. *Icarus* 239: 46–73.
- Milani, A., Knežević, Z., Spoto, F., and Paolicchi, P. 2019. Asteroid Cratering Families: Recognition and Collisional Interpretation. *Astronomy & Astrophysics* 622: 18 A47.
- Milley, E. P. 2010. Physical Properties of Fireball-Producing Earth-Impacting Meteoroids and Orbit Determination through Shadow Calibration of the Buzzard Coulee Meteorite Fall. MSc thesis, University of Calgary, Alberta, Canada, p. 167.
- Milley, E. P., Hildebrand, A. R., Brown, P. G., Noble, M., Sarty, G., Ling, A., and Maillet, L. A. 2010. Pre-Fall Orbit of the Buzzard Coulee Meteoroid. GeoConvention Canada 2010—Working with the Earth. Calgary, Canada. Abstract id.0974\_GC2010, 4 pp.
- Mitchell, A. M., Reddy, V., Sharkey, B. N. L., Sanchez, J. A., Burbine, T. H., Le Corre, L., and Thomas, C. A. 2020. Constraining Ordinary Chondrite Composition Via Near-Infrared Spectroscopy. *Icarus* 336: 113426.
- Möller, A., and Knöfel, A. 2023. Der Meteoritenfall in Elmshorn am 25. April 2023. *Meteoros* 26: 158–166.
- Molnar, L. A., and Haegert, M. J. 2009. Details of Recent Collisions of Asteroids 832 Karin and 158 Koronis. AAS/DPS Meeting #41, Abstract 41, id.27.05.
- Morate, D., de León, J., De Prá, M., Licandro, J., Pinilla-Alonso, N., Campins, H., Arredondo, A., Marcio, C. J., Lazzaro, D., and Cabrera-Lavefrs, A. 2019. The Last Pieces of the Primitive Inner Belt Puzzle: Klio, Chaldaea, Chimaera, and Svea. *Astronomy & Astrophysics* 630: 14 A141.

- Morbidelli, A., and Gladman, B. 1998. Orbital and Temporal Distributions of Meteorites Originating in the Asteroid Belt. *Meteoritics & Planetary Science* 33: 999–1016.
- Morbidelli, A., Bottke, W. F., Nesvorný, D., and Levison, H. F. 2009. Asteroids Were Born Big. *Icarus* 204: 558–573.
- Morbidelli, A., Gonczi, R., Froeschle, C., and Farinella, P. 1994. Delivery of Meteorites Through the  $\nu_6$  Secular Resonance. *Astronomy & Astrophysics* 282: 955–979.
- Mothé-Diniz, T., and Nesvorný, D. 2008. Tirela: An Unusual Asteroid Family in the Outer Main Belt. *Astronomy & Astrophysics* 492: 593–98.
- Moutinho, A. L. R., Zurita, M., Zucolotto, M. E., and Tosi, A. 2020. Santa Filomena. *Meteoritical Bulletin* 109.
- Nakamura, T., Noguchi, T., Tanaka, M., Zolensky, M. E., Kimura, M., Tsuchiyama, A., Nakato, A., et al. 2011. Itokawa Dust Particles: A Direct Link between S-Type Asteroids and Ordinary Chondrites. *Science* 333: 1113–16.
- Nathues, A., Mottola, S., Kaasalainen, M., and Neukum, G. 2005. Spectral Study of the Eunomia Asteroid Family: I. Eunomia. *Icarus* 175: 452–463.
- Nesvorný, D., Bottke, W. F., Dones, L., and Levison, H. F. 2002. The Recent Breakup of an Asteroid in the Main-Belt Region. *Nature* 417: 720–771.
- Nesvorný, D., Bottke, W. F., Levison, H. F., and Dones, L. 2003. Recent Origin of the Solar System Dust Bands. *The Astrophysical Journal* 591: 486–497.
- Nesvorný, D., Bottke, W. F., Vokrouhlický, D., Morbidelli, A., Jedicke, R., Lazzaro, D., Ferraz-Mello, S., and Fernandes, J. A. 2006. Asteroid Families. In *Asteroids Comets Meteors 2005 (Proceedings of IAU Symposium 229)*. Búzios, Brazil, August 2005, edited by D. Lazzaro, S. Ferraz-Mello, and J. Fernandez, 289–299. Cambridge: Cambridge University Press.
- Nesvorný, D., Brož, M., and Carruba, V. 2015. In *Asteroids IV*, edited by P. Michel, F. E. DeMeo, and W. F. Bottke, 297–321. Tucson, AZ: University of Arizona Press.
- Nesvorný, D., Jenniskens, P., Levison, H. F., Bottke, W. F., Vokrouhlický, D., and Gounelle, M. 2010. Cometary Origin of the Zodiacal Cloud and Carbonaceous Micrometeorites. Implications for Hot Debris Disks. *The Astrophysical Journal* 713: 816–836.
- Nesvorný, D., Rogerio, D., Bottke, W. F., Jedicke, R., Naidu, S., Chesley, S. R., Chodas, P. W., et al. 2023. NEOMOD: A New Orbital Distribution Model for Near-Earth Objects. *The Astronomical Journal* 166: 30–55.
- Nesvorný, D., Roig, F., Vokrouhlický, D., and Brož, M. 2024. Catalog of Proper Orbits for 1.25 Million Main-Belt Asteroids and Discovery of 136 New Collisional Families. *The Astrophysical Journal Supplement Series* 274: 19–25.
- Nesvorný, D., Vokrouhlický, D., and Bottke, W. F. 2006. The Breakup of a Main-Belt Asteroid 450 Thousand Years Ago. *Science* 312: 1490.
- Nesvorný, D., Vokrouhlický, D., Morbidelli, A., and Bottke, W. F. 2009. Asteroidal Source of L Chondrite Meteorites. *Icarus* 200: 698–701.
- Nishizumi, K., and Caffee, M. W. 2012. CM Chondrites from Multiple Parent Bodies: Evidence from Correlated Mineralogy and Cosmic-Ray Exposure Ages. *43rd Lunar and Planetary Science Conference (LPI Contribution 1608)*, abstract #2758.
- Nishizumi, K., Caffee, M. W., Hamajama, Y., Reedy, R. C., and Welten, K. C. 2014. Exposure History of the Sutter's Mill Carbonaceous Chondrite. *Meteoritics & Planetary Science* 49: 2056–63.
- Noonan, J. W., Reddy, V., Harris, W. M., Bottke, W. F., Sanchez, J. A., Furfaro, R., Brown, Z., et al. 2019. Search for the H chondrite parent body among the three largest S-type asteroids: (3) Juno, (7) Iris, and (25) Phocaea. *The Astrophysical Journal* 158: 8–213.
- Noonan, J. W., Volk, K., Nesvorný, D., and Bottke, W. F. 2024. Dynamical Feasibility of (3) Juno as the Parent Body of the H Chondrites. *Icarus (New York, N.Y.)* 408: 115838.
- Novaković, B., Dell'Oro, A., Cellino, A., and Knežević, Z. 2012. Recent Collisional Jet from a Primitive Asteroid. *Monthly Notices of the Royal Astronomical Society* 425: 338–346.
- Novaković, B., Tsiganis, K., and Knežević, Z. 2010. Dynamical Portrait of the Lixiaohua Asteroid Family. *Celestial Mechanics and Dynamical Astronomy* 107: 35–49.
- Novaković, B., Tsirvoulis, G., Granvik, M., and Todovic, A. 2017. A Dark Asteroid Family in the Phocaea Region. *The Astronomical Journal* 153: 8–266.
- Novaković, B., Vokrouhlický, D., Spoto, F., and Nesvorný, D. 2022. Asteroid Families: Properties, Recent Advances, and Future Opportunities. *Celestial Mechanics and Dynamical Astronomy* 134: 60–34.
- O'Brien, D. P., Marchi, S., Morbidelli, A., Bottke, W. F., Schenk, P. M., Russell, C. T., and Raymond, C. A. 2014. Constraining the Cratering Chronology of Vesta. *Planetary and Space Science* 103: 131–142.
- Oberst, J., Heinlein, D., Köhler, U., and Spurný, P. 2004. The Multiple Meteorite Fall of Neuschwanstein: Circumstances of the Event and Meteorite Search Campaigns. *Meteoritics & Planetary Science* 39: 1627–41.
- Okazaki, R., Yoneda, S., and Yamaguchi, A. 2023. Noble Gas Compositions of Koshigaya, Komaki, Narashino, Hachioji, and Sone Meteorites. Annual meeting of the Geochemical Society of Japan. Abstract id.70.0–113.
- Oszkiewicz, D. A., Kankiewicz, P., Włodarczyk, I., and Kryszczyńska, A. 2015. Differentiation Signatures in the Flora Region. *Astronomy & Astrophysics* 584: 14–A18.
- Ozdín, D., Plavcan, J., Hornáková, M., Uher, P., Porubčan, V., Veis, P., Rakovský, J., Tóth, J., Konečný, P., and Svoren, J. 2015. Mineralogy, Petrography, Geochemistry, and Classification of the Kosice Meteorite. *Meteoritics & Planetary Science* 50: 864–879.
- Ozdín, D., Spurný, P., Borovicka, J., Shrbeny, L., Povinec, P., Macke, R., and Tóth, J. 2024. Pusté Úlany. *Meteoritical Bulletin* 113.
- Palmer, M., and Scott, J. 2024. Takapō. *Meteoritical Bulletin* 113.
- Palotai, C., Sankar, R., Free, D. L., Howell, J. A., Botella, E., and Batchelder, D. 2019. Analysis of the 2016 June 2 Bolide Event over Arizona. *Monthly Notices of the Royal Astronomical Society* 487: 2307–18.
- Paolicchi, P., Spoto, F., Knežević, Z., and Milani, A. 2019. Ages of Asteroid Families Estimated Using the YORP-Eye Method. *Monthly Notices of the Royal Astronomical Society* 484: 1815–28.
- Parker, A., Iverzic, Z., Juric, M., Lupton, R., Sekora, M. D., and Kowalski, A. 2008. The Size Distributions of Asteroid Families in the SDSS Moving Object Catalog 4. *Icarus* 198: 138–155.
- Patzek, M., Hoppe, P., Bischoff, A., Visser, R., and John, T. 2020. Hydrogen Isotopic Composition of CI- and CM-Like Clasts from Meteorite Breccias—Sampling Unknown Sources of Carbonaceous Chondrite Material. *Geochimica et Cosmochimica Acta* 272: 177–197.

- Pauls, A., and Gladman, B. 2005. Decoherence Time Scales for “Meteoroid Streams”. *Meteoritics & Planetary Science* 40: 1241–56.
- Pavela, D., and Novaković, B. 2019. Dynamical Evolution of König and Karma Asteroid Families. EPSC-DPS Joint Meeting 2019, Id.EPSC-DPS2019 Id.1080.
- Pavela, D., Novaković, B., Carruba, V., and Radovic, V. 2021. Analysis of the Karma Asteroid Family. *Monthly Notices of the Royal Astronomical Society* 501: 356–366.
- Popova, O. P., Jenniskens, P., Emel’yanenko, V., Kartashova, A., Biryukov, E., Khaibrakhmanov, S., Shuvalov, V., et al. 2013. Chelyabinsk Airburst, Damage Assessment, Meteorite Recovery, and Characterization. *Science* 342: 1069–73.
- Povinec, P. P., and Tóth, J. 2015. The Fall of the Košice Meteorite. *Meteoritics & Planetary Science* 50: 851–52.
- Pratesi, G., Moggi, C. V., Greenwood, R. C., Franchi, I. A., Hammand, S. J., Di Martino, M., Barghini, D., et al. 2021. Cavezzo—The Double Face of a Meteorite: Mineralogy, Petrography and Geochemistry of a Very Unusual Chondrite. *Meteoritics & Planetary Science* 56: 1125–50.
- Reddy, V., Carvano, J. M., Lazzaro, D., et al. 2011. Mineralogical Characterization of the Baptistina Asteroid Family: Implications for K/T Impactor Source. *Icarus* 216: 184–197.
- Reddy, V., Sanchez, J. A., Bottke, W. F., Cloutis, E. A., Izawa, M. R. M., O’Brien, D. P., Mann, P., et al. 2014. Chelyabinsk Meteorite Explains Unusual Spectral Properties of Baptistina Asteroid Family. *Icarus (New York, N.Y.)* 237: 116–130.
- Rhoden, A. R., Walsh, K. J., Gattelle, G. M., Avdellidou, C., and Delbo, M. 2020. On the Origin of the Largest Inner Main Belt D-type Asteroid. *51st Lunar and Planetary Science Conference (LPI Contribution 2326)*, abstract #2843.
- Riebe, M. E. I., Plant, A., Meier, M. M. M., Will, P., Krämer, A.-K., Bischoff, A., Maden, C., and Busemann, H. 2022. Almahata Sitta Ureilites – Noble Gases and Cosmic Ray Exposure Ages. *85th Annual Meeting of the Meteoritical Society 2022 (LPI Contribution No. 2695)*, id.6258.
- Riebe, M. E. I., Welten, K. C., Meier, M. M. M., Wieler, R., Barth, M. I. F., Ward, D., Laubenstein, M., et al. 2017. Cosmic-Ray Exposure Ages of Six Chondritic Almahata Sitta Fragments. *Meteoritics & Planetary Science* 52: 2353–74.
- Rivkin, A. S., Emery, J. P., Howell, E. S., Kareta, T., Noonan, J. W., Richardson, M., Sharey, B. N. L., et al. 2022. The Nature of Low-Albedo Small Bodies from 3  $\mu$ m Spectroscopy: One Group that Formed within the Ammonia Snow Line and One that Formed beyond it. *The Planetary Science Journal* 3: 34 153.
- Rubin, A. E. 2010. Impact Melting in the Cumberland Falls and Mayo Belwa Aubrites. *Meteoritics & Planetary Science* 45: 265–275.
- Rubin, A. E., and Bottke, W. F. 2009. On the Origin of Shocked and Unshocked CM Clasts in H-Chondrite Regolith Breccias. *Meteoritics & Planetary Science* 44: 701–742.
- Ruesch, O., Hiesinger, H., Blewett, D. T., Williams, D. A., Buczkowski, D., Scully, J., Yingst, R. A., et al. 2014. Geologic Map of the Northern Hemisphere of Vesta Based on Dawn Framing Camera (FC) Images. *Icarus* 244: 41–59.
- Sanchez, J. A., Reddy, V., Thirouin, A., Bottke, W. F., Kareta, T., De Florio, M., Sharkey, B. N. L., Battle, A., Cantillo, D. C., and Perason, N. 2024. The Population of Small Near-Earth Objects: Composition, Source Regions, and Rotational Properties. *The Planetary Science Journal* 5: 45 131.
- Sansom, E. K., Bland, P. A., Towner, M. C., Devillepoix, H. A. R., Cupak, M., Howie, R. M., Jansen-Sturgeon, T., et al. 2020. Murrili Meteorite’s Fall and Recovery from Kati Thanda. *Meteoritics & Planetary Science* 55: 2157–68.
- Sato, K., Miyamoto, M., and Zolensky, M. E. 1997. Absorption Bands near 3  $\mu$ m in Diffuse Reflectance Spectra of Carbonaceous Chondrites: Comparison with Asteroids. *Meteoritics & Planetary Science* 32: 503–7.
- Schenk, P. M., Neesemann, A., Marchi, S., Otto, K., Hoogenboom, T., O’Brien, D. P., Castillo-Rogez, J., Raymond, C. A., and Russell, C. T. 2022. A Young Age of Formation of Rheasilvia Basin on Vesta from Floor Deformation Patterns and Crater Counts. *Meteoritics & Planetary Science* 57: 22–47.
- Scherer, P., and Schultz, L. 2000. Noble Gas Record, Collisional History and Pairing of CV, CO, CK and Other Carbonaceous Chondrites. *Meteoritics & Planetary Science* 35: 145–153.
- Schmedemann, N., Kneissl, T., Ivanov, B. A., Michael, G. G., Wagner, R. J., Neukum, G., Ruesch, O., et al. 2014. The Cratering Record Chronology and Surface Ages of (4) Vesta in Comparison to Smaller Asteroids and the Ages of HED Meteorites. *Planetary and Space Science* 103: 103–130.
- Schmitz, B., Farley, K. A., Goderis, S., Heck, P. R., Bergström, S. M., Boschi, S., Claeys, P., et al. 2019. An Extraterrestrial Trigger for the Mid-Ordovician Ice Age: Dust from the Breakup of the L-Chondrite Parent Body. *Science Advances* 5: eaax4184.
- Schrader, D. L., Coutis, E. A., Applin, D. M., Davidson, J., Torrano, Z. A., Foustoukos, D., Alexander, C. M. O’D., et al. 2024. Tarda and Tagish Lake: Samples from the same outer Solar System asteroid and implications for D- and P-type asteroids. *Geochimica et Cosmochimica Acta* 380: 48–70.
- Schult, C., Stober, G., Keuer, D., and Singer, W. 2015. Radar Observations of the Maribo Fireball over Juliusruh: Revised Trajectory and Meteoroid Mass Estimation. *Monthly Notices of the Royal Astronomical Society* 450: 1460–64.
- Scott, E. R. D. 2020. Iron Meteorites: Composition, Age, and Origin. Oxford Research Encyclopedia of Planetary Science [cited 2024 October 12]. Available from: <https://oxfordre.com/planetaryscience/view/10.1093/acrefore/9780190647926.001.0001/acrefore-9780190647926-e-206>.
- Scott, E. R. D., and Herzog, G. F. 2021. Short Cosmic-Ray Exposure Ages of CI and CM Chondrites May Reflect Disintegration of Volatile-Rich Asteroids at Perihelion. *52nd Lunar and Planetary Science Conference (LPI Contribution No. 2548)*, Id.1833.
- Scott, J. M., Vida, D., Behan, D., Boothroyd, M. R., Burgin, D. L., Grieg, D., McKellar, P., et al. 2024. New Zealand’s Meteor Camera Network Leads to Recovery of the Tekapo/Takapō Meteorite. *eMeteorNews* 9: 155–58.

- Šegon, D., Korlevic, K., Andreic, Z., Vida, D., Novoselnik, F., and Skokic, I. 2018. Ten Years of the Croatian Meteor Network. *WGN, Journal of the International Meteor Organization* 46: 87–95.
- Shober, P. M., Caffee, M. W., and Bland, P. A. 2024. Cosmic-Ray Exposure Age Accumulated in near-Earth Space: A Carbonaceous Chondrite Case Study. *Meteoritics & Planetary Science* 59: 2695–2717.
- Shober, P. M., Courtot, A., and Vaubaillon, J. 2025. Near Earth Stream Decoherecy Revisited: The Limits of Orbital Similarity. *Astronomy & Astrophysics* 693: 20 A28.
- Shober, P. M., Devillepoix, H. A. R., Sansom, E. K., Towner, M. C., Cupák, M., Anderson, S. L., Benedix, G., et al. 2022. Arpu Kuilpu: An H5 from the Outer Main Belt. *Meteoritics & Planetary Science* 57: 1146–57.
- Šhrbený, L., Krzesinska, A. M., Borovička, J., Spurný, P., Tyminski, Z., and Kmiecik, K. 2022. Analysis of the Daylight Fireball of July 15, 2021, Leading to a Meteorite Fall and Find near Antonin, Poland, and a Description of the Recovered Chondrite. *Meteoritics & Planetary Science* 57: 2108–26.
- Smith, T., He, H., Li, S., Ranjith, P. M., Su, F., Gattacceca, J., Braucher, R., and ASTER-Team. 2021. Light Noble Gas Records and Cosmic Ray Exposure Histories of Recent Ordinary Chondrite Falls. *Meteoritics & Planetary Science* 56: 2002–16.
- Spoto, F., Milani, A., and Zoran, K. 2015. Asteroid Family Ages. *Icarus* 257: 275–289.
- Spurný, P. 1994. Recent Fireballs Photographed in Central Europe. *Planetary and Space Science* 42: 157–162.
- Spurný, P. 2016. Instrumentally Documented Meteorite Falls: Two Recent Cases and Statistics from all Falls. In *Proceedings IAU Symposium No. 318, Asteroids: New Observations, New Models, Honolulu, United States, August 3–7, 2015*, edited by S. R. Chesley, A. Morbidelli, R. Jedicke, and P. Farnocchia, 69–79. Cambridge: Cambridge University Press.
- Spurný, P., Bland, P. A., Borovička, J., Towner, M. C., Šhrbený, L., Bevan, A. W. R., and Vaughan, D. 2012. The Mason Gully Meteorite Fall in SW Australia: Fireball Trajectory, Luminosity, Dynamics, Orbit and Impact Position from Photographic Records Asteroids, Comets, Meteors. Proceedings of the Conference Held May 16–20, 2012, Niigata, Japan, abstract #6369.
- Spurný, P., Bland, P. A., Šhrbený, L. I., Borovička, J., Ceplecha, Z., Singelton, A., Bevan, A. W. R., et al. 2012. The Bunburra Rockhole Meteorite Fall in SW Australia: Fireball Trajectory, Luminosity, Dynamics, Orbit, and Impact Position from Photographic and Photoelectric Records. *Meteoritics & Planetary Science* 47: 163–185.
- Spurný, P., Bland, P. A., Šhrbený, L., Towner, M. C., Borovička, J., Bevan, A. W. R., and Vaughan, D. 2011. The Mason Gully Meteorite Fall in SW Australia: Fireball Trajectory and Orbit from Photographic Records. 74th Annual Meeting of the Meteoritical Society, August 8–12, 2011 in London, UK. Published in: *Meteoritics & Planetary Science Supplement Series* 74: Id.5101.
- Spurný, P., Borovička, J., and Šhrbený, L. 2022. A Bright Bolide in the Early Evening Sky on June 25, 2022, Probably Ended in a Meteorite Fall in SW Slovakia. [cited 2024 September 1]. Available from: [https://www.asu.cas.cz/~meteor/bolid/2022\\_06\\_25/index.html](https://www.asu.cas.cz/~meteor/bolid/2022_06_25/index.html).
- Spurný, P., Borovička, J., and Šhrbený, L. 2024a. Atmospheric Entry and Fragmentation of the Small Asteroid 2024 BX1: Bolide Trajectory, Orbit, Dynamics, Light Curve, and Spectrum. *Astronomy & Astrophysics* 686: 8 A67.
- Spurný, P., Borovička, J., and Šhrbený, L. 2024b. A Very Bright Bolide Over Austria Associate With a Meteor Shower Captured in Detail by the European Bolide Network Instruments. [cited 2024 December 1]. Available from: <https://www.gnews.cz/en/culture/a-very-bright-bolide-over-austria-associated-with-a-meteorite-fall-captured-in-detail-by-the-instruments-of-the-european-bolide-site/>.
- Spurný, P., Borovička, J., Baumgarten, G., Haack, H., Heinlein, D., and Sørensen, A. N. 2017. Atmospheric Trajectory and Heliocentric Orbit of the Ejby Meteorite Fall in Denmark on February 6, 2016. *Planetary and Space Science* 143: 192–98.
- Spurný, P., Borovička, J., Haack, H., Singer, W., Jobse, K., and Keuer, D. 2013. Trajectory and Orbit of the Maribo CM2 Meteorite from Optical, Photoelectric and Radar Records. *Meteoroids 2013*. Proceedings of the Conference Held August 26–30, 2013, Poznan, Poland. Abstract #111.
- Spurný, P., Borovička, J., Haloda, J., Šhrbený, L., and Heinlein, D. 2016. Two Very Precisely Instrumentally Documented Meteorite Falls: Žďár nad Sázavou and Stubenberg—Prediction and Reality 79th Annual Meeting of the Meteoritical Society (LPI Contribution No. 1921), id. #6221.
- Spurný, P., Borovička, J., Kac, J., Kalenda, P., Atanackov, J., Kladnik, G., Heinlein, D., and Grau, T. 2010. Analysis of Instrumental Observations of the Jesenice Meteorite Fall on April 9, 2009. *Meteoritics and Planetary Science* 45: 1392–1407.
- Spurný, P., Borovička, J., Šhrbený, L., Ronge, L., and Heinlein, D. 2019. The Hradec Kralove (CZ) and Renchen (DE) Meteorite Falls – Recovery of Meteorites Exactly According to Prediction Based on Records Taken by the European Fireball Network. Oral presentation at *Meteoroids 2019*, June 17–21, 2019. Bratislava, Slovakia. Abstract. [cited 2024 September 17]. Available from: <https://www.asu.cas.cz/articles/1229/19/meteorit-hradec-kralove-nalezene-v-predpovezene-oblasti>; Also: [https://fmph.uniiba.sk/fileadmin/fmfi/microsites/kafzm/daa/Meteoroids2019\\_files/abstracts/oral/O\\_69.pdf](https://fmph.uniiba.sk/fileadmin/fmfi/microsites/kafzm/daa/Meteoroids2019_files/abstracts/oral/O_69.pdf).
- Spurný, P., Borovička, J., and Šhrbený, L. 2020. The Žďár Nad Sázavou Meteorite Fall: Fireball Trajectory, Photometry, Dynamics, Fragmentation, Orbit, and Meteorite Recovery. *Meteoritics & Planetary Science* 55: 376–401.
- Spurný, P., Haloda, J., and Borovička, J. 2013. Benešov Bolide—Surprising Outcome of Exceptional Story After Twenty Years. In Proceedings of the International Meteor Conference, *La Palma, Canary Islands, Spain 20–23 September 2012*, edited by M. Gyssens, and P. Roggemans, pp. 106–7. Mechelen: International Meteor Organization.
- Spurný, P., Haloda, J., Borovička, J., Šhrbený, L., and Halodová, P. 2014. Reanalysis of the Benešov Bolide and Recovery of Polymict Breccia Meteorites—Old Mystery Solved after 20 Years. *Astronomy & Astrophysics* 570: idA39: 14.
- Spurný, P., Oberst, J., and Heinlein, D. 2003. Photographic Observations of Neuschwanstein, a Second Meteorite from the Orbit of the Příbram Chondrite. *Nature* 434: 151–53.
- Suttle, M. D., King, A. J., Schofield, P. F., Bates, H., and Russell, S. S. 2021. The Aqueous Alteration of CM

- Chondrites, a Review. *Geochimica et Cosmochimica Acta* 299: 219–256.
- Tagliaferri, E., Spalding, R., Jacobs, C., and Erlich, A. 1994. Detection of Meteoroid Impacts by Optical Sensors in Earth Orbit. In *Hazards Due to Comets and Asteroids*, edited by T. Gehrels, M. S. Matthews, and A. Schumann, 199–220. Tucson, AZ: University of Arizona Press.
- Takenouchi, A., Yoneda, S., Yamaguchi, A., Okazaki, R., Takahashi, N., Shirai, N., Fujiwara, Y., and Kataoka, R. 2021. The First Fall-Observed and Recovered Meteorite in Japan: Narashino meteorite. Japan Geoscience Union Meeting 2021. Abstract id.PPS07-04.
- Takir, D., and Emery, J. P. 2012. Outer Main Belt Asteroids: Identification and Distribution of our 3- $\mu$ m Spectral Groups. *Icarus (New York, N.Y.)* 219: 641–654.
- Takir, D., Emery, J. P., and McSween, H. Y. 2015. Toward an Understanding of Phyllosilicate Mineralogy in the Outer Main Asteroid Belt. *Icarus* 257: 185–193.
- Takir, D., Emery, J. P., Bottke, W. F., and Arredondo, A. 2024. Origin of Asteroid (101955) Bennu and its Connection to the New Polana Family. *Scientific Reports* 14: 15965.
- Tanbakouei, S., Trigo-Rodríguez, J. M., Llorca, J., Moyano-Camero, C. E., Williams, I. P., and Rivkin, A. S. 2021. The Reflectance Spectra of CV-CK Carbonaceous Chondrites from the Near-Infrared to the Visible. *Monthly Notices of the Royal Astronomical Society* 507: 651–662.
- Tatsumi, E., de León, J., Popescu, M., Licandro, J., and Tiaut, F. 2021. Near Ultraviolet Observations of Polana, Eulalia, and Themis Families: Origin of Ryugu and Bennu. EuroPlanet Science Congress 15: id.2021–283.
- Tatsumi, E., Vilas, F., de León, J., Popescu, M., Hasegawa, S., De Prá, M., Tiaut-Ruano, F., and Licandro, J. 2024. Near-Ultraviolet Absorption Distribution of Primitive Asteroids from Photometric Survey. II. Collisional Families. *Astronomy & Astrophysics* 693: 27.
- Terfelt, F., and Schmitz, B. 2021. Asteroid Break-Ups and the Meteorite Delivery to Earth the Past 500 Million Years. *Proceedings of the National Academy of Sciences of the United States of America* 118: 8 32020977118.
- Thompson, M. S., Loeffler, M. J., Morris, R. V., Keller, L. P., and Christoffersen, R. 2019. Spectral and Chemical Effects of Simulated Space Weathering of the Murchison CM2 Carbonaceous Chondrite. *Icarus* 319: 499–511.
- Toliou, A., Granvik, M., and Tsirvoulis, G. 2021. Minimum Perihelion Distances and Associated Dwell Times for Near-Earth Asteroids. *Monthly Notices of the Royal Astronomical Society* 506: 3301–12.
- Tosi, A., Zucolotto, M. E., Andrade, D. P., Winter, O. C., Mourao, D. C., Sfair, R., Ziegler, K., Perez, P. D., et al. 2023. The Santa Filomena Meteorite Shower: Trajectory, Classification, and Opaque Phases as Indicators of Metamorphic Conditions. *Meteoritics & Planetary Science* 58: 621–642.
- Tóth, J., Kornos, L., Duris, F., Zigo, P., Kalmancok, D., Világi, J., Simon, J., et al. 2018. AMOS from Slovakia, Canary Islands, and Chile. In *Proceedings of the International Meteor Conference. Serbia, 21–24 September 2017*, edited by M. Gyssens, and R. J.-L. Petnica, 16–17. Mechelen: IMO.
- Towner, M. C., Jansen-Sturgeon, T., Cupak, M., Sansom, E. K., Devillepoix, H. A. R., Bland, P. A., Howie, R. M., Paxman, J. P., Benedix, G. K., and Hartig, B. A. D. 2022. Dark-Flight Estimates of Meteorite Fall Positions: Issues and a Case Study Using the Murrili Meteorite Fall. *The Planetary Science Journal* 3: 16 44.
- Trigo-Rodríguez, J. M., Borovička, J., Spurný, P., Ortiz, J. L., Docobo, J. A., Castro-Tirado, A. J., and Llorca, J. 2006. The Villalbeta de la Peña Meteorite Fall: II. Determination of Atmospheric Trajectory and Orbit. *Meteoritics & Planetary Science* 41: 505–517.
- Trigo-Rodríguez, J. M., Lyytinen, E., Gritsevich, M., Moreno-Ibáñez, M., Bottke, W. F., Williams, I., Lupovka, V., Dmitriev, V., Kohout, T., and Grokhovsky, V. 2015. Orbit and Dynamic Origin of the Recently Recovered Annama's H5 Chondrite. *Monthly Notices of the Royal Astronomical Society* 449: 2119–27.
- Tsiganis, K., Knežević, Z., and Varvoglis, H. 2007. Reconstructing the Orbital History of the Veritas Family. *Icarus* 186: 484–497.
- Tsirvoulis, G. 2019. Discovery of a Young Subfamily of the (221) Eos Asteroid Family. *Monthly Notices of the Royal Astronomical Society* 482: 2612–18.
- Unsalan, O., Jenniskens, P., Yin, Q.-Z., Kaygisiz, E., Albers, J., Clark, D. L., Granvik, M., et al. 2019. Howardite Fall in Turkey: Source Crater of HED Meteorites on Vesta and Impact Risk of Vestoids. *Meteoritics & Planetary Science* 54: 953–1008.
- Vernazza, P., Binzel, R. P., Thomas, C. A., DeMeo, F. E., Bus, S. J., Rivkin, A. S., and Tokunaga, A. T. 2008. Compositional Differences between Meteorites and near-Earth Asteroids. *Nature* 454: 858–860.
- Vernazza, P., Marsset, M., Beck, P., Binzel, R. P., Birlan, M., Cloutis, E. A., DeMeo, F. E., Dumas, C., and Hiroi, T. 2016. Compositional Homogeneity of CM Parent Bodies. *The Astronomical Journal* 152: 54–63.
- Vernazza, P., Zanda, B., Binzel, R. P., Hiroi, T., DeMeo, F. E., Birlan, M., Hewins, R., Ricci, L., Barge, P., and Lockhart, M. 2014. Multiple and Fast: The Accretion of Ordinary Chondrite Parent Bodies. *The Astrophysical Journal* 791: 120, 22 pp.
- Vida, D., Segon, D., Gural, P. S., Brown, P. G., McIntyre, M. J. M., Dijkema, T. J., Pavletic, L., et al. 2021. The Global Meteor Network—Methodology and First Results. *Monthly Notices of the Royal Astronomical Society* 506: 5046–74.
- Vida, D., Segon, D., Segon, M., Atanackov, J., Ambrozik, B., McFadden, L., Ferriere, L., et al. 2021. Novo Mesto Meteorite Fall—Trajectory, Orbit and Fragmentation Analysis from Optical Observations. 15th Europlanet Science Congress 2021, id.EPSC2021-139.
- Viikinkoski, M., Vernazza, P., Hanuš, J., le Coroller, H., Tazhenova, K., Carry, B., Marsset, M., et al. 2018. (16) Psyche: A mesosiderite-like asteroid? *Astronomy & Astrophysics* 619: 10 L3.
- Visuri, J. J., and Gritsevich, M. I. 2021. Introducing the FireOwl—Data Processing Software of the Finnish Fireball Network. 84th Annual meeting of the Meteoritical Society, held August 15–21, 2021, Chicago, Illinois (LPI Contribution No. 2609), id.6093.
- Vokrouhlický, D., Brož, M., Bottke, W. F., Nesvorný, D., and Morbidelli, A. 2006. The Peculiar Case of the Agnia Asteroid Family. *Icarus* 183: 349–361.
- Vokrouhlický, D., Brož, M., Bottke, W. F., Nesvorný, D., and Morbidelli, A. 2006. Yarkovsky/YORP Chronology of Asteroid Families. *Icarus* 182: 118–142.
- Vokrouhlický, D., Pravec, P., Durech, J., Bolin, B., Jedicke, R., Kusnirák, P., Galád, A., et al. 2017. The Young

- Datura Asteroid Family. Spins, Shapes, and Population Estimate. *Astronomy & Astrophysics* 598: id.A91: 19.
- Walsh, K. J., Delbó, M., Bottke, W. F., Vokrouhlický, D., and Lauretta, D. S. 2013. Introducing the Eulalia and New Polana Asteroid Families: Re-Assessing Primitive Asteroid Families in the Inner Main Belt. *Icarus* 225: 283–297.
- Wasson, J. T., and Kallemeyn, G. W. 1988. Compositions of Chondrites. *Philosophical Transactions of the Royal Society of London. Series A, Mathematical and Physical Sciences* 325: 535–544.
- Welten, K. C., and Caffee, M. W. 2024. Cosmogenic Radionuclides in the Stubenberg LL6 Chondrite Fall—Evidence for a Recent Breakup Event of a Meter-Sized Object in Space. 86th Annual Meeting of the Meteoritical Society (LPI Contribution No. 3036), id.6460.
- Welten, K. C., Caffee, M. W., and Nishizumi, K. 2016. The Complex Cosmic Ray Exposure History of Jesenice (L6): Possible Evidence for Ejection from Parent Body by Tidal Disruption or YORP Related Effects. *47th Lunar and Planetary Science Conference* (LPI Contribution no. 1903), abstract #2924.
- Welten, K. C., Lindner, L., van der Borg, K., Loeken, T., Scherer, P., and Schultz, L. 1997. Cosmic-Ray Exposure Ages of Diogenites and the Recent Collisional History of the Howardite, Eucrite and Diogenite Parent Body/Bodies. *Meteoritics & Planetary Science* 32: 891–902.
- Welten, K. C., Meier, M. M. M., Caffee, M. W., Laubenstein, M. L., Nishizumi, K., Wieler, R., Bland, P. A., Towner, M. C., and Spurný, P. 2012. Cosmic-Ray Exposure Age and Preatmospheric Size of the Bunburra Rockhole Achondrite. *Meteoritics & Planetary Science* 47: 186–196.
- Wetherhill, C. 1967. Collisions in the Asteroid Belt. *Journal of Geophysical Research* 72: 2429–44.
- Wetherhill, C. 1985. Asteroidal Source of Ordinary Chondrites. *Meteoritics & Planetary Science* 20: 1–22.
- Wieler, R. 2002. Cosmic-Ray-Produced Noble Gases in Meteorites. *Reviews in Mineralogy and Geochemistry* 47: 125–170.
- Williams, D. A., Denevi, B. W., Mittlefehldt, D. W., Mest, S. C., Schenk, P. M., Yingst, R. A., Buczkowski, D. L., et al. 2014. The Geology of the Marcia Quadrangle of Asteroid Vesta: Assessing the Effects of Large, Young Craters. *Icarus* 244: 74–88.
- Willman, M., Jedicke, R., Nesvorný, D., Moskovitz, N., Ivezic, Z., and Fevig, R. 2008. Redetermination of the Space Weathering Rate Using Spectra of Iannini Asteroid Family Members. *Icarus* 195: 663–673.
- Xu, Y.-B., and Zhou, L.-Y. 2020. Transit of Asteroids across the 7/3 Kirkwood Gap under the Yarkovsky Effect. *Astronomy & Astrophysics* 637: id.A19: 9.
- Yamaguchi, A., Takenouchi, A., Okazaki, R., and Yoneda, S. 2020. Narashino. *Meteoritical Bulletin* 109.
- Yang, B., Hanuš, J., Brož, M., Chrenko, O., Willman, M., Ševeček, P., Masiero, J., and Kaluna, H. 2020. Physical and Dynamical Characterization of the Euphrosyne Asteroid Family. *Astronomy & Astrophysics* 643: id.A38: 9.
- Zande, B., Egal, A., Steinhaus, A., Bouley, S., Colas, F., Ferrière, L., Vida, D., et al. 2023. Recovery and Planned Study of the Saint-Pierre-le-Viger Meteorite: An Achievement of the FRIPON/Vigie-Ciel Citizen Science Program. 86th Annual Meeting of the meteoritical society. 13–18 August 2023, Los Angeles, CA (LPI Contribution No. 2990), id. 6206.
- Zappalà, V., Bendjoya, P., Cellino, A., Farinella, P., and Froeschlé, C. 1995. Asteroid Families: Search of a 12,487-Asteroid Sample Using Two Different Clustering Techniques. *Icarus* 116: 291–314.
- Zappatini, A., Gnos, E., Hofmann, B., and Lindemann, S. 2024. Raja. *Meteoritical Bulletin* 113.
- Zappatini, A., Hofmann, B. A., Gnos, E., Eggenberger, U., Gfeller, F., Kruttasch, P. M., Sansom, E. K., et al. 2024. 86th Annual meeting of the Meteoritical Society 2024 (LPI Contrib. No. 3036), id.6140.
- Zappatini, A., Hofmann, B., and Gnos, E. 2022. Al-Khadhaf. *Meteoritical Bulletin* 112.
- Zolensky, M. E., Fries, M., Utas, J., Chan, Q. H.-S., Kebukawa, Y., Steele, A., Bodnar, R. J., et al. 2016. 30 C Chondrite Clasts in H Chondrite Regolith Breccias: Something Different. *Meteoritics & Planetary Science* 51: 6488.
- Zolensky, M. E., Takenouchi, A., Mikouchi, T., Gregory, T., Nishizumi, K., Caffee, M. W., Velbel, M. A., et al. 2021. The Nature of the CM Parent Asteroid Regolith Based on Cosmic Ray Exposure Ages. *Meteoritics & Planetary Science* 56: 49–55.
- Zolensky, M. E., Weisberg, M. K., Buchanan, P. C., and Mittlefehldt, D. W. 1996. Mineralogy of Carbonaceous Chondrite Clasts in HED Achondrites and the Moon. *Meteoritics & Planetary Science* 31: 518–537.
- Zolensky, M., and Le, L. 2024. How are H Chondrites Like HEDs? Frequent Presence of CI and CM Xnoliths. 86th Annual Meeting of the Meteoritical Society 2024 (LPI Contribution. No. 3036), abstract# 6160.
- Zolqdek, P., Wisniewski, M., and Polakowski, K. 2012. Fireball over Denmark on 17 January 2009. *Journal of the International Meteorological Organization* 37: 182–84.
- Zuluaga, J. I., Cuartas-Restrepo, P. A., Ospina, J., and Sucerquia, M. 2019. Can We Predict the Impact Conditions of Meter-Sized Meteoroids? *Monthly Notices of the Royal Astronomical Society Letters* 486: L69–L73.
- Zurita, M. 2020. Rock Found in Tiros (Brazil) Is a Meteorite from Vesta that Had its Fall Filmed in May. [cited 2024 October 9]. Available from: <https://www.bramonmeteor.org/bramon/en/rocha-encontrada-em-tiros-e-um-meteorito-vindo-de-vesta-que-teve-sua-queda-filmada-em-maio/>. Also: Bolide over Minas Gerais - 05/08/2020. Online: <https://www.bramonmeteor.org/bramon/en/bolido-sobre-gerais-08-05-2020/>
- Zurita, M., Andrade, D., and Zucolotto, M. E. 2020. Tiros. *Meteoritical Bulletin* 109.